LBL-32689
UC-404

Center for Advanced Materials

CAM

Interaction in Polysilazane / SiC Powder Systems

Y.P. Boiteux
(Ph.D. Thesis)

July 1992

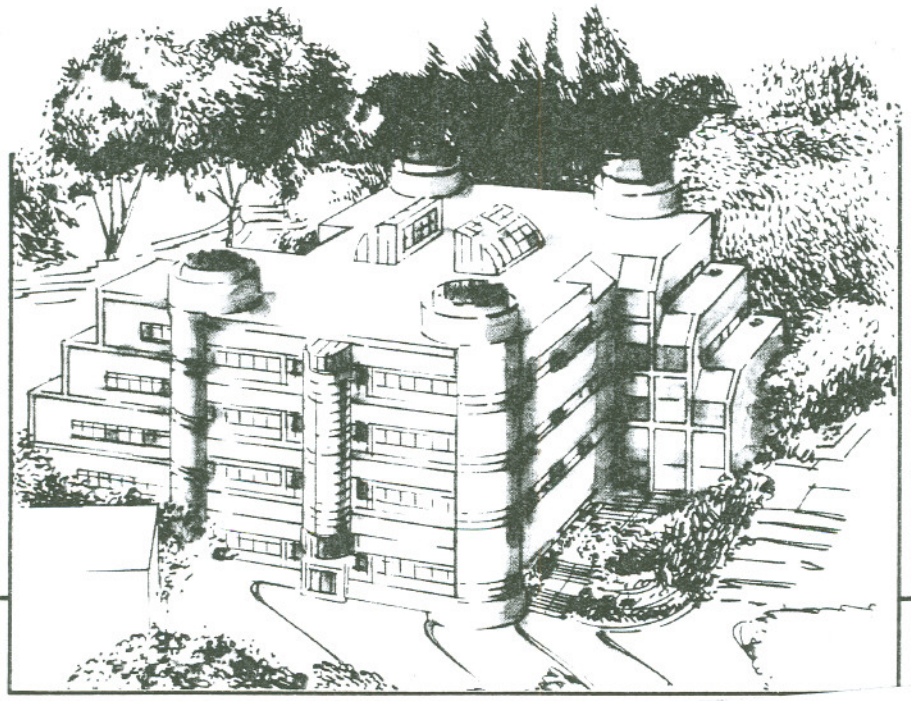

LBL-32689
REFERENCE COPY
Does Not
Circulate
Copy 1
Bldg. 50 Library.

Materials and Chemica
Lawrence Berkeley Laboratory
ONE CYCLOTRON ROAD, BERKELEY, CA 94720 • (415) 486-4755

Prepared for the U.S. Department of Energy under Contract DE-AC03-76SF00098

DISCLAIMER

This document was prepared as an account of work sponsored by the United States Government. Neither the United States Government nor any agency thereof, nor The Regents of the University of California, nor any of their employees, makes any warranty, express or implied, or assumes any legal liability or responsibility for the accuracy, completeness, or usefulness of any information, apparatus, product, or process disclosed, or represents that its use would not infringe privately owned rights. Reference herein to any specific commercial product, process, or service by its trade name, trademark, manufacturer, or otherwise, does not necessarily constitute or imply its endorsement, recommendation, or favoring by the United States Government or any agency thereof, or The Regents of the University of California. The views and opinions of authors expressed herein do not necessarily state or reflect those of the United States Government or any agency thereof or The Regents of the University of California and shall not be used for advertising or product endorsement purposes.

Lawrence Berkeley Laboratory is an equal opportunity employer.

LBL-32689
UC-404

Interaction in Polysilazane / SiC Powder Systems

Yves P. Boiteux
Ph.D. Thesis

Department of Materials Science and Mineral Engineering
University of California

and

Center for Advanced Materials
Materials Sciences Division
Lawrence Berkeley Laboratory
University of California
Berkeley, CA 94720

July 1992

This work was supported by the Director, Office of Energy Research, Office of Basic Energy Sciences, Materials Sciences Division, of the U.S. Department of Energy under Contract No. DE-AC03-76SF00098.

Interaction in Polysilazane / SiC Powder systems

by Yves P. Boiteux

Abstract

The consolidation of ceramic precursor / ceramic powder systems upon heating is investigated. This research explores new moderate temperature fabrication routes to structural ceramics. It also opens new pathways to near-net shape forming techniques.

A polysilazane (silicon nitride precursor) is chosen as ceramic precursor. The filler material is a sub-micron SiC powder. Prior to the investigation, a scheme is developed to optimize the volume fraction of precursor to be added to the powder. The proposed strategy aims at maximizing the density of the compacted samples in the green state. Different techniques are then presented to improve the homogeneity of precursor distribution in the mixture. In particular, a microencapsulation technique is developed that leads to a uniform coating of precursor on individual SiC particles.

Upon pyrolysis of these systems containing 20 wt% polysilazane, little shrinkage occurs. Therefore, the observed consolidation does not involve significant volume or grain boundary diffusion in the filler material (SiC). Microstructure observations confirm that the silicon carbide particles do not coarsen during the heat treatment. Using various electron microscopy techniques, the role of the precursor phase is investigated. The precursor, upon pyrolysis, transforms into an amorphous ceramic phase that acts as a cement between the SiC particles. Depending upon its composition this cement phase can remain amorphous up to 1500°C; overall, it is best described as a siliconoxycarbide with or without traces of nitrogen. The elimination of nitrogen in the amorphous phase indicates that the filler material (SiC) has a strong influence on the pyrolysis behavior of

the chosen polysilazane. It is found that the amorphous ceramic phase may crystallize between 1400 and 1500°C, and that, depending on the nature of the gas environment, the crystalline phases were SiC, Si or Si_3N_4.

Mechanisms explaining the strength increase upon heat treatment are proposed. During precursor conversion, a redistribution of the precursor occurs by action of capillary forces or via vapor phase diffusion and recondensation of volatile monomers. The confined pyrolysis of the precursor results in an increase of residual ceramic matter being decomposed inside the sample. An interfacial reaction between the native silica-rich surface layer on silicon carbide particles and the precursor derived phase explains the high strength of the materials.

TABLE OF CONTENTS

Acknowledgements

CHAPTER 1 : INTRODUCTION 1
1.1 Processing of Si_3N_4 and SiC ceramics 1
1.2 Precursors : a new trend in ceramic synthesis. 3
1.3 Development of precursors for SiC and Si_3N_4. ceramics. 3
1.4 Background on polysilanes and polysilazanes. 4
1.5 Polysilanes and polysilazanes as binders. 8

CHAPTER 2 : RESEARCH OBJECTIVES 11
2.1 Consolidation phenomena in precursor/powder system upon pyrolysis.. 11
2.2 Goal 11
2.3 General approach 12
2.4. Limitation of scope 13

CHAPTER 3 : UNCONFINED PYROLYSIS 15
3.1 Introduction 15
3.2 Experiment 15
3.3 Results 17
3.4 Discussion 20

CHAPTER 4: PROCESSING OF SiC/POLYSILAZANES MATERIALS 23
4.1 Introduction 23
4.2 Background 24
4.3 Selection of precursor loading 25
4.4 Sample preparation 26
4.5 Results and discussion 31
4.6 Conclusion 36

CHAPTER 5 : MICROSTRUCTURE AND PHASE ANALYSIS 37
5.1 Introduction 37
5.2 Experiments 37

5.3 Results and discussion 39
5.4 Conclusion 45

CHAPTER 6 : MECHANICAL PROPERTIES 47
6.1 Introduction 47
6.2 Experimental 48
6.3 Results 48
6.4 Source of macroscopic flaws 49

CHAPTER 7 : GENERAL DISCUSSION 51

CHAPTER 8 : CONCLUSION 56

REFERENCES 58

LIST OF TABLES 62

LIST OF FIGURES 66

Acknowledgments

First I would like to express my gratitude to my advisor, Professor L.C. De Jonghe, who, during the many years of my stay at LBL, has continuously given new life to my efforts. His remarkable knowledge of so many different scientific fields can only inspire a total admiration

Also to be thanked are Professors Searcy and Louie, who have accepted the delicate task to review this "manuscript". Their participation and guidance during the qualifying examination helped me focus my research.

Obtaining a PhD at Berkeley is also the opportunity to meet people with various backgrounds. I am particularly grateful to John Holthuis, James Wu and John Jacobson, outstanding members of the technical staff, who have done more than can be expected from them to facilitate my experiments. The discussions we shared will not be forgotten. Question : Who can recite french poetry fifty years after learning it ? There are many other persons who have contributed directly and indirectly to this work, among them Erlene F., Jim S., Hank B. Bob I., Peter R. and all the workshop members.

Special thanks will go to Chuck Echer and Dr.Kanan Krishnan of the National Center for Electron Microscopy, for their assistance in the analytical part of the electron microscopy work. The microscopy could not have been possible without the devoted help from Wendy, who assisted me in the preparation of the sample. There are also those who know things, no, I mean, really, a lot of things and don't keep it for themselves, Tom Richardson and Steve Visco to name them.

Too many (ex-)students should be mentioned that have made my stay more enjoyable, first the core of the coffee club, Jian Ding, Dale Olson, Mike Kollrack, Dave Kapolnek and Tim Kueper (who actually never drank coffee). I also have to thank Ty, Craig, Mani, Thea, Chi, Shari, King-Fu and Jiang-Tsair Lin, Shun Wu, Mahesh and all the

so many souls that, at some point, I have met. I will not forget my ex-office-mate, Naomi Naito, for the unbelievable support she displayed during the preparation of my examination. Of course, there are those who helped me not forget my French, Jean-Christophe Giron, Pascal Gruffel, Alain Claverie and Picard. Those who shared the same interest in the game of volley-ball are too numerous to be cited, but they have also contributed to help me keep my sanity.

And yet, all of this may not have been possible without the courageous altruism of my late sister Anne who disappeared just a month before this work was completed from a long and painful illness that she alone decided not to inform me about. I dedicate this thesis to her, because she had already received all the love I could give.

CHAPTER 1 INTRODUCTION

1.1 Processing of Si_3N_4 and SiC ceramics.

The efficiency of current gas turbine engines is limited by their maximum operating temperature. To raise this temperature substantially, technology has turned to structural ceramics to find new materials that do not creep at high temperature. Silicon carbide[1] and silicon nitride[2], both in monolithic and composite forms, have been the workhorses of research programs for more than twenty years. These materials possess the required properties. Those properties are low density (to minimize centrifugal forces at high rpm), good thermal stability, oxidation and corrosion resistance, and low creep at high temperature. However, the widespread use of structural ceramics for application under severe conditions has fallen well short of expectation, mainly because of the brittleness of SiC and Si_3N_4. Significant progress in reliability, however, has been achieved by implementing cleaner processing procedures and by using finer and purer starting materials. The strength of ceramics is very sensitive to the presence of flaws as a result of their low toughness. The elimination of flaws in structural ceramics is still the number one problem facing the ceramist of the 1990s. Large flaws can originate from contamination (any foreign particle with deleterious effect during packing and sintering) or from residual porosity associated with a locally poor packing of the particles. Additional flaws can even be created during the consolidation stage due to inhomogeneous densification rates. Since flaws are introduced during processing it is useful to reconsider the different stages of fabrication of a typical ceramic article.

In stage one, a powder is prepared that contains the material of interest, plus additives and various binders. The homogeneity of the distribution of the various components will depend on the efficiency of the mixing procedure. Local variations in concentration of

additives can affect adversely the densification rates between neighboring regions. At stage two, the powder mixture is compacted into a "green" structure. Additions of organic binders usually alleviate poor packing by allowing rearrangement of particles. Ideally, a green compact should be characterized by a uniform pore size distribution. When applicable, forming techniques based on the sedimentation of colloidal suspensions lead to more homogeneous green structures. During the last stage the compact is fired into a dense object. Typical flaws observed in the final microstructure are large grains and voids. Both of these flaws can be to some extent eliminated by a careful microstructure evolution control[3]. Finally, machining flaws can be strength limiting because they affect the surface or sub-surface of the parts, which are often subject to the highest tensile stresses and consequently are the more likely regions for cracks to form[4].

This brief review of a conventional fabrication process has pointed out the main origins of flaws in a ceramic part. Conceptually, a more direct fabrication procedure may eliminate most of the problems described earlier (impurities, inhomogeneous mixing, particle packing and large residual porosity). It would rely on organometallic polymers (called ceramic precursor) that could be shaped using conventional plastic forming techniques and transformed[5] directly into ceramic objects upon thermal decomposition. An example of such a new concept is the formation of oxide ceramic from alkoxides and the fabrication of small parts via the sol-gel process. This technique, of course, relies on the availability of suitable "precursors", and is particularly well adapted for oxide ceramics. For SiC and Si_3N_4 however the sol-gel technique is not applicable. The synthesis of inorganic polymer precursors to ceramics was proposed by Chantrell and Popper more than twenty five years ago. An excellent review[6] focuses on the synthesis of precursors for SiC and Si_3N_4 ceramics.

1.2 Precursors : a new trend in ceramic synthesis.

A ceramic precursor can be defined as a chemical (usually an inorganic polymer) that can be transformed into a solid ceramic upon either heating or addition of another reagent. Upon transformation most of the organic side groups are eliminated and the residue is composed of the inorganic elements often in an amorphous state. The starting materials used to prepare the precursors can be purified by a variety of distillation techniques, which ensures a precursor of high purity and therefore a very pure ceramic phase after pyrolysis.

Precursors can be used effectively for thin film applications where conventional powder processing is inadequate. They have been considered for the synthesis (by mixing at a molecular level) of materials with complex atomic arrangements such as some multicomponent oxides[7]. Last but not least, precursors have been synthesized to mass produce fiber material (for example the Nicalon™ fibers[8](Si, C, O), and the Tyranno™ fibers[9] (Si, Ti, C, O)). Other interesting materials can be synthesized via the precursor route, for example boron nitride from B-triamino-N-tris (trimethylsilyl) borazine[10]. Since this work focuses on Si- based ceramics, the following section takes a closer look at the existing precursors for SiC and Si_3N_4.

1.3 Development of precursors for SiC and Si_3N_4 ceramics.

Silicon-chained polymers with hydrocarbon side groups have been known for a long time but the chemists who synthesized the early polymers did not consider their pyrolytic properties. It was the search for purer and finer starting materials and for more direct forming techniques that pushed ceramists to be interested in the precursors called polysilanes (for SiC) and polysilazanes (for Si_3N_4). More research on organosilicon chemistry was needed to understand how the precursors could be manipulated (chemically

or thermally) to maximize the amount of ceramic residue after pyrolysis. The early success of Yajima[11] and his team in preparing siliconoxycarbide fibers triggered a flurry of investigations on new precursors synthesis[12 13 14].

It is interesting to note that the carbon fiber technology[15] had been developed almost twenty years earlier. There are obvious parallels between the production of carbon fibers and that of SiC fibers from suitable precursors, most notably the similarity between polymeric chains and the common need to control the cross linking of the molecules while minimizing carbon (or silicon) losses.

The synthesis of new SiC and Si_3N_4 precursors is not limited to the fabrication of fibers. For example, thin films coating (Si_3N_4) have been deposited on various substrates by plasma assisted polymerization[16]. Paint-spraying techniques of polysilazanes solutions are being developed[17 18] to protect carbon/carbon composites from oxidation at elevated temperature.

In this work, precursors are investigated as potentially active binders. This will be developed in section 1.5. It is, however, necessary at this time to learn more about these precursors and the following sections describe briefly the main characteristics of both polysilanes and polysilazanes. As the precursors investigated are all polymers, the words "polymers" and "precursors" will be used interchangeably.

1.4 Background on polysilanes and polysilazanes.

In 1863, the synthesis of alkyl substituted silanes was reported by Friedel and Crafts[19]. This discovery is regarded as the starting point of the field of organosilicon chemistry. It took years of dedicated research[20] before significant progress led to practical applications. In the 1940s the field took off rapidly with the advent of silicone polymers whose properties could be tailored by molecular weight and viscosity control during

synthesis. Polymers based on the four elements silicon, carbon, nitrogen and oxygen, offer a wide variety of properties that chemists are just beginning to explore.

Of all the polymers that can be synthesized from various combinations of these elements only those with specific pyrolytic properties are of interest to the ceramist. The main property of a precursor is called "yield". There are however different definitions of the word. The "theoretical yield" is the calculated amount of solid material (expressed in percentage of a given initial mass of precursor) obtained after pyrolysis, assuming ideal reaction mechanisms, usually involving no loss of silicon. The experimental yield is the amount of solid residue as measured, for instance by thermogravimetry analysis (TGA), after decomposition of the polymer. The pyrolytic product is often composed of a mixture of materials, and one can define the "specific" yield as the amount of, say, SiC, from the pyrolysis of a given amount of precursor. What certainly complicates a comparison between precursors is that yields depend on many experimental parameters such as heating rates, final heating temperature and gas environment. Furthermore, the pyrolysis can be "confined " or "unconfined". Unconfined pyrolysis refers to the conversion of the polymer in bulk form. If particles or fibers or any other solid phase substrate is added to the precursor, the word "confined pyrolysis" is used to indicate that the decomposition reaction can be altered by the presence of a filler material.

The following section discusses separately some specific features relative to polysilanes and polysilazanes.

1.4.1 Polysilanes

Polysilanes are inorganic polymers based on a Si-Si backbone. They can be linear (polydimethylsilanes) or contain rings with a wide range of molecular weights. They are typically prepared by reaction between chlorosilanes (or other halosilanes) and alkylsilanes[21]. In most cases the reaction is conducted in solution (Tetrahydrofuran) with sodium or potassium as catalysts. As polymers, they have interesting optical properties (long UV

absorption), and have found applications in the photoresist technology. Upon thermal decomposition certain polysilanes convert into SiC or SiC +C mixtures. A great deal of work[22] has focused on the different factors influencing the SiC yield of various precursors. . For the precursor to yield a significant amount of ceramic phase, its stoichiometry (C:Si ratio) must be as close as 1:1 as possible (otherwise large amount of carbon phases can be expected). It is, however, not a sufficient condition. To illustrate this, consider the pyrolysis of linear polydimethylsilane[23] . At 800° C the ceramic residue is practically nil. The mechanisms of reversion or retroversion reaction explain the low yield. The linear polymer chain can bend back upon itself and cyclic species can separate from the chain and become volatile. If the polymer chain is long and the side groups not too bulky the reaction can repeat itself until the whole chain is consumed. If nothing prevents the decomposition (i.e. unconfined pyrolysis conditions), the ceramic yield will inevitably be low. The substitution of methyl groups by more bulky groups can inhibit the reversion reaction but it means a considerable increase of the C:Si ratio. This problem can be solved by cross linking or branching of the polymer prior to pyrolysis. Cross linking is the onset of a 3-D network formation and it can be effected by UV radiation, oxidation or curing. The large oxygen concentration found in the early Nicalon™ fibers originate from such a cross linking in air. The presence of oxygen in the precursors can limit the stability of the pyrolyzed phases at high temperature.

To form SiC it is preferable to start from a polycarbosilane, i.e. a precursor with a Si-C backbone[24]. Polycarbosilanes can be prepared from polysilanes under high pressure[25]. Increasing work is being conducted on precursor synthesis to maximize the ceramic yield without introducing oxygen.

Polysilanes are still expensive experimental products. Table 1.1 lists some of the commercially available precursors along with cost and yield.

1.4.2 Polysilazanes

The second important class of inorganic precursors contains polymers with -Si-N- repeating units. The side groups attached to Si and to N can be H, CH_3 or any alkyl chains. They have received less attention than polysilanes maybe because of the relative instability of Si-N bonds in oxygen or water containing atmospheres. Although known for some time, Si-N containing polymers or polysilazanes have only recently been considered as potential precursors to ceramics. They can be synthesized by reaction between chlorosilanes and primary or secondary amines[26]. Products with various degrees of polymerization are obtained by changing reaction time and temperature. Polymerization results from the formation of radicals and from rearrangement reactions that promote Si-N bonds by elimination of volatiles. Polysilazanes have often a branched structure or are made of rings containing three or four Si-N units. Curing or cross linking is also an important step in the conversion process. To maximize the ceramic yield the polymer must have some "latent reactivity". This term describes the ability of the polymer to cross link and to create branches before it can be depolymerized through reversion reactions. Typically, Si-H and N-H bonds provide some latent reactivity.

Most polysilazanes contain more carbon than nitrogen, so it is not surprising to find sometimes mixtures of SiC and Si_3N_4 in the pyrolysis products. The decomposition mechanisms are complex. They involve a competition between Si-C and Si-N bond formation from radicals. In addition, the transformation mechanisms depend strongly on the nature or the pyrolysis gas atmosphere. The presence of a filler material will also influence the composition of the final products; to quote Rice[6] "even in cases where the polymer microstructure appears to be Si-N based, ceramic materials are derived that contain significant and sometimes predominant quantities of SiC derived from pendant carbon

groups". Polysilazanes containing no carbon atoms have been synthesized by Seyferth[27] but are not commercially available. Silicon nitride rich fibers have been obtained by pyrolysis of hydridopolysilazanes but they still contain some carbon[28] . Whether or not a carbon-free Si_3N_4 fiber necessitates a carbon-free precursor is an interesting question. Indeed, Okamura et al[29]. have prepared Si_3N_4 fibers by pyrolysis of a polycarbosilane in NH_3. To address the problem of phase prediction after pyrolysis, much more understanding of the (Si, C, N, O) system is needed. The discussion of phase formation and phase stability is further complicated by the existence, up to elevated temperatures, of metastable amorphous phases.

A list of some commercially available polysilazanes is given in Table 1.2. Most of the high-yield precursors are still experimental products and not available on the market. The particular sensitivity of both polysilanes and polysilazanes to UV radiation and oxidation limits their shelf-life to about 3 months. The slow degradation of the polymer is characterized by the release of NH_3 molecules (for polysilazanes) and the formation of insoluble microgels.

1.5 Polysilanes and polysilazanes as binders.

Although the transformation of inorganic precursors into solid ceramic materials has been successfully applied to the fabrication of fibers, thin films and small objects, the fabrication of large parts by pyrolysis of a precursor faces serious obstacles. The density of a typical precursor is about $1 g/cm^3$, that of the final ceramic is 3, therefore a very large shrinkage is expected upon pyrolysis if the final product is not to contain pores. In most cases, the shrinkage is not uniform and cracks form[30]. To overcome this difficulty, Yajima[31] was the first to consider mixing a precursor with a ceramic powder (a coarse SiC) and pyrolyzing the mixture. He found that consolidation of such a mixture could be effected by a relatively low temperature pyrolysis (1100°C), whereas the conventional sintering temperature for SiC is about 2000°C. Little is known about the microstructure of the

material except that the total porosity was measured at *ca.* 30% and the flexural strength reached 60 MPa. Further processing improvements led to a material with a flexural strength of 250 MPa. This early experiment proved that strong solids made of high temperature resistant material could be fabricated at temperatures at which conventional sintering mechanisms do not operate. Materials similar to those prepared by Yajima are the object of this work. Strictly speaking, the interaction phenomena between the precursor and a ceramic powder upon heating should not be called "sintering" (terminology used by Yajima). In the present work the words "consolidation" and "strengthening" will be used. Similar interaction has been observed on a variety of systems[32 33 34] all involving SiC or Si_3N_4 as filler material and a polysilane or polysilazane as precursor/binder. State-of-the art porous materials obtained by pyrolysis of polysilazanes / SiC systems at 1400°C have flexural strength in excess of 450 MPa[33]. This modulus of rupture is comparable to that of fully dense SiC, but the hardness is lower due to the presence of 20 to 30 % porosity, which makes them readily machinable[32] . Parts with complex geometry can be fabricated by injection molding or extrusion techniques, taking advantage of the thermoplasticity of the precursor[35, 36].

Up to now, these materials have been developed and their properties improved by a systematic optimization of the processing parameters. Yet, little is actually known about the consolidation mechanisms itself, i.e. the reaction at the particle/precursor interface during pyrolysis. An intrinsic role of the filler particles in the mixture can be ruled out since at low processing temperature (<1500°C) the self diffusion coefficients of both C and Si are too small to permit significant mass transport between the filler particles by surface diffusion or evaporation-condensation. The objective of this work is to elucidate the role of the precursor.

In this introduction, I have tried to explain, from a ceramist' viewpoint, how ceramic precursors came about. Yajima's early work was only the starting point of a field of research that has grown enormously since. The materials presented here are not considered for specific applications. They could be used as preforms that could be infiltrated by metals. The surface porosity could be filled via CVI (chemical infiltration technique) to obtain materials with soft

cores and hard skins. As-pyrolyzed materials present an interesting example of high strength ceramics with large residual total porosity. The consolidation mechanism, already significant at moderate temperature, cannot be left unexplored.

CHAPTER 2 RESEARCH OBJECTIVES

2.1 Consolidation phenomena in precursor/powder system upon pyrolysis.

Although the mechanical properties of these pyrolyzed ceramic precursor / ceramic powder materials have been significantly improved since the pioneering work of Yajima, the mechanisms by which the consolidation takes place are still not understood. The study of the influence of important processing parameters has not brought enough insight as to the fundamental phenomena taking place in the sample during the conversion of the precursor. A literature review points to four major references that describe the fabrication of similar materials by pyrolysis of various systems[31,32,33,34]. A system consists of a precursor and powder. There are basically two problems in the approach used so far by previous workers. First, not enough is known about the pyrolytic behavior of the precursor in a simpler environment, that is, without the presence of a filler phase (here the ceramic powder). Secondly, the microstructure observations have not focused on the most important piece of the puzzle, namely the neck region between the filler particles, where the precursor derived phase is most likely to play an important role.

2.2 Goal

It is thus the aim of this work to investigate the role of a precursor in the consolidation effect observed during the pyrolysis of a compacted precursor ceramic powder mixture. The emphasis will be on understanding and quantifying the mechanisms by which the particle to particle contact are strengthened.

2.3 General approach

The materials described in this work are not commercially available. Consequently, it was decided that the samples on which characterization is performed should be prepared in-house. Thus, it is possible to monitor the evolution of the microstructure of the samples at various stages during processing.

There are two basic approaches that can be considered in order to study the interaction precursor/particle upon heating. One may want to simplify the geometry by investigating a macro-model of the contact (figure 2.1a). Basically, a thin layer of precursor could be sandwiched between two SiC discs. This sandwich could then be heated slowly in a furnace and the microstructure of the interface characterized by various imaging and analytical techniques. The second approach is to study the problem on a real system (fig. 2.1b), that is to say, add the precursor to a fine ceramic powder, pyrolyze the compacted mixture and characterize the microstructure at different stages during processing.

The second approach was selected after some consideration about the role of the powder network on the consolidation phenomena. As the precursor is pyrolyzed, gases evolve from the sample. In the model contact, the geometry is such that the gases have to escape at the periphery of the sandwich whereas in real samples the volatile species could permeate or diffuse through the pore channels between the packed particles. The powder network determines the location of the precursor. Ideally, it sits in the interstices between the particles. This means that no pocket of precursor exists larger than the volume of a particle, whereas, in the model contact, the precursor exists as one continuous thin film. One can anticipate that the total interfacial contact area between the precursor and the ceramic particles is an important factor in the consolidation during pyrolysis. In the

"sandwich" model, the interfacial area is orders of magnitude smaller than in the real sample. For this reason, the second approach is preferred.

After selection of a particular precursor, the pyrolytic behavior is investigated in the absence of a filler phase. The motivation behind this preliminary study is to collect valuable information about the phases, the microstructure evolution, the crystallization temperature and the precursor to ceramic transformation mechanisms in unconfined pyrolysis conditions.

One chapter will be dedicated to sample preparation and to some important physical properties such as density and shrinkage. The microstructure of the pyrolyzed samples will be characterized by electron microscopy techniques with an emphasis on locating the pyrolyzed form of the precursor in the sample. Finally, some preliminary mechanical property evaluations will be discussed.

2.4. Limitation of scope

In this investigation one must define a system, that is select a precursor and a ceramic powder. Because consolidation has been evidenced on all possible combinations, namely polysilane or polysilazane and either SiC or Si_3N_4 as filler material, the selection will be dictated by the following consideration. As can be expected, one of the most difficult tasks will be to monitor the evolution of the precursor phase as it is pyrolyzed into a ceramic solid, similar in composition to the filler. Therefore, if SiC is used as the ceramic powder, then a polysilazane can be considered as precursor, since it will be transformed into some nitrogen containing phase, possibly Si_3N_4, which could be distinguished easily from the filler material. This choice gives *a priori* a good chance to conduct successfully an analytical investigation of the sample to understand the role of the precursor in the early

consolidation. The problem of the location of the polymer derived phase became apparent in most of the previous investigations.

CHAPTER 3 UNCONFINED PYROLYSIS

3.1 Introduction

Before investigating the pyrolytic behavior of the polymeric precursor in the presence of a filler material it is important to study its decomposition in simpler environmental conditions. In this chapter, a selected polysilazane will be pyrolyzed in bulk form at different temperature and under various gas atmospheres. These conditions are referred to as *unconfined* pyrolysis. The present chapter describes the conversion of a precursor in terms of weight loss, microstructure evolution, nature of pyrolyzed phases and crystallization mechanisms. The literature provides some useful information about the pyrolysis of polysilazanes[37] but its is clear that despite general common features the transformation precursor to ceramic will depend on the specific molecular structure of the initial precursor, for given pyrolysis conditions.

3.2 Experiment

The precursor was purchased from Huls-Petrarch chemicals[0] . The chemical structure of this polysilazane copolymer is represented on fig 3.1. It is a viscous liquid at room temperature and must be kept away, as much as possible, from long exposure to air and to UV light. Its unconfined pyrolysis yield is 50-55% of solid ceramic residue. Its main pyrolytic product is Si_3N_4 .

---

[0] Huls America, Inc., (formerly Petrarch Systems) Piscataway. NJ

The pyrolyses were conducted in two types of furnaces. One was a graphite element furnace where temperatures below 1200°C were controlled by a Tungsten-Rhenium thermocouple. Above 1200°C the temperature was monitored by pyrometry. Typically, 0.5 g of precursor was poured into an Al_2O_3 boat, then the sample was inserted in the furnace. The chamber was vacuumed to 10^{-5} Hg mm before the pyrolysis to flush out any oxygen. Nitrogen was run at atmospheric pressure over the sample. The heating rate, although not critical in this experiment, was set at 10°C/min and the final temperature of the one-hour heat treatment ranged from 500 to 1700°C. This range covers the expected crystallization temperature which, for other polysilazanes, has been measured between 1400 and 1500°C. One experiment was conducted in vacuum in a tungsten element furnace. However, to prevent damage to the elements the first phase of the pyrolysis must be conducted in a quartz tube furnace up to 800°C. Indeed, during precursor decomposition, Si-based vapors escape from the polymer (usually low molecular weight species). These vapors can redeposit on the hot W elements creating WSi_2. Mazdiyasni[38] reports the failure of a Pt-Pt / 10%Rh thermocouple tip during pyrolysis of a Si_3N_4 precursor at 1500-1600°C. The failure was traced to the formation of a low melting $PtSi_x$ phase.

The microstructure of the pyrolyzed pieces collected from these experiments were characterized by scanning electron microscopy. Gold coating was necessary for all samples as charging occurred on non-coated specimens. Phases were analyzed by X-ray diffraction (Cu K-α radiation, λ= 0.154 nm). The spectra were compared to those of standards provided by the JCPDS library.

3.3 Results

3.3.1 Observation during pyrolysis.

From the weight loss vs. T (fig 3.2) it can be seen that the major structural transformation of the precursor ends at about 600°C. The transformation that takes place is a complex set of elimination and cross linking reactions. The weight loss (45 %) corresponds to the loss of volatile species containing Si and small gas molecules. The nature and amount of these volatiles could not be analyzed with our laboratory equipment but the typical fragments of the decomposition of a polysilazane are summarized in table 3.1. One of the main difficulties in collecting information about volatile compounds is due to the wide range of their molecular weights. Initially, between 100 and 200°C, low molecular weight silazanes separate from the precursor. Between 200 and 500°C, higher molecular weight fragments become volatile. Above 500°C, mostly small gas molecules are detected as organic fragments are being eliminated from the pyrolyzed phase. At 600-700°C no more weight loss occurs and the main transformation to an inorganic solid has ended. During the pyrolysis experiments conducted in quartz tubes, viscous deposits of polymeric materials were found on the cooler parts of the tube. Similar observations were reported by Schilling[22]. It is believed that this redeposition is due to the recondensation of some Si-rich volatiles.

3.3.2 Microstructure

3.3.2.1 Pyrolysis in Nitrogen

The morphology of the precursor pyrolyzed at 1000°C is shown on fig. 3.3. The outer and fracture surfaces show no sign of discrete features, indicative of a glassy structure. Most of the larger pieces have curled or wrapped under shrinkage stresses. One can see that if the formation of large objects would be difficult by direct polymer pyrolysis.

No sign of crystallinity is apparent by SEM. At 1400°C, the product develops a spongy microstructure (fig. 3.4). A surface layer is reminiscent of the amorphous state before crystallization. The particle size is less than 50 nm and very uniform. The nano-particles appear to be sintered together along short chains.

At 1500°C and above, nucleation and growth occurs from the amorphous phase (fig. 3.5 a) and the existing crystallites coarsen (fig. 3.5b). At higher temperature (1700°C), the morphology of some particles (long faceted grains) reveals a second mechanism of crystal growth. It is believed that a vapor-liquid-solid transformation mechanism can explain the formation of these whiskers[39](fig. 3.6 a). The presence of a sphere at the tip of the whiskers points to the presence (at high temperature) of a liquid phase, in which Si-rich vapors have dissolved. The supersaturation in Si and C (or N) in the liquid sphere leads to the precipitation or growth of perfect SiC or Si_3N_4 crystals along a preferred orientation (total surface energy). The spheres are believed to contain impurities (such as iron), which makes the growth of whiskers possible from a melted droplet at about 1500°C. On the same sample, facetted crystallites reach a size of about 1 micron (fig. 3.6 b).

3.3.2.2 Vacuum pyrolysis.

At 1400°C in vacuum, whiskers were observed that grew from the surface of the pyrolyzed precursor (fig 3.7 a). These whiskers are not single crystal, they are a collection of crystals stacked along a common direction. Their growth mechanism is unknown. As the pyrolysis was conducted in vacuum (10^{-5} -10^{-6} mmHg) it is not likely that these whiskers are made of SiO_2. Similar whisker observations have been reported[40]. Figure 3.7 b shows the surface microsturcture made of small (<500 nm) facetted crystals.

The microstructure at 1500°C is shown in fig. 3.8 a and b. The bulk is made of spherical particles, about 60 nm in diameter. The surface morphology reveals an advanced stage of coarsening of the finer microstructure. Neck formation is evident. For positive pressure pyrolysis, the surface microstructure indicates a lesser degree of coarsening than

that of bulk phase. Here, the reverse is true. The microstructure difference can be explained by a thermal gradient between surface and bulk or by a surface segregation affecting the coarsening mechanisms. On some of the particles facetting is observed which indicates that every particle is a single crystal with facets that minimize its total surface energy. For SiC faceting occurs mostly on (111) and (110) planes.

3.3.2 Phase analysis

3.3.2.1 Nitrogen pyrolysis

X-ray diffraction spectra of precursor pyrolyzed at up to 1200°C do not indicate the formation of any crystalline phases. Therefore, up to 1200°C the PDP (precursor derived phase) can be considered amorphous. At 1400°C a transformation may have taken place as indicated by the broad peaks centered around 0.25 nm (fig. 3.9). At 1500°C, α-Si_3N_4 and β-SiC are clearly identifiable. The peaks are sharper, which indicates growth of the crystallites. Upon further heating at 1600 and 1700°C, the silicon nitride to silicon carbide ratio increases with temperature. At these temperature, the new crystallized phases may not be formed from the amorphous phase but rather by converting SiC into Si_3N_4. The relative stability of Si_3N_4 vs. SiC has been the object of several investigations[41,42]. In the conditions of the experiment, there are two opposing factors. In a graphite furnace the activity of carbon is close to 1. The reaction is conducted under a nitrogen flow, so pN_2 is 0.1 MPa. The reaction to consider is,

$$Si_3N_4 + 3C \rightleftharpoons 3\ SiC + 2\ N_2$$

Above 1460°C, at pN_2=1atm, the two phases can coexist as seen on fig. 3.10.
Below 1460°C, if SiC forms, it should transformed into Si_3N_4 but it is well known that this reaction is kinetically limited and not actually dominant. If Si_3N_4 forms, thermodynamically it will be stable, in the presence of C up to 1460°C. Carbon can either originate from the heating elements made of graphite or from excess carbon in the

precursor. Above the equilibrium temperature, Si_3N_4 can consume all the excess carbon and transform into SiC. No carbon in graphitic form was detected by X-ray diffraction. It is therefore difficult using thermodynamic arguments to predict the nature of the phases after pyrolysis. The following section illustrates this complexity by considering pyrolyses in vacuum.

3.3.2.2. Vacuum pyrolysis

The X-ray diffraction pattern of PS 116 pyrolyzed at 1500°C in vacuum is shown in fig. 3.11. The material is composed of a mixture of β-SiC and recrystallized Si. These phases are actually predicted to be the stable phases at this temperature under high vacuum conditions[43]. Upon heating between 1200 and 1500°C, additional gases were released as indicated by the pressure gauge fluctuations. These gases are most likely H_2, NH_3 and CH_4.

The phase analysis indicates that the conversion to a ceramic material in vacuum depends strongly on the gas atmosphere. The elimination of nitrogen from the amorphous solid phase can be explained by facile Si-N bond scission, leaving the more stable Si-C bond. Referring to fig.3.10, Si_3N_4 decomposes above 1000°C in high vacuum, whereas SiC is still stable. In nitrogen atmosphere, the difference in stability is less pronounced, explaining why both Si_3N_4 and SiC were detected.

3.4 Discussion

The conversion of a precursor into a ceramic phase can be divided into two stages. At about 500 to 700°C, an amorphous phase containing Si, C, N (and O) is formed. An unknown quantity of hydrogen is present in the amorphous material in bonds such as N-H,

Si-H[37]. This amorphous state is maintained up to about 1400°C, temperature at which crystallization starts. Initially, an extremely fine grained and uniform microstructure is obtained. Nucleation and growth has been evidenced as the major transformation mechanism especially for the bulk structure. Other features, such as whisker-like crystals, clearly indicate that another mechanism can be active, particularly at higher temperature. From our results, it is difficult to conclude that the crystallization started at a well determined temperature. Most of the nucleation takes place between 1200 and 1400°C. A definite grain structure becomes visible between 1400-1500°C. Upon crystallization a small exothermic peak is detected by differential scanning calorimetry[44]. This is surprisingly very different from the crystallization of amorphous Si_3N_4 particles[45], for which a very large heat of transformation was recorded. The main difference between the two systems is that, for the latter, the nucleation of the new crystalline phase occurred on a very narrow temperature range[46]. Our observations indicate that for more complex precursors (containing C and N atoms), the transformation is not as sharp.

The microstructure observations indicate that upon transformation very high specific surface structures are formed. The porosity is clearly large and open. The size of the pores increases as the particles grow and grain boundaries are eliminated by coarsening. The particles growth is possible via surface diffusion and vapor phase transport. At 1400-1500°C volume diffusion does not play a major role for SiC. The vapor-liquid-solid mechanisms occurring at higher temperature must be initiated on randomly distributed liquid phases. The liquid droplets are usually found to be Fe-rich[39]. Another possible mechanism for whisker growth is by vapor phase deposition at an emerging screw-dislocation. For such mechanisms to occur, the whisker must have some available free-space to grow, hence in a confined environment whisker formation will be limited, or the size of the whiskers will be determined by the size of the pore they grow in. Our observations indicate that whisker growth is primarily a free-surface phenomenon.

Even under well-controlled pyrolysis conditions, it is possible to observe different types of microstructure in the same sample. The micrographs selected for each temperature represent the most common microstructure found in a given sample. The co-existence of various microstructures is certainly due to gradients in chemical composition or the influence of impurities (furnace-borne). The literature indicates also quite large variations in microstructure or phase obtained after pyrolysis[27,37,47]. Phase separation is even possible in the polymeric state, if the precursor is composed of chains with a wide range of molecular weights[48].

For the reasons presented above it is not possible, at this time, to predict precisely the pyrolytic behavior of the polysilazane in a SiC powder environment. Clearly. the presence of SiC particles should promote the formation of a SiC-like phase. If the sample is pyrolyzed in nitrogen, Si_3N_4 and SiC may be found to coexist. The crystallization temperature in the presence of a seed material is expected to be lower, but other factors can come into play. If the silica-rich surface layer modifies the composition of the amorphous phase, the precursor could remain in an amorphous state up to higher temperature.

CHAPTER FOUR PROCESSING OF SiC/POLYSILAZANES

4.1 Introduction

As mentioned earlier, materials described in this research are not available commercially. An increasing effort is aiming at improving their mechanical properties and their reliability through a series of process developments[49]. This type of research requires large amounts of precursor and therefore is costly. A more scientific route is chosen here to evidence at least on some small scale the strong interaction between the precursor and a ceramic powder upon heat treatment. The present chapter deals mainly with some aspects of the fabrication of experimental specimens.

There is, actually, no set methodology for preparing a sample and the procedure described here will make use of information collected in the literature and other conventional techniques. The objective of this chapter is to explain the choices of some processing parameters.

The sample preparation is separated into three phases. In phase 1, the precursor/powder mixture is prepared with the obvious goal to obtain a uniform distribution of precursor. Phase 2 describes the forming technique and its influence of sample volumetric composition. At the end of this phase, the sample will referred to as "green body". The controlled pyrolysis is discussed in Phase 3, This is followed by a heat treatment up to 1500°C . Density changes, composition evolution and porosity can be monitored at each processing step.

4.2 Background

The original work of Yajima describes a conventional method for sample preparation using hexane as a solvent. The precursors are only soluble in non-polar solvents like toluene or tetrahydrofuran. The presence of water can cause the polymer to precipitate or phase separate. Actually, the latter property can be used to elaborate a new mixing technique called micro encapsulation which will discussed more in detail later. So, in general, the presence of water is detrimental to the processing of samples, and all container must be thoroughly cleaned and dried before use. There are not enough details in Yajima's original paper to find out where the strength-limiting flaws are introduced. He adopted a simple room temperature compression molding technique that seemed to give a homogeneous green body. Similar forming techniques were used in other references[32,33]. Depending on the effect of temperature on the viscosity of the precursor, a compression at moderate temperature may enhance the compatibility of the mixture[34]. More complicated techniques such as injection molding and extrusion can be used to produce more complex shapes. These processes require the formulation of complex binder systems. Techniques based on slip casting or centrifuge casting may introduce the problem of phase separation. The SiC filler is about three times as dense as is the precursor and, upon settling, the top layers of the sample would be polymer rich whereas the bottom layers would be depleted in precursor. This variation in precursor distribution would lead one side of the sample to bloat or crack while the other side would not consolidate. If this separation can be prevented, the fabrication of samples via consolidation of sterically stabilized dispersions should be revisited.

Plastic forming techniques have been the logical choice of many investigations for the simple reason that the precursor is a thermoplastic polymer. The amount of precursor

is an important parameter to choose before the mixture can be prepared. It will determine to some extent the rheological behavior of the blend.

4.3 Selection of precursor loading

Based on a simple model first developed by Schwartz[50], the selection of an optimum volume fraction of precursor can be rationalized. The strategy is to maximize the density of the green body by proper selection of the polymer loading (V_p). All the volumes, except as indicated otherwise, listed in the equations refer to volume fractions.

Let ρ_s be the density of the powder compact in the absence of precursor, and let ρ_p be the density of the precursor. If one assumes that the precursor can be added without modifying the volume fraction of powder filler material, then the density of the green sample, ρ, is,

$$\rho = \rho_s + V_p.\rho_p \text{ (Eq.1)}$$

in this case , the volume fraction of filler is constant. Equation(1) is represented by a straight line of slope ρ_p. Two parallel lines (a) and (b) are drawn on fig.4.1, corresponding to two powders with different compaction behaviors. A third line (c) is drawn representing the density, ρ_m, of an imaginary pellet containing a volume fraction V_p of precursor and $1-V_p$ volume fraction of SiC, assuming that they can vary from 0 to 1. If ρ_{SiC} designates the density of filler material, then the density of such a pellet is represented by the following equation,

$$\rho_m = V_p.\ \rho_p + (1-V_p).\rho_{SiC} \text{ (eq.2)}$$

The intersection between the curve (a) and (c) determines the optimum amount of precursor. It maximizes the density of the green body. To the right of this point, the addition of an excess precursor at the expense of SiC particles results in a decrease of density. Whereas to the left of the optimum, the sample still contains porosity that, ideally,

can be filled up with precursor without displacing the SiC filler. So, according to this simple model, the optimum amount of precursor, V^*_p, should be,

$$V^*_p = 1 - \rho_s / \rho_{SiC} \quad \text{(eq.3)}$$

Numerically, this corresponds to 16.5 and 24.5 wt% of precursor for the two powders represented by the two curves (a) and (b). Whether or not this optimum value of density can be reached by eliminating all porosity will be discussed later.

4.4 Sample preparation

4.4.1 Precursor/powder mixture preparation

4.4.1.1 Conventional method

Once the composition of the mixture has been selected, the precursor is dissolved in an organic medium such as toluene or tetrahydrofuran (fig. 4.2). A second dispersion is prepared by adding the selected amount of SiC powder (β-SiC[&]) to the same organic solvent. A dispersant (Oloa™ 1200[%]) is also added to improve the quality of the SiC dispersion. The two solutions are carefully homogenized separately by ultrasound agitation, then mixed together and further homogenized using a magnetic stirrer or an ultrasonic bath. Before drying the mixture a high speed shear mixer[+] is used at around 8000 rpm for about 5 minutes. After a homogeneous dispersion is obtained the solvent is removed in a rotoevaporator[$] under vacuum. A heated oil bath maintains the temperature

---

[&] B-SiC 21, Ferro Corp., Cleveland, OH.

[%] Chevron Chemicals, Oronite Additives Div., San Francisco, CA

[+] Model L-04719-10, Cole Parmer Inst. Company, Chicago, Il.

[$] Model RE-46, Yamato Scientific Co., LTD., Japan

of the dispersion at 70° C. The dry mixture is formed of loosely agglomerated cakes that can be crushed in a mortar and pestle and ball-milled to a fine flowable powder. Spray-drying of the dispersion results in clogging of the spray nozzle. This method of solvent removal is not recommended. Once the powder is ball-milled and sieved it can be stored for further use. Figure 4.3 presents the powder / polysilazane mixture before milling.

4.4.1.2 Alternate method : Microencapsulation

An alternate method for preparing the blend was explored to tackle the problem of homogeneous distribution of polymer phase in the mixture. If one assumes that the presence of the precursor is indispensable for significant local strengthening to occur then its homogeneous distribution must be regarded as important.

The procedure presented below is termed "coacervation" or the more modern word "micro encapsulation". As early as 1945, Kruytt[51] described the phenomenon of coacervation as follows:" If one starts from a sol, that is, the solution of the colloid in an appropriate solvent, then according to the nature of the colloid, various changes (temperature, addition of a substance) can bring about a reduction of the solubility as a result of which a larger part of the colloid separates out in a new phase". The novelty of our application is to control the formation of polymer-rich precipitates and to form a coating layer on each individual SiC particles. The step-by-step procedure is detailed in fig.4.4.

This technique is based on the incompatibility of the precursor with a polar solvent. First, a dispersion of SiC + polymer is prepared in toluene. Constant agitation of the solution is necessary. The most effective agitation was provided by an ultrasonic horn. To induce phase separation, ethanol, the non-solvent, was added drop by drop. Initially, some precipitation can take place but the coacervates are redissolved in the mostly non-polar medium. At the critical point (defined as the volume of ethanol to be added, per volume of toluene initially in solution, necessary to prevent re-dissolution of polymer-rich

coacervates), the mixing action is stopped. For our choice of solvent and non-solvent, the critical point is reached for about a 1 to 1 ratio of the two liquids. Toluene and ethanol are partially miscible but the high energy mixing forces complete miscibility. In the absence of SiC particles, spherical shaped polymer-rich coacervates are formed. The size of the sphere depends on the intensity of the mixing action. Under high shear stress provided by the ultrasound probe, the coacervation occurs preferentially around the dispersed SiC particles (fig. 4.5). This preferential coacervation has been demonstrated not only for a polysilazane but also for a polysilane precursor. The micro encapsulated SiC particles formed under high energy mixing are stable even when the ultrasonic horn is turned off. It is possible that the coacervates contain more than one SiC particle and the long term stability of SiC/polymer entities is questionable. The system can obviously reduce the high energy precursor/(polar)medium interface by coalescing with similar systems. The coacervated system may be reversibly de-coacervated by adding the first solvent, namely toluene.

This technique is an exploratory procedure, not a well understood process. Additional experimentation would be needed to benefit fully from the apparent improved homogeneity in precursor distribution. In particular, it is not known what effect the addition of a polar (O-H) medium has on the molecular structure of the precursor. Also, once the precursor is coacervated, one must find a way to prevent massive flocculation or design a procedure that can take advantage of this flocculation.

4.4.2 Compaction

Samples (1 1/4 x 1/2 x 1/4 inch^3) were uniaxially pressed at 5 to 10 ksi (35 to 70 MPa) in a double-action tungsten carbide die at room temperature. The samples were weighed and measured to calculate their density. All specimens were then isostatically pressed at 100 ksi (700 MPa) at room temperature in rubber bags. The goal was to reduce

porosity and correct the density variations caused by unaxial pressing. After isostatic pressing, the volumetric compositions of the samples were determined.

4.4.3 Debinding and Post heat treatment.

4.4.3.1 Debinding

This phase deals with the conversion of the polymer into a ceramic upon heating. In order to choose a safe heating schedule, one can find out the temperature range over which the weight loss of the precursor alone is maximum and estimate the rate of pyrolysis gas evolution corresponding to this temperature. Practically, a slow heating rate is used throughout the conversion process, typically 0.5 to 1°C/min. Fig 4.6 represents the heating cycle used under nitrogen flow in a quartz tube furnace up to about 1000°C . The samples were held at 1000°C for about one hour. The furnace power was then turned off and the specimens ballistically cooled under nitrogen flow. Post-pyrolysis densities, total weight losses and shrinkage data were measured. The density was determined by weight and linear measurement as well as by Archimedes' method. To apply the latter procedure it was necessary to coat the sample with a thin layer of vacuum grease that did not dissolve in glycerol (the displaced medium). The yield of the precursor in confined pyrolysis was calculated by,

$$Y = 1 - (\Delta m/m) / M_p \quad \text{(Eq. 4)}$$

where $\Delta m/m$ is the weight loss of the sample upon pyrolysis and M_p is the initial mass fraction or polymer loading. This equation assumes that no weight loss occurs for a powder compact without precursor, which is a very good approximation for SiC in nitrogen up to 1500°C.

To compare the pyrolytic behavior of the polysilazane in both confined and unconfined pyrolysis the weight loss vs. temperature was recorded (Cahn@ micro balance

---

@ Microbalance Model 1000, Cahn Instruments Inc., Cerritos, CA.

model) on a 20 wt% precursor/80 wt% SiC sample heated under a low pressure of nitrogen up to 800°C. Although it had been reported[37] that no difference was detected between the two behaviors, others[52] had consistently found higher ceramic yield when a filler is added. Actually, the data reported by Blum did not refer to a compacted mixture but to the dry uncompacted mixture which would explain why he found almost superimposing weight loss curves.

4.4.3.2 Post heat treatments.

The maximum operating temperature of the tube furnace was 1200°C, therefore it was not possible to heat treat the sample in the same set-up. A high temperature graphite element furnace[#] was used to complete the heat treatment to 1500°C. This temperature was arbitrarily chosen, keeping in mind that the precursor derived phase could crystallize between 1400 and 1500°C. All the heat treatments were conducted in nitrogen. Because the precursor had already been transformed into a solid phase during the debinding phase, higher heating rates, typically, 5 to 10°C/min could be chosen. The samples were maintained at the highest temperature for one hour and cooled in the furnace under nitrogen flow.

The microstructure of the collected specimens can be characterized fully as will be explained in chapter 5. In the present chapter results concerning the early evolution of microstructure are presented along with physical properties, such as densities and shrinkage, and volumetric composition change.

[#] Astro HTG-7010G, Thermal technologies, Concord, NH.

4.5 Results and discussion

4.5.1 Volumetric composition before pyrolysis : Optimization of initial precursor loading

The experimental results are summarized in fig 4.7. The two sets of points correspond to our data and to Schwartz's results[53] (his data points had to be corrected so as to account for his choice of filler material). For low polymer loading the measured densities, ρ', of samples lie close to the lines predicting the densities on the basis of available porosity being filled up with precursor, without affecting the compaction behavior of the filler material. However, the data indicate that as the volume fraction of polymer reaches its optimal value (as defined earlier), it becomes difficult to decrease the residual total porosity. The residual porosity, p, can be read directly from the graph or calculated from,

$$p = 1 - \rho'/\rho_m \quad \text{Eq.(5)}$$

There is an actual decrease of the volume fraction of filler material in the sample containing initially more than 30 % vol. of precursor. The porosity decreases, however, to 5% for the 20wt% sample. The data also evidence the importance of the compactability of the filler powder on the density of the green body. For a powder compacting poorly a larger amount of precursor can be added to reach maximum green density. The volumetric composition as a function of polymer loading is shown on fig 4.8. For each composition, the results represent an average over at least six samples.

The question to be addressed here is the following: what causes the deviation from ideal packing behavior i.e. deviation from the simple replacement of pores by precursor as the volume fraction of polymer increases?

The formation of a rigid network of filler particles determines the limit of compactability of the sample. Hence, the load (at maximum isostatic pressure) is supported by a skeleton of touching spheres or touching agglomerates. Thus, the presence

of strong agglomerates, especially for higher volume fraction of precursor, could explain why the maximum green density is not reached. Such strong agglomerates have been observed in the sieved powder before compaction. The deviation from ideal behavior makes it possible to add more precursor phase than the predicted limit. Indeed, amounts of up to 30 % by weight (57 vol%) have been used[34] without the expected problems of cracking. Schwartz[44] predicted that if the ideal limit is surpassed then the sample could be described as a particulate-reinforced plastic, where the SiC filler would not form a continuous rigid network but be dispersed in a polymeric matrix. In this case, the sample would collapse or crumble upon pyrolysis. The difference between some experimental results and the prediction of simple models may be explained by the limited flowability of the precursor during compaction. In the model, it is assumed that the polymer acts like a low viscosity fluid not capable of sustaining an applied load, which causes its perfect redistribution into the open space between the ceramic particles. External factors such as the addition of other organic lubricants, as well as compression molding at temperature for which the viscosity of the precursor is reduced. may contribute to narrow the gap between predictions and experimental results.

It has been assumed that the best strategy in choosing the polymer loading was to maximize the density of the green body. One should ask, however, whether this strategy comes in direct conflict with the objective of obtaining a damage-free pyrolysis of the sample. The addition of anthracene[35](a sublimable material) has been suggested to minimize bloating, by creating some open porosity to allow the pyrolysis gases to escape the sample.

There are many other factors that can influence the strength of pyrolyzed samples. The preceding analysis showed little gain in density between samples containing 5 to 20 wt% of precursor. It seems therefore that there might not be a strong correlation between initial precursor content and mechanical properties[34].

It is concluded that initial precursor contents varying between 10 and 20 wt% can produced the expected strengthening effect. But, clearly, the local consolidation of the sample will rely more on a homogeneous distribution of precursor than the addition of an optimum amount.

4.5.2 Weight loss vs. temperature: Yield and shrinkage.

The ceramic yield (defined as weight of ceramic residue per unit weight of precursor) of the polysilazane in unconfined pyrolysis conditions ranges from 50 to 55 % . However, the yield of the same precursor under confined pyrolysis has been found consistently higher, up to 70 %. This was verified for various precursor loadings (between 5 and 20 wt%) and various shapes of samples. For a given pyrolysis and a given sample shape the weight losses are very reproducible from one sample to another; typically, the difference is less than 1 %. This result shows that, at least macroscopically, the precursor content is uniform in the different samples.

Fig. 4.9 presents the comparison between two weight loss curves vs. temperature. The dotted line refers to the precursor in confined pyrolysis. In addition to.the difference in amount of ceramic residue found between the two experiments one can notice that some of the finer details of the precursor weight loss curve are lost in the presence of a filler. This could mean that the SiC powder has altered the decomposition process of the precursor[52] (adsorption of decomposing species on the SiC particles surfaces). The shift of the curve to the right (decomposition of the precursor at higher temperature) could indicate a diffusion or permeation limited process of the volatile species through the network of the pores as the pyrolysis proceeds. In the present case, pores are small (<50 nm) and the decomposing species have, at least at the beginning, molecular masses ranging from 100 to 200 so that collisions between the molecules may control the debinding process[54].

The linear shrinkage of the samples was measured after pyrolysis. Shrinkage increases from 0.5 to 3 % for increasing precursor content (5 to 20 wt %). This indicates, especially for highly loaded samples, that a certain fraction of precursor is actually present at the contact point between the filler particles. Clearly, only some small rearrangement of the rigid network occurs upon pyrolysis. Such rearrangement is observed for samples not containing precursor. This observation is an early indication that the filler particles, here SiC, do not densify, as expected at 1500°C. So, consolidation does not take place by strengthening of the neck via volume or grain boundary diffusion.

4.5.3 Volumetric composition of sample after pyrolysis.

Upon conversion to a solid phase the precursor undergoes a very large density change, from 1 to 2-3 g/cm^3 .The true density of the pyrolyzed phase has been measured by Helium pycnometry[34] (2.65 g/cm^3 at 1400°C). It increases with temperature until it reaches that of a crystalline state. Before crystallization the pyrolyzed phases are best described as amorphous silicon-(oxy)-carbonitrides[55]. The second important feature of the amorphous phases is the presence of nanosize porosity[56].

Let us estimate the volume fraction V_g of pyrolyzed phase assuming that it is a phase of density ρ_g . Let V' be the volume fraction of filler material after pyrolysis and ρ' the density of the pyrolyzed sample. then

$$\rho' = \rho_{SiC}.V' + \rho_g.V_g \quad \text{(Eq. 6)}$$

V' can be derived from the selected volume fraction of precursor in the green body, V^*_{SiC} , the porosity, p_O, of the sample in the green state and the volume shrinkage, S (S is defined by $S=(V_{final}-V_{initial})/V_{initial}$ and is a negative number).

$$V' = (1/1+S).(1-p_O).V^*_{SiC}$$

Vf^*_{SiC} can be calculated from the initial mass fraction of filler material, Mf^*_{SiC} ,

$$V_g = \frac{1}{\rho_g} \cdot (\rho' - \frac{\rho_{SiC}}{1+S} \cdot (1 - p_o) \cdot \frac{1}{1 + \frac{\rho_p}{\rho_{SiC}} \cdot \frac{1 - M^*_{SiC}}{M^*_{SiC}}}) \quad \text{Eq.7}$$

Numerically, for ρ_p=1, ρ_{SiC} =3.2 M^*_{SiC}= 80%, p_o= 7% and ρ'= 2.1. Assuming a volume shrinkage of 10 % and ρ_g=2.6 one can estimate the volume fraction of the precursor phase after pyrolysis at 10%.

Another way to calculate V_g from the ceramic yield Y is given by

$$V_g = Y \rho_p V_p / \rho_g \quad \text{Eq.(8)}$$

with Y= 60 % and V_p= 42%, we find V_g= 9 vol%

In equation (7) the influence of Y is hidden in the value of ρ' which is measured by Archimedes' method.

Even if there were no residual porosity in the green body, because of the loss of precursor (represented by the quantity Y) and the change of density, it is impossible to have a continuous (fully dense) phase between the SiC filler particles. Therefore pore volume must be created in the interparticle volume and the precursor derived phase may contain many very small pores. This was speculated on by Niihara[32] but no microstructural evidence was given. Equation (8) shows also that V_g is proportional to V_p. For reasons that will become clear in the next chapter (microstructure) it seems rational to choose a large precursor loading. In view of the density results after pyrolysis (fig. 4.10) one could choose 15 wt % but the differences are small. The microstructures described in chapter 5 will refer to a sample containing initially 20 %wt. of precursor.(43.5 %vol.).

4.6 Conclusion

This section has described the preparation of a typical sample. The choice of precursor content was justified by considering the expected and measured volumetric compositions of samples made with various amounts of polysilazane.

The slow pyrolysis in nitrogen did not lead to any cracking or bloating of the sample, even for sample containing large volume fractions of precursor. The measured ceramic yield was always found to be higher than the expected value obtained in unconfined pyrolysis. This observation suggests that redistribution of the polymer via vapor phase transport is possible during the pyrolysis. The precursor could also redistribute itself through the particle network, driven by capillary forces, the way liquids do during drying or during liquid phase sintering[56]. This would depend mainly on the viscosity of the precursor at temperature is increased.

The low shrinkage observed during heat treatment rules out a significant densification of the sample. Hence, consolidation occurs without major densification.

CHAPTER FIVE MICROSTRUCTURE AND PHASE ANALYSIS

5.1 Introduction

In chapter three, relevant data were collected on the pyrolytic behavior of the precursor in unconfined pyrolysis. In the present chapter, we focus on samples prepared as described in chapter four. Unless mentioned otherwise the samples contained initially 20 wt % of polysilazane and 80 wt.% SiC, and were pyrolyzed at 1500° C in nitrogen.

Microstructural observations are aiming at tracking down the evolution of the precursor as it is pyrolyzed into a ceramic phase. It would be easier for microstructure evaluation to prepare a sample with large SiC particles, then, the identification of the precursor phase would be immediate[31]. However, it has been shown that using finer filler materials leads to stronger materials[23]. So it was decided to conduct all observations on samples filled with a 0.2-0.3 μm SiC powder.

5.2 Experiments

Very few techniques offer high resolution imaging and analytical capabilities. The most adequate techniques are scanning electron microscopy and transmission electron microscopy with X-ray and energy loss spectrometers.

Samples were cut using a diamond saw, polished with SiC paper down 1200 grit size. The final polishing was performed using successively 6 and 1 micron diamond pastes. Some fracture surface were also examined. All (SEM) samples required gold coating for high magnification observations. In this case, X-ray analysis was not possible since gold absorbs strongly all the low energy X-ray of interest (O at 532 eV, N at 400 eV and C at

285 eV). Carbon coating was not a solution since carbon is one of the elements to be analyzed in the samples. For these reasons, it was not possible or difficult in SEM (scanning electron microscopy) to collect, during the same session, both information relative to the microstructure and information concerning the elemental composition and distribution of phases. It should be noted that in SEM/EDS (energy dispersive spectroscopy) or WDX (wavelength dispersive spectroscopy), the zone being analyzed is not determined by the size of the beam hitting the sample but by the penetration depth of the primary electron in the sample and the mean free path of the X-rays produced in this region.

Macroscopically, crystalline phases were analyzed by X-ray diffraction*. It became clear that because of the extremely small scale at which the interaction between the precursor and the filler material took place, a much higher resolution instrument was needed, namely a transmission electron microscope.

A thin specimen made from the pyrolyzed material was prepared as follows. Out of the bars pyrolyzed at 1500°C small squares (2 x 2 x 0.5 mm^3) were cut using a diamond saw. These small squares were glued to a glass mount and polished down to a 80 μm thickness using SiC paper. The sample was turned over, reglued and polished so as to obtain two parallel polished faces. A calibrated die= was used to monitor approximately the thickness reduction. The samples mounted on glass stubs were transferred to a dimpler$ and ground using a soft brass wheel covered with diamond paste. At the end of this stage the sample's thickness is about 10-20 μm. A visual check by transparency is extremely useful in determining the end of the dimpling stage, since dimpling must be stopped before perforation. The glass mount and the sample are carefully rinsed and

---

* Krystalloflex, Siemens, Germany.

= Model 623, Gatan, Warrendale, PA

$ Model 656, Gatan, Warrendale, PA.

dried. Under an optical microscope silver paint is dabbed on the edges of the sample and a slotted 3 mm copper grid is positioned on top of the sample and slightly pressed to spread the paint. The silver paint is set by thermal treatment at 90°C for 1 hr. The glue is then dissolved and the sample is stored away ready for the nest step. Ion-milling[$$] using Argon ions was performed at 5 kV with an attack angle of 15°.

Various microscopes have been used : Philips EM 301[@@] (inspection), Philips EM 400 (Observation and microdiffraction), two JEOL[%%] 200 CX , one dedicated for high resolution microscopy and the other dedicated for microanalysis. The latter one is equipped with a ultra thin window EDS[##] detector capable of detecting and quantifying elements down to Z=6. Electron loss spectra were acquired by a EELS spectrometer[+] with parallel detection.

5.3 Results and discussion

5.3.1. SEM

Fig 5.1 represents (800°C in Nitrogen) a typical polished surface of a sample after pyrolysis at 800°C in nitrogen. The rather uneven surface topography is a consequence of large amounts of residual porosity. Some particles were pulled out during polishing, showing that the bonding strength between the particles and the precursor is still low. Certain areas (fig. 5.2) show little porosity on a small scale. Although not clearly visible on

---

[$$] Dual Ion Mill Model 600, Gatan, Warrendale, PA

[@@] Philips, Eindhoven, The Netherlands.

[%%] Jeol Corp., Japan.

[##] Model 3400, Kevex (Fisons Instruments), Valencia, CA.

[+] Model 666, Gatan, Warrendale, PA.

the micrograph, the particle network seems dense. There is not a sharp interface between the particles, but the existence of a continuous phase is still difficult to assert unambiguously.

The microstructures of samples pyrolyzed at 1000 and 1200°C are shown respectively on fig 5.3 and 5.4. The lower magnification micrographs indicate the presence of numerous cracks that surround denser regions (30-100 μm). These flaws are processing related. The microstructure reveals that the cohesion or bonding between these denser areas is weak and that the cementing action of the precursor phase took place locally in the agglomerates and not in between them. The material between the denser regions was not consolidated and was very likely pulled out during polishing. The agglomerates have the desired microstructure, i.e. dense and crack-free. Fig 5.4 b gives a better account of the microstructure of a dense region. Very little porosity can be seen. The size of the filler particles being 200 to 300 nm, the precursor phase is represented by the smallest features observable (10 nm) (fig 5.5). These small features cannot be analyzed by EDS for elemental composition.

At 1500°C the only visible change in the microstructure, as observed on a fracture surface (fig 5.6), is the growth of elongated grain in the form of short whiskers. They range between 10 and 300 nm in length and their diameter is fairly constant around 30 to 40 nm. These whiskers can be found mostly in the open voids between dense regions (fig. 5.7). They grew from the precursor phase, most likely, via a vapor-liquid-solid mechanism. Because of their size and small volume, reliable information cannot be collected by EDS analysis. The overall microstructure reveals no coarsening and extremely fine grained material is still visible, which means that not all the precursor has transformed into whiskers.

The microstructure as revealed by SEM is still difficult to interpret. There is no clear identification of the precursor derived phase except when, in some location and for higher processing temperature, it is visible in the form of short whiskers. At this stage it is

not possible to correlate consolidation of the structure with the interaction between particle and precursor. The large dense areas have the desired microstructure with little porosity. However, the lack of control during initial processing is evidenced by the presence of large cracks surrounding the dense regions.

5.3.2 Phase analysis by X-ray diffraction

The X-ray diffraction spectra (fig. 5.8) of samples pyrolyzed at 1000, 1200 or 1500°C indicate the presence of SiC as the only crystalline phase, which is the phase of the filler material. For sample pyrolyzed up to 1400°C the precursor derived phase may still be amorphous, according to the results of chapter three. The presence of a filler phase can lower the free energy change during crystallization of the precursor phase by providing nucleation sites.

A slight surface discoloration tending toward greenish hues was observed in samples treated at 1000°C. At 1200°C the samples have a distinctive light green surface layer (0.2 mm) and 1500°C the whole sample has changed from black/gray to light green. This color sequence clearly indicative of the diffusion of nitrogen atoms in the bulk of the SiC filler particles. However, these changes are not correlated with a phase transformation. If the precursor derived phase could not be detected as a different crystalline phase for the samples heat treated at 1500°C in nitrogen, then only two possibilities exist. Either the new phase is still amorphous and therefore does not contribute to any peak in the spectrum or the precursor transformed into mostly β-SiC, which cannot be distinguished from the powder filler phase.

5.3.3 TEM

Fig. 5.9 is a bright field image (amplitude contrast only) of the microstructure of a sample near the edge of the perforation. This microstructure, composed of small SiC

particles, is very uniform in the thin region around the hole where observations are possible. The particle size (0.2-0.3 μm) is practically identical to that of the original filler material, confirming the SEM observations. Furthermore, no shape change of the particle (no smoothening of edges or obvious rounding of apices) is seen. The presence of smaller particles (d<0.1 μm) indicates that coarsening effects did not affect the microstructure. There is little interaction between particles themselves. At low magnification the particles seem to be stacked in a rather porous 3-D network. Most of the selected area diffraction patterns taken from areas such as fig. 5.10 reveal a microcrystalline SiC with the characteristic (111) ring at 0.25 nm and no other reflection inside this ring. However, in some rare instances, two additional faint rings were detected at 0.335 and 0.446 nm. The first ring could be interpreted as graphite (d_{0002}=0.336 nm). Excess carbon can be expected as a minor pyrolysis product of polysilazane[28]. The reflection at 0.446 nm could come from some small β-Si_3N_4, but since these reflections were not seen over most of the sample one can conclude that the major pyrolysis phase is not Si_3N_4. This result is in agreement with Matsumoto's[47], who studied by X-ray diffraction the influence of filler material on the nature of the pyrolysis products of a polysilazane. The whiskers described in an earlier section were also visible particularly in crack-like openings near the hole of the TEM sample (fig. 5.11). It is firmly believed that these elongated features have grown from the precursor derived phase either from amorphous films or from small nuclei via processes necessitating large amounts of Si-rich vapor phase. The detection of whiskers in entangled arrays can be interpreted as follows. If a certain region of the sample contains a high concentration of precursor phase (inhomogeneous distribution) then upon transformation a void will be created due to the shrinkage of the precursor into a solid phase. Open-space is a necessary condition for easy vapor transport, and, because the local partial pressure of Si is high, whisker growth is particularly observed in regions that were initially rich in polymer. Free-surface of precursor derived ceramics showed similar whisker formation.

At higher magnification, it was possible to evidence a continuous amorphous phase as shown in fig. 5.12. The two arrows indicate the location of the amorphous phase bridging the SiC particles. The interfacial bonding seem strong. The amorphous nature of the interparticle phase was confirmed by microdiffraction in the STEM mode (probe size <10 nm) as illustrated on fig.5.13. The diffracting particle was close to a (111) orientation. Several microdiffraction patterns were collected from the bridge and all confirmed an amorphous state. The interparticle phase always appears in lighter contrast probably due to its thinness and lower density. Typically, glassy structures in the Si-C-O-N system have lower densities than the crystalline phases, such as SiC or Si_3N_4 . From the micrographs, the extent of the phase seems to vary between locations, and without such a phase, the strength of the bond between two particles would only be due to van der Waals forces, i.e. weak. Even non-touching particles can be connected with some small amounts of amorphous phase. So, even if the volume fraction of SiC is reduced, it is possible that the consolidation effects are more significant for large volume fractions of precursor phase. Strong solid bridges connect separated particles. It is extremely difficult to evidence the role of the binding phase between two almost touching spheres. Such a microstructure is shown on fig. 5.14. The arrows outline the edges of two silicon carbide particles. There is no sign of an interface in the interparticle phase. The existence of a native silica layer present on all SiC particles surfaces had been evidenced in an earlier work[58]. Since the two SiC particles are bonded together via the precursor derived phase it would be expected to find some variation in contrast between the SiO_2 and the amorphous phase. The lack of such contrast could indicate that some interdiffusion has taken place between the silica surfaces and the amorphous phase. It is not known if an oxidation pre-treatment would influence the microstructure or the nature of the interaction. Niihara[32] had investigated the influence of post heat treatment at 1400°C in air. He found that the room temperature strength was increased considerably. Two possible interpretations were given. A crack healing process could have taken place during the post treatment, thus reducing the size of

flaws at the surface of the sample. The second argument was that the bonding characteristics of the amorphous phase between the SiC particles could be modified by oxidation. However, no experimental observation was available to confirm these possibilties.

5.3.2 Phase analysis

Using an ultra thin window detector, it was possible to quantify the composition of the amorphous phase at different locations in the sample. Fig. 5.15 shows a large amorphous area that has remained stable in the shape of a C. The arrow indicates the exact location of the probe during analysis. The composition at this location, which is obtained after background removal, peak fitting and thickness determination (=45 nm), is $SiC_{2.7}O_{1.1}N_{0.1}$. Mass absorption coefficients are taken into account in all the k-factors for composition analysis. The C:Si:N ratio is initially 3:2:2 , therefore, the composition of the amorphous phase at the first location indicates a loss of both silicon and nitrogen. Actually, nitrogen has been almost totally eliminated. Similar nitrogen elimination has been reported[59]on methyldipolysilazane fiber after heat treatment at 1400°C. The slow evolution of CO and N_2 from the fibers leads to the crystallization of silicon carbide. Such a large excess of carbon could lead to precipitates of graphite, but none were detected in this amorphous phase. A second analysis was performed on an amorphous feature adjacent to the first location (fig. 5.16). The feature analyzed showed a darker contrast, indicative of a higher concentration of strong scatterers. The composition was found to be $SiC_{1.1}O_{0.6}$ with nitrogen level too low to be reliably quantified. A definite adjustment toward the composition of SiC was identified. The precursor derived phase still amorphous after the 1500°C heat treatment must be in a metastable state. Under the particular experimental conditions the crystalline phase most likely to form is SiC. This necessitates the nucleation of SiC embryos, which can be achieved by solid state diffusion in the siliconoxycarbide

phase along with the elimination of oxygen and carbon as CO gas. EDS analysis was also conducted on isolated elongated features found in crack-like openings (fig 5.17). One composition was extremely rich in silicon, ($SiC_{0.32}O_{0.25}$).

It is therefore not possible to describe the composition of the precursor phase as one average composition. Very large variations can exist locally in apparently homogeneous phases. The local stoichiometry determines to some extent the ability of this phase to crystallize, if further heating is applied, in the crystalline form closest to its composition. Other investigations[44] for materials heat treated at 1300°C report the presence of a continuous Si-C-N amorphous phase. However, the microstructures for higher heat treatment temperature are not presented.

To confirm some of the results obtained by EDS, phases were also analyzed by energy loss spectroscopy. Precursor derived phases located in different regions of the sample were analyzed with the goal to detect nitrogen. The expected K-edge is located at 400 eV. Small concentrations of nitrogen, typically less than 5 to 10 %, were detected in amorphous phases (fig. 5.18). To prove that nitrogen did not come from the pyrolysis atmosphere a SiC particle was analyzed, as shown in fig. 5.19. The absence of a detectable amount of nitrogen confirms our assumption. The Si-L edge shapes of an amorphous feature and a β-SiC particle are compared on fig. 5.20. The similarity of the electron loss near edge structures indicates that in the amorphous phase Si has a chemical environment similar to that of Si in SiC.

5.4 Conclusion

The microstructure observations have confirmed the role of the precursor derived phase as the cementing material that connects the individual SiC particles and give the sample its strength. The positive identification of a continuous amorphous phase was,

however, not possible at every neck between particles. In terms of composition, we were able to conclude that the filler material has influenced the decomposition reaction of the polymer. No Si_3N_4 was positively identified.

CHAPTER SIX MECHANICAL PROPERTIES

6.1 Introduction

Materials prepared by co-pyrolysis of a precursor/powder mixture were developed serendipitously. Indeed, the initial intent was to use these precursors as sintering aids to obtain fully dense SiC with improved microstructure. However, the materials had relatively high strength after a heat treatment at moderate temperature that did not allow the sample to sinter. What is most interesting for many ceramists is the high strength reported in the literature despite the large residual porosity after heat treatment. One would expect the strength of a porous body to obey the following equation[60],

$$\sigma = \sigma_0(1-\exp(-bp))$$

with b a scalar ranging from 1 to 4, p the sample porosity and σ_0 an average strength of fully dense SiC. Clearly, the data published in the literature cannot be represented by this equation. The high strength could be justified by the extremely small size of the pores (<10 nm). The nature of the porosity in precursor derived phases has been discussed by Lipowitz et al.[56]. Pores in PDP were originally cylindrical nanochannels that allowed gas evolution to occur. These channels collapsed through instability into a series of closed pores. As temperature is increased pores coalesce, but the total porosity decreases as the density of the precursor derived phase tends toward that of the crystalline phase closest in stoichiometry.

To view the material as a homogeneous porous ceramic is however erroneous. As demonstrated in chapter five, the material is best described as a mosaic of SiC microcrystals cemented together by a Si-C-O amorphous phase. Ideally, the mechanical properties depend on the strength of the interface between two SiC particles. The

evolution of the strength of this interface should be characterized by evaluating the mechanical properties of samples processed at different temperatures. In an attempt to do so several strength evaluation were conducted as explained in the next paragraph.

6.2 Experimental

Samples containing 20 wt% polysilazane-80 wt% SiC were pyrolyzed in nitrogen at different temperatures, namely 1000, 1200 and 1500°C. Test bars (3 x 3 x 30 mm^3) were cut using a diamond saw. The edges were beveled and the tensile side was polished using a 1 micron diamond paste. The flexural strength was measured by 4-pt bend testing at room temperature at a cross speed of 0.05 mm/mn. If the load at fracture is designated by P, the modulus of rupture can be calculated from,

$$\sigma = 3\ P\ a\ /\ b\ h^2$$

where a is the half difference between the width of the top and bottom supports, b and h are respectively the width and the thickness of the sample.

6.3 Results

Figure 6.1 summarizes the strength data. The strengths measured are much lower than those published in the literature. Clearly, all the samples broke prematurely due to the presence of large flaws. The highest strength recorded was around 100 MPa. Actually these results are comparable to those obtained by Yajima before infiltration/pyrolysis cycles. The origin of flaws will be discussed in the next paragraph and some guidelines regarding their elimination will be given.

If any trend can be derived from the strength data collected, then it seems that the interaction precursor phase/powder increases with processing temperature. This could be

related to the density increase of the amorphous phase. The higher processing temperature can allow more interfacial reaction between the precursor derived phase and the silica-rich surfaces of the SiC particles. At 1500°C some of the precursor derived phase may already have crystallized. Is it possible to correlate higher strength and crystallization of the amorphous cement phase? The crystallization of amorphous Si_3N_4 powder is known to be highly exothermic[45]. However, the DTA curve of a precursor derived phase does not exhibit a strong exothermic peak upon crytallization. So, there might not be a strong correlation between crystallization of the amorphous phase and increase in strength. The literature provides two examples[32,34] of materials with high strength (300 to 450 MPa) in which the authors claimed that the precursor derived phase is still amorphous.

The elimination of surface flaws by repeated precursor impregnation /pyrolysis cycles can dramatically increase the modulus of rupture[31]. Mechanisms of surface porosity elimination have been reported by Mazdyiasni[48]. He observed that whiskers similar to the one detected in both SEM and TEM filled up pores in a bird's nest pattern. Surface porosity can also be eliminated by oxidation heat treatment[32,34]. Flexural strengths after 10 min at 1400°C in air were increased from 300 to 450 MPa.

6.4 Source of macroscopic flaws

A critical review of the processing procedure of our samples should evidence the stage at which flaws are introduced. Observations of polished surfaces have shown the presence of large agglomerated regions weakly bonded to one another. It is believed that such agglomerates formed during the preparation of the blend. After vacuum evaporation the mixture is made of cakes that are first allowed to dry overnight to eliminate all residual solvent. There is a dilemma in the next preparation step. If the mixture is not properly dried then upon ball-milling the ZrO_2 balls used get coated with a uniform layer of

precursor/powder blend. If the mixture is completely dried then it is not possible to crush the strong agglomerates seen on fig. 6.2. If the agglomerated structure is still seen after pyrolysis it means that it did not disappear during uniaxial and isostatic pressing. There are two modifications to the preparation of samples that can be suggested. The addition of a processing aid, an organic lubricant, could promote the deformation of the agglomerates under an applied stress. The second processing improvement would be to compress mold the blend at moderate temperature (100 to 150°C). Over this temperature range the thermoplastic properties of the polysilazanes can also improved packing uniformity.

The elimination of large flaws should be the main focus of future work. This should be conducted on smaller samples (typically 1/4" in diameter) so as to keep research cost down. Once conditions are found that minimize the large flaw population the processing can be scaled up to bending bar sizes and further mechanical testing can follow.

CHAPTER SEVEN GENERAL DISCUSSION

The goal of this study was to understand some of the mechanisms taking place upon pyrolysis in a polysilazane/SiC compact. Most of the relevant literature has focused on a more macroscopic approach to the problem, i.e. on the influence of external processing parameters such as initial precursor content. Such investigations require large amounts of starting material in order to develop and optimize the fabrication process. In the present work we have evidenced some of the fundamental interaction between the filler material and the decomposing precursor.To justify the need for a such an investigation, it is important to recall that without addition of a precursor a solid made of compacted SiC particles exhibits no consolidation when subjected to the same heat treatment. Hence, the presence of the precursor is the only factor that can explain the unexpected high strength of the porous material.

Macroscopically little shrinkage was observed upon heat treatment. This seems to indicate that the precursor, in its polymeric state, is primarily located in the interparticle voids. Then, in each void, resembling in shape a octahedral site in a fcc structure, the precursor can undergo a large density change upon transformation without affecting the overall dimensions of the sample. A sample, without precursor, subject to the same heat treatment does not undergo any shrinkage at all. This confirms that no densification takes place. Regardless of mechanisms (evaporation-condensation, surface or volume diffusion) the kinetics of mass transport would be extremely slow for a 1500°C heat treatment. So the strength of the material cannot be explained by the redistribution of mass from one filler particle to another or by neck formation through atom diffusion from positive to negative curvature regions. In that sense, the filler particles, by themselves do not play a significant role in the strengthening of the sample. The particle size of the filler material

may play an important role. If the strength of the material increases with decreasing particle size, as suggested by the results of Yajima and those of Niihara, then the total interfacial area between the precursor and the filler particles may be an adequate parameter to quantify the interaction. At the same time, the size of critical flaws may be reduced by using a finer powder .

The macroscopic characterization of the material evidenced that upon confined pyrolysis more ceramic residue was retained than was predicted from free or unconfined pyrolysis. The thermal decomposition of a polysilazane releases volatile silazane monomers that are detached from the polymer chain via retroversion reactions. Some of these silazanes escape from the sample. Another fraction of volatile silazanes may be trapped inside the compact or readsorb on the surfaces of the SiC particles. As temperature increases, these species would decompose thermally inside the sample. There is, however, no microstructural evidence to support this mechanism. Since this redistribution mechanism relies on volatile species, it would apply primarily to precursors that releases large amounts of monomers, i.e. low yield precursors. Such mechanisms may be important in Niihara's work[32] on polysilastyrene / SiC systems. The "polysilastyrene" has a low ceramic yield of about 20-25 %, and yet the average flexural strength of his test samples is 280 MPa. Not enough experimental data are available today to establish a strong correlation between this mechanism, coined internal micro-CVD (fig. 6.3), and the mechanical properties of the materials.

A second strengthening mechanism (Fig.6.4) is suggested by the microstructure observations. It has been possible to identify, by TEM, in locally dense regions, a continuous phase. This phase was mostly present between SiC particles, providing strong bridges responsible for the local consolidation of the compacted powder. The phase can also be seen as a pore filler that can reduce the size of the flaws from which cracks can initiate. The analyses of fracture surfaces in the sample indicate that cracks propagate between the strong, dense regions and not through them. So the agglomerates have a high

cohesive strength. The strengthening by the precursor seems only effective if the packing density of SiC particles is high, which means that large pockets of precursor in the green body will become weak links in the pyrolyzed material. Attention has been given in this work to some promising micro encapsulation techniques aiming at improving the distribution of precursor phase in the sample.

One can make very simple estimates of the size of necks formed between two touching SiC particles assuming the geometry of Fig. 6.5. In our case the neck material is only composed of polymer derived phases. Equation (7) of chapter four can be used to obtain an estimate of the volume fraction of precursor derived phase after pyrolysis. Let N be the average coordination number of a SiC particle, h the half thickness of the neck and R the radius of the particle. The volume, per SiC particle, of neck material for one contact is,

$$V_{1/2neck} = \pi.b^2.h - \pi.h^2(R - h/3),$$

with $(R - h)^2 + b^2 = R^2$. By expressing the ratio between the volume fraction of precursor, V_g, to that of SiC, V', we have,

$$V_g / V' = N\, V_{1/2neck} / V_{particle} = N\, (\pi.b^2h - \pi.h^2.(R - h/3))/4\pi R^3/3,$$

setting $x = h/R$, the equation to solve is

$$3.N/4.(x^2 - 2x^3/3) = V_g / V',$$

Numerically, if V_g= 10% and V'= 50% and N= 12, then x is 0.2. So, even for large amount of precursor loading (20wt%), the average neck size is relatively small.

Even if the model gives a rough estimate of the extent of neck formation, ultimately what controls the strength of a sample is the strength of the interface between two SiC particles. The bond is formed by two SiC/precursor interfaces and a thin amorphous phase. Upon failure the weakest link will break first. The strong interface between the PDP and the SiC particle can be explained by some interdiffusion between the SiO_2-rich surface layer present on all SiC particle and the amorphous phase. Indeed, by

analytical electron microscopy the PDP was found to be oxygen rich, that is, contain more oxygen than a SiC particle of the same thickness.

Thermodynamically, the following reaction is possible between surface silica and excess carbon in the PDP,

$$SiO_2 + C \rightarrow SiC + 2\ CO\ (T>1000^{o}C)$$

Other competing reactions can also take place depending on the local vapor pressure of CO. There are at least two other possible explanations for the detection of oxygen in the precursor phase. For practical reasons it was not possible to prepare samples in an oxygen-free atmosphere. Hence, the surface of the polymer may have oxidized or hydrolyzed according to,

$$\text{-Si-N-} + H_2O \rightarrow \text{Si-OH} + NH_3$$

It is believed that the hydrolysis reaction only occurs at the surface of the polymer but if the precursor is finely divided the surface area in contact with air or moisture may be large and oxygen contamination significant. It has also been assumed that once the sample is pyrolyzed (500-800°C), it is no longer oxygen sensitive. But the formation of Si-O-Si bonds has been reported[61] in precursor pieces pyrolyzed at 1000°C. This observation illustrates the need for improved research facilities where the sample can be prepared in an oxygen and moisture-free environment. Since oxygen is an important contamination element in practically all research involving precursors, it would have been desirable to be able to measure its concentration between the different preparation steps of the sample.

Finally, it is possible, as suggested by observation of pyrolyzed phases in chapter three, that the neck between filler particles has been strengthened by Ostwald ripening mechanisms involving the high surface energy nanophase created just upon crystallization. There is a large driving force for this phase to lower its total surface energy and this can be accomplished by elimination of free surfaces, namely coarsening of the nanophase and/or growth of the neck region at the particle contact area at the expense of the newly crystallized precursor phase. This mechanism is only valid if the heat treatment

temperature allows the crystallization of the precursor derived phase. In the present case, this is possible since the polysilazane is known to crystallize in a ceramic phase between 1400 and 1500°C.

The short whiskers seen both TEM and SEM do not play a role in the consolidation. It is difficult to assert how much bonding they provide between particles they connect. Their growth indicates a locally poor packing of the SiC filler particles that has created the open space necessary for the elongated features to grow. If the growth of these whiskers can be controlled, it might be possible to tailor a microstructure of SiC particles with *insitu* SiC whiskerization. Such microstructures are currently being developed[62].

CHAPTER EIGHT CONCLUSION

This work has reported the results from detailed microstructural investigations and macroscopic physical properties measurements. The goal was to evidence the major mechanisms for consolidation of a powder/precursor compact pyrolyzed at relatively low temperature. Some of the mechanisms are directly revealed by microstructural observation despite the small scale at which interaction takes place. Others are inferred from more macroscopic measurements and from investigations aimed at analyzing each component of the system individually.

It is the formation of chemical bonds between the precursor derived phase and the SiC particles that gives the material its cohesion and unexpected high strength. The ability to form strong bonds is due in part to the reactivity of the precursor phase even after cross linking. This reactivity can be attributed to the presence of hydrogen[37] in the amorphous solid phase at temperature up to 1200°C. For the ceramist the strengthening can be justified by the formation of neck between SiC particles, these necks are not formed by sintering mechanisms involving the SiC filler particles but are the results of the local decomposition of the original polymer at the neck region.

Despite some difficulties encountered in the interpretation of the microstructural observations, the experimental approach has yielded interesting clues as to some of the most logical interaction mechanisms. Yet, the pursuit of a similar investigation would benefit from slight modifications. First, one should find a polysilazane containing only silicon, nitrogen and hydrogen and no carbon. This could be achieved in collaboration with a chemistry department interested in polysilazane synthesis. The pyrolysis of such polysilazane would undoubtedly yield measurable quantities of Si_3N_4 making the phase analysis a little easier. If, at first, one is only interested in microstructure characterization,

a better choice of filler material would be an easily recognizable powder, such as large (4 μm) SiC particles. If the focus is on fabricating high strength samples then a fine powder, such as the one selected, would be preferred. Also, to elucidate the role of surface silica one could try to prepare a sample in an oxygen-free environment, or as much as possible quantify the evolution of oxygen in the precursor during fabrication of the samples.

Last but not least, this study has shown that microstructure control is still the most challenging task a ceramist has to face. Despite the particular care brought to the preparation of the samples severe limitations in mechanical properties were introduced by the presence of large flaws. The control of macroscopic inhomogeneities should be the focus of more experimental work. Pressure-casting of the still flowable powder/precursor paste or heat-assisted compression molding with addition of organic lubricants are some suggested routes toward the elimination of flaws in the microstructure.

Structural ceramic fabrication via pyrolysis of precursors is still a very active field of research. The author hopes this present work will provide a source of valuable information for those involved in the application of precursors as binders for monolithic or composite ceramics.

References

1. Johnson C.A., Prochazka S., "Investigation of Ceramics for High Temperature Applications", Naval Air Development Center, NADC-75228-30, 1977.

2. Prochazka S., Greskovich C.D., "Development of a Sintering Process for High Performance Silicon Nitride", AMMRC TR-78-32, 1978.

3. Lange F.F., *J. Am. Ceram. Soc.*, **72** [1], 3-15, 1989.

4. Singh J., *Advanced Ceramic Materials*, **3**, [1] 18-27, 1988.

5. Chantrell P.G., Popper E.P., in "Special Ceramics", Popper ed. p.87-102, Academic Press, New York, 1964.

6. Wynne K.J. , Rice R.W., *Annu. Rev. Mater. Sci.*, **14**, 297, 1984.

7. Hardy A.B. *et al.*, "Ultrastructure Processing of Advanced Ceramics", p.407, Ed. by J. D. Mackenzie and D. R. Ulrich, Wiley, NY, 1987.

8. Yajima S., Hayashi J., Omori M., 1978, U.S. Patent 4,052,430.

9. Yajima *et al.*, *J. Mater. Sci.*, **16**,1349-1355, 1981.

10. Paciorek K.J.L. *et al.*, *ibid* ref. 7, p.89-97

11. Yajima S., Hayashi J., Omori M., Okamura K., *Nature* **260**, 683, 1976.

12. West R. *et al.*, *Am. Ceram. Soc. Bull.*, **62** [8] 899, 1983.

13. Schilling, Jr. C.L., Wesson J.P., Williams T.C., *ibid* ref 12, p.912.

14. Wills R.R., Markle R., Mukherjee S., *ibid* ref 12, p.904.

15. Jenkins G.M., Kawamura K., "Polymer Carbons-Carbon fibre, Glass and Char", London, Cambridge Univ. Press, 1976.

16. Beatty C. L., "Ultrastructure Processing of Ceramics, Glasses and Composites", p.272, Ed. by L.L. Hench and D.R. Ulrich, Wiley, NY 1984.

17. Ethyl Corporation, technical information release.

18. Coblenz W.S. *et al.*, "Proceedings of the Nineteenth University Conference on Ceramic Science, North Carolina State University, Nov. 9, 1982.

19. Friedel and Crafts, *Ann.*, **136**, 203, 1865.

20. West R., "Organopolysilanes" in Silicon Compounds (technical publication, Huls-Petrarch chemicals).

21. Kippling , *Proc. Roy, Soc.* A, **59**, 139, 1937.

22. Schilling, Jr. C.L., Wesson J.P., Williams T.C., "Organosilane Polymers IV: Polycarbosilane Precursors for Silicon Carbide", O.N.R., TR-80-1, 1980.

23. Yajima *et al.*, *J. Mater. Sci.*, **13**, 2569-2576, 1978.

24. Fritz G., Matern E., "Carbosilanes", Springer-Verlag, Berlin, 1986.

25. Yajima *et al.*, *J. Am. Ceram. Soc.*,**59**, 326, 1976.

26. Stock A., Somieski K., *Ber. dt. chem. Ges.*, **54**, 740, 1921.

27. Seyferth *et al.*, *J. Am. Ceram. Soc.* C-13-C-14, 1983.

28. Legrow *et al.*, "Better Ceramics through Chemistry II", Ed. by Brinker, Clark and Ulrich, MRS Symposium proceedings vol.73, p.533, 1986.

29. Okamura *et al.*, *ibid* ref 7, p.501.

30. Bishop *et al.*, Ceramic Transactions, Vol. 1 in Ceramic Powder Science II, B, ed. by Messing, Fuller and Hausner.

31. Yajima *et al.*, *Am. Ceram. Soc. Bull.*, **56** [12], 1060-1063, 1977.

32. Niihara *et al.*, *ibid* ref7, p.547.

33. Schwartz *et al.*, *Advanced Ceramic Materials*, **3** [4], 320-323, 1988.

34. Semen J., Loop J.G., *Ceram. Eng. Sci. Proc.* **11** [9-10],1387-1394, 1990.

35. Su S., GTE technical memorandum TM-0136-05-89-066, 1989.

36. Mutsuddy B., "High Tech Ceramics", p.571, Ed. P. Vincenzini, 1987.

37. Blum *et al.*, *J. Mater. Sci.*, **24**, 1707-1718, 1989.

38. Mazdyiasni K.S., Cooke C.M, *J. Amer. Ceram. Soc.*, **56** [12], 628-633, 1973.

39. Messier D.R., Wong P., *J. Amer. Ceram. Soc.*, **56** [12],480-485, 1973.

40. Blum Y., private communication.

41. Greil P., Tanaka H., Petzow G., *ibid* ref 36. p.1011.

42. Nickel K. *et al.*, *Advanced Ceramic Materials*, **3**, [6], p.557-562, 1988.

43. Wada H., Wang M.J., "Whisker and Fiber Toughened Ceramics", p.63-72, Ed. by R.A. Bradley, 1988.

44. Semen J., Loop J.G., unpublished results.

45. Prochazka S., Greskovitch C., *Am. Ceram. Soc. Bull.*, **57** [6], 579-586, 1978.

46. Yamada *et al.*, *J. Mater. Sci.*, **2**, 275-278, 1983.

47. Matsumoto R.L.K., "Crystallization of Pyrolyzed Polysilazanes", presented at the Annual Meeting of the MRS , San Francisco, 1989.

48. Mazdyiasni K.S., West R., David L., *J. Am. Ceram. Soc.*, **61** [11-12], 504-508, 1988.

49. Rogers J.J. *et al.*, *Ceram. Eng. Sci. Proc.*, **10** [7-8], 833-836, 1989.

50. Schwartz K.B., Rowcliffe D.J., *J. Am. Ceram. Soc.*, **69** [5], C-106-C-108, 1986.

51. Kruyt H.R., "Colloid Science", p.243, ed. by H.R. Kruyt, Vol. II, Elsevier, 1949.

52. Jamet *et al.*, *Ceram. Eng. Sci. Proc.*,**5** [7-8], 677-694, 1984.

53. Schwartz K.B., Blum Y., "Better Ceramics through Chemistry III", p.483-488, MRS symposium proceedings vol. 121, 1988.

54. German R.M., International Journal of Powder Metallurgy", **23** [4], 237-245, 1987.

55. Lipowitz *et al.*, *Advanced Ceramic Materials*, **2** [x], 121, 1987.

56. Lipowitz *et al.*, *J. Mater. Sci.*, **25**, 2118-2124, 1990.

57. Shaw T., Mat. Res. Symp. Proc., **73**, 215-223,1986.

58. Rahaman M., Boiteux Y.P., De Jonghe L.C., *Am. Ceram. Soc. Bull.*, **65** [8], 1986.

59. Chaim R., Heuer A.H., *J. Am. Ceram. Soc.*, **71** [11], 960-969, 1988.

60. Rice R.W., "Microstructural Dependence of Mechanical Properties", *Treatise of Material Sciences and Technology*, Vol. II, p.199 (1977).

61. Riedel *et al.*, *J. Eur. Ceram. Soc.*, **5**, 213-222, 1989.

62. Blum Y., unpublished work.

List of Tables

Table 1.1 : Commercial polysilanes (source Huls/Petrarch chemicals)

Table 1.2 : Commercial polysilazanes (source Huls/Petrarch chemicals)

Table 3.1 : Pyrolysis gases from a polydisilylazane (ref Blum Y. ref 37)

POLYSILANES

Description [CAS #]	Form	Solvent	λmax	Other	Thermal	Char % at 800° by TGA	10g
Poly(cyclohexylmethyl) silane	solid	Toluene THF	320		Tg: 93°	5-10% N_2 30-35% air	S 199
Polydihexylsilane	solid						199
Poly(dimethylsilane) [28883-63-8]	solid	Hot fluorene Hot phenanthrene				20-25%	
Poly(phenylmethylsilane)	solid	Toluene	337		Tg: 112-122°		169
(90%) Dimethylsilane-10% Dimethylsiloxane Copolymer P	liquid	THF, Toluene	258	S.G. 0.94			169
(50%) Cyclohexylmethylsilane (50%) Dimethylsilane Copolymer	solid	Toluene	304		Tg: 100°	10-15% N_2 30-35% air	169
(50%) Dimethylsilane (50%) Phenylmethylsilane Copolymer (Polysilastyrene)	solid	THF, Toluene			Tg: 85-92°		

Table 1.1 : Commercially available polysilanes (source Huls/Petrarch)

POLYSILAZANES

Description	Structure	d_4^{25}	Visc.	Char % 700°	MW	SG	10g
Poly (1,1-dimethyl-silazane) Crosslinked	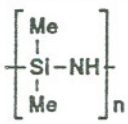		>1000	10-15			≤ 99
Poly (1,1-dimethyl-silazane) Telomer	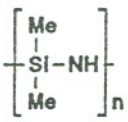	1.042	6000-8000	5-10	750		99
Poly (1,2-dimethyl-silazane P	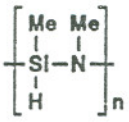	0.99	600-800	15-20	760		99
(1,2-dimethylsilazane) (1-methylsilazane) Copolymer P	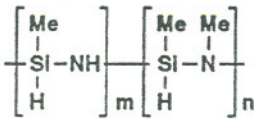	1.04	70.2	50-55		1.024	99
N-Methylsilazane Resin in Toluene, 25% Solids RI 1,494 (25)	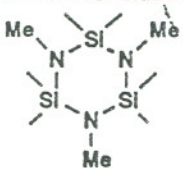			50-55 (800°)			99

Table 1.2 : Commercially available polysilazanes (source Huls/Petrarch chemicals)

Temperature (°C)	Gases
350	Trace—$Me_3SiOSiMe_2H$, $(Me_3Si)_2NH$
400	Trace—Me_2SiH_2, Me_4Si, Me_3SiOH, $Me_3SiOSiMe_2$ $(Me_3Si)_2NH$
450	Trace—$Me_3SiOSiMe_2H$, $(Me_3Si)_2NH$ + CH_4
500	Trace—Me_2SiH_2, Me_4Si, Me_3SiOH + CH_4
550	CH_4
600	CH_4
650	CH_4
700	CH_4
800	CH_4

Table 3.1 : Pyrolysis gases from a polydisilylazane (Blum Y. ref. 37)

List of Figures

Figure 2.1 : Possible approaches to investigate interaction.

Figure 3.1 : Polysilazanes PS 116 (Huls/Petrarch chemicals)

Figure 3.2 : Thermogravimetry analysis of PS 116.

Figure 3.3 : Microstructure of pyrolyzed polysilazanes; 1000°C, N_2.

Figure 3.4 : Microstructure of pyrolyzed polysilazanes; 1400°C, N_2.

Figure 3.5 : Microstructure of pyrolyzed polysilazanes; 1600°C, N_2.

Figure 3.6 : Microstructure of pyrolyzed polysilazanes; 1700°C, N_2.

Figure 3.7 : Microstructure of pyrolyzed polysilazanes; 1400°C, vacuum.

Figure 3.8 : Microstructure of pyrolyzed polysilazanes; 1500°C, vacuum.

Figure 3.9 : X-ray diffraction spectra of pyrolyzed polysilazanes in N_2 :
a:1400°C, b:1500°C, c: 1600°C, d: 1700°C.

Figure 3.10 : Stability diagram of SiC and Si_3N_4.

Figure 3.11 : X-ray diffraction spectrum of pyrolyzed polysilazanes; 1500°C, vacuum.

Figure 4.1 : Selection of precursor loading : green density vs. precursor content.

Figure 4.2 : Flow chart of conventional processing.

Figure 4.3 : Powder/polysilazane mixture (conventional processing).

Figure 4.4 : Micro-encapsulation flow chart.

Figure 4.5 : Micro-encapsulated SiC powder.

Figure 4.6 : Heating schedule for 20 wt% PS 116 / SiC samples.

Figure 4.7 : Measured green densities vs. precursor content.

Figure 4.8 : Volumetric composition as a function of initial precursor content.

Figure 4.9 : Comparison of pyrolysis behaviors : Precursor vs. Precursor + filler.

Figure 4.10 : Densities (relative to ρ_{SiC}) of pyrolyzed samples vs. initial precursor content.

Figure 5.1 : Polished surface of sample pyrolyzed at 800°C, N_2.

Figure 5.2 : High magnification of sample pyrolyzed at 800°C, N_2, showing dense area.

Figure 5.3 : Polished surface of sample pyrolyzed at 1000°C in N_2.

Figure 5.4 : Polished surface of sample pyrolyzed at 1200°C in N_2.

Figure 5.5 : Evidence of precursor derived phase (1000°C, N_2).

Figure 5.6 : Fracture surface of pyrolyzed sample (1500°C, N_2).

Figure 5.7 : Preferred location of whiskers in less dense regions.

Figure 5.8 : X-ray diffraction of pyrolyzed sample (1500°C, N_2).

Figure 5.9 : TEM of pyrolyzed sample (bright field).

Figure 5.10 : Electron diffraction ring pattern : microcrystalline SiC.

Figure 5.11 : TEM of elongated features (polymer derived phase).

Figure 5.12 : TEM of amorphous phase (pdp) binding SiC particles.

Figure 5.13 : TEM and micro-diffraction of amorphous bridge.

Figure 5.14 : High resolution micrograph of neck region between two particles.

Figure 5.15 : Energy dispersive spectroscopy of amorphous region($SiC_{2.7}O_{1.1}N_{0.1}$)

Figure 5.16 : Energy dispersive spectroscopy of amorphous region (see arrow) ($SiC_{1.1}O_{0.6}$).

Figure 5.17 : Energy dispersive spectroscopy of amorphous whisker in crack-like opening ($SiC_{0.3}O_{0.25}$).

Figure 5.18 : Energy loss spectroscopy of precursor derived phase: N content less than 5 % at.

Figure 5.19 : Energy loss spectroscopy of reference SiC particle.

Figure 5.20 : Comparison between Si-L near edge structures in β-SiC and in polymer derived phase.

Figure 6.1 : Flexural strength as a function of heat treatment temperature.

Figure 6.2 : Possible source flaws: agglomerates formed during processing.

Figure 6.3 : Consolidation mechanism: redistribution of precursor via vapor phase transport during pyrolysis.

Figure 6.4 : Consolidation mechanism: Interfacial reaction involving silica-rich surface layer and polymer derived phase.

Figure 6.5 : Geometry of reinforced particle contact area.

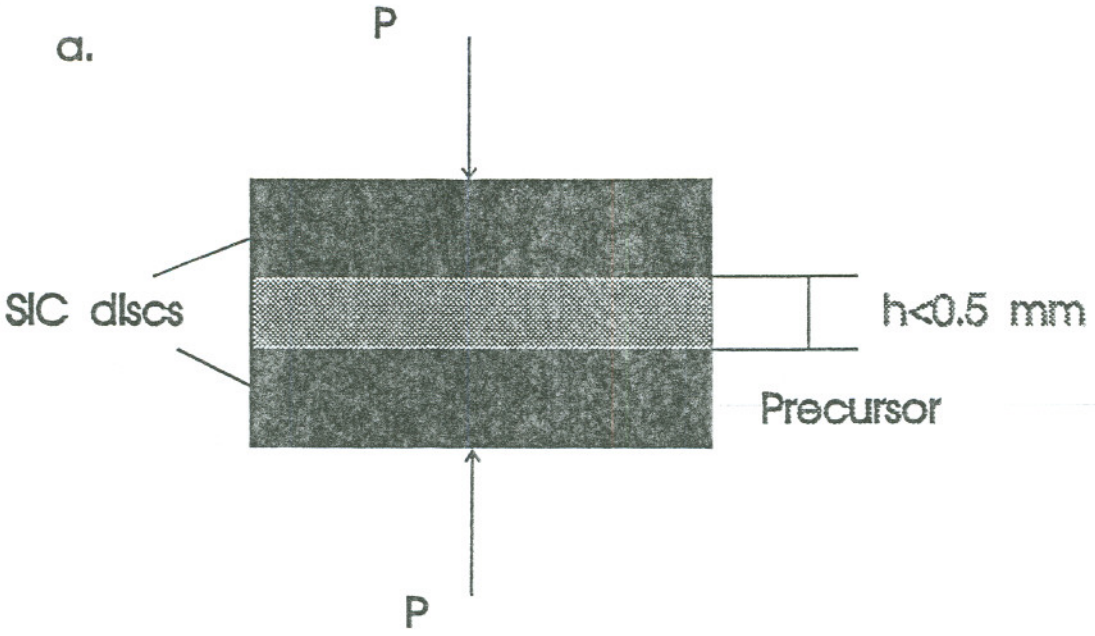

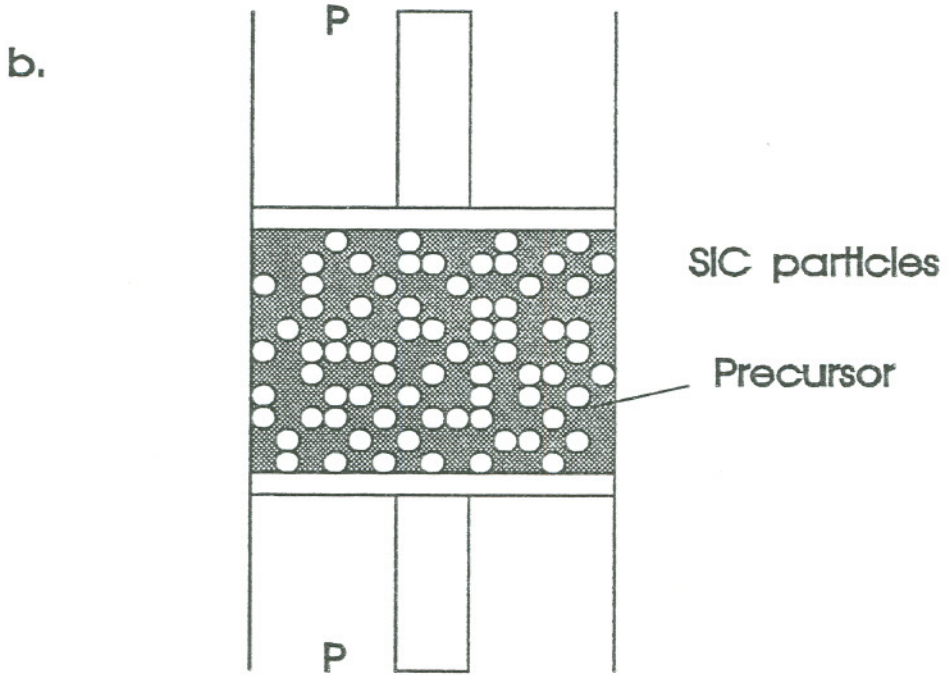

Figure 2.1 : Possible approaches for experimental investigation
a. Model macroscopic contact
b. Real system

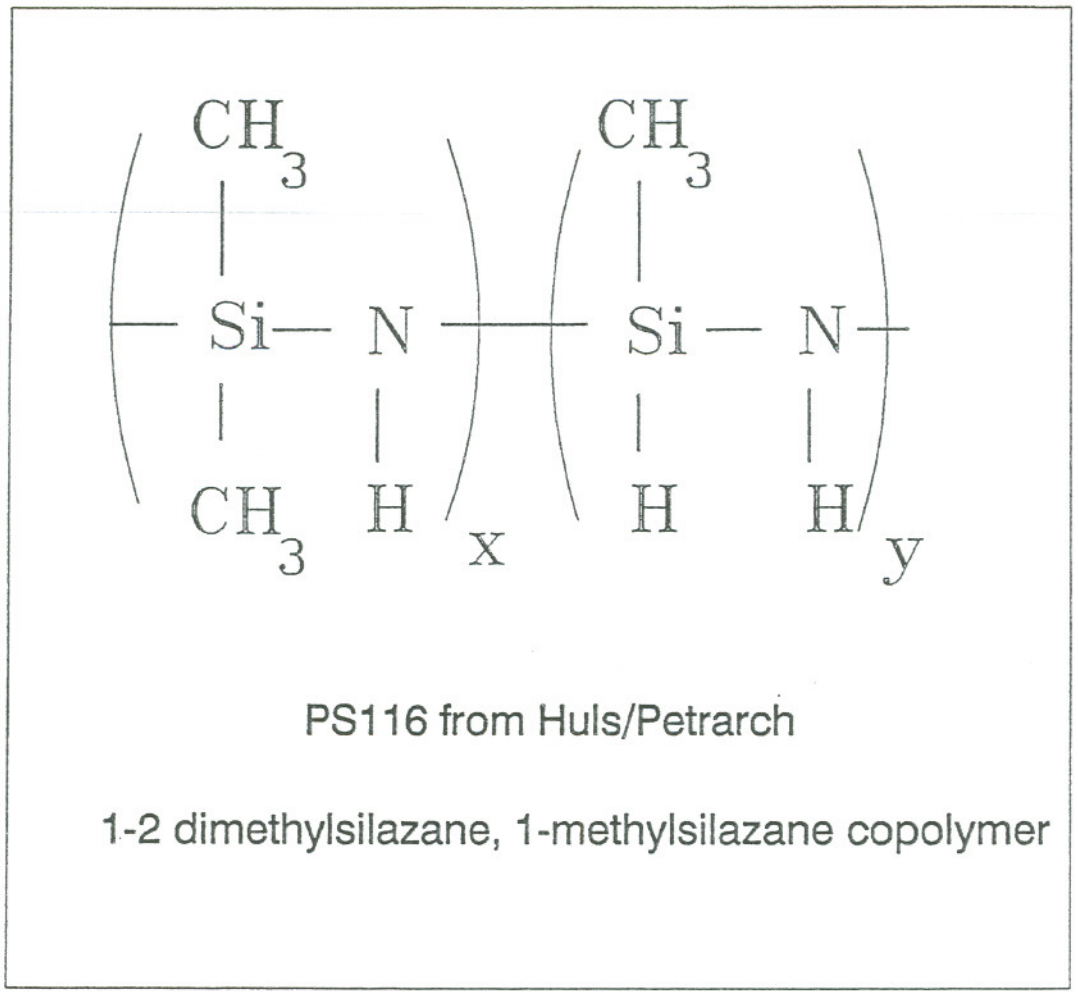

Figure 3.1 : Polysilazanes PS 116 (Huls/Petrarch chemicals)

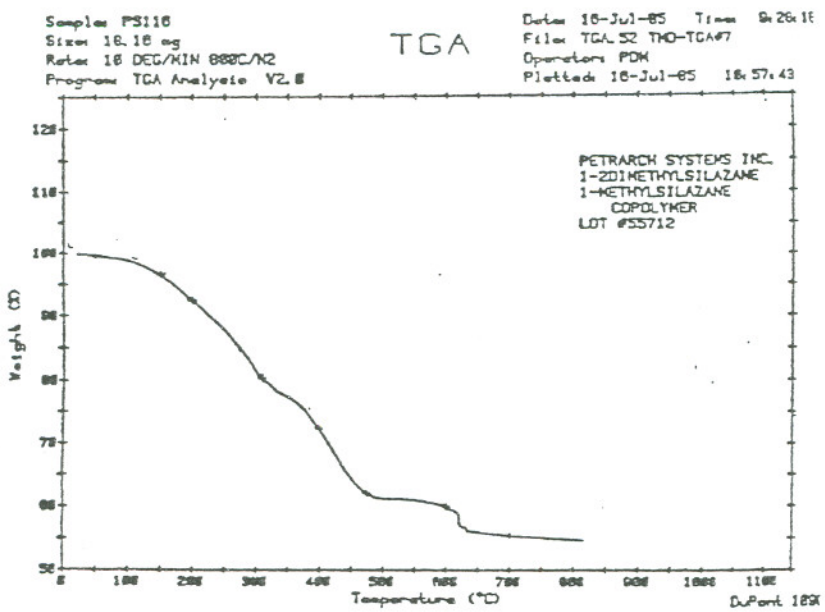

Figure 3.2 : Thermogravimetry of PS 116

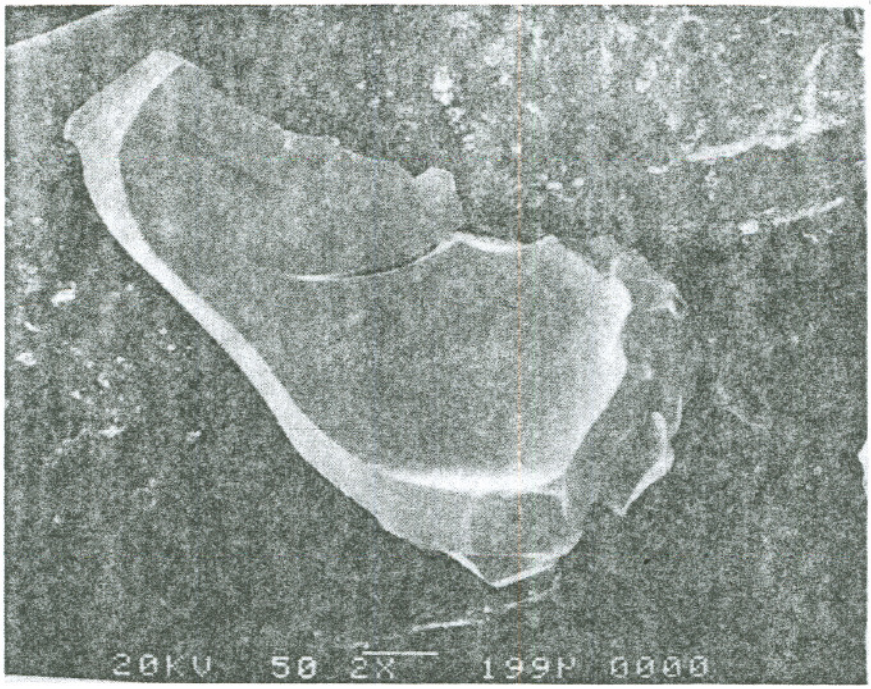

A

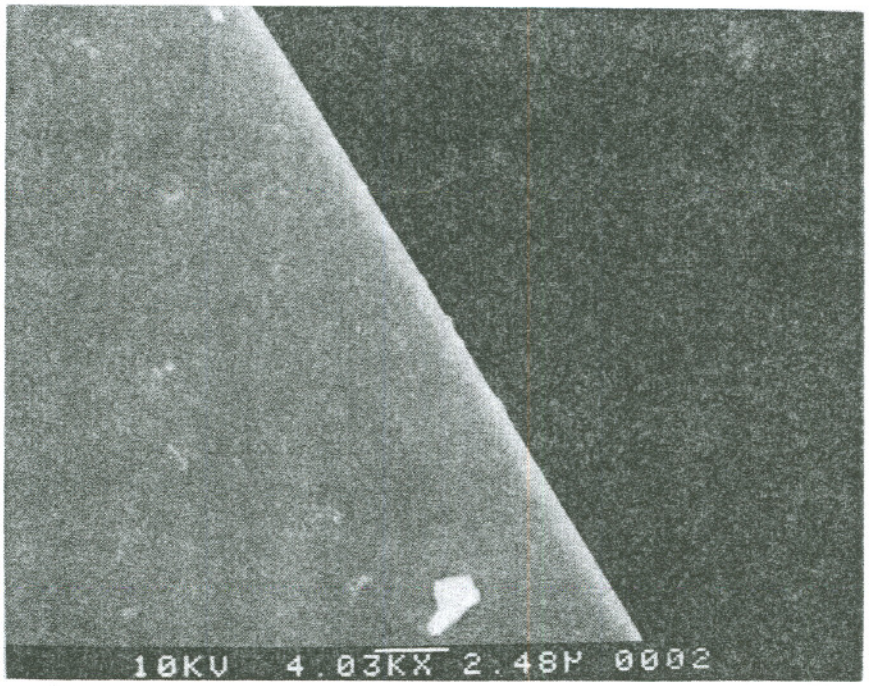

B

Figure 3.3 : Microstructure of pyrolyzed polysilazanes, 1000°C, N_2.

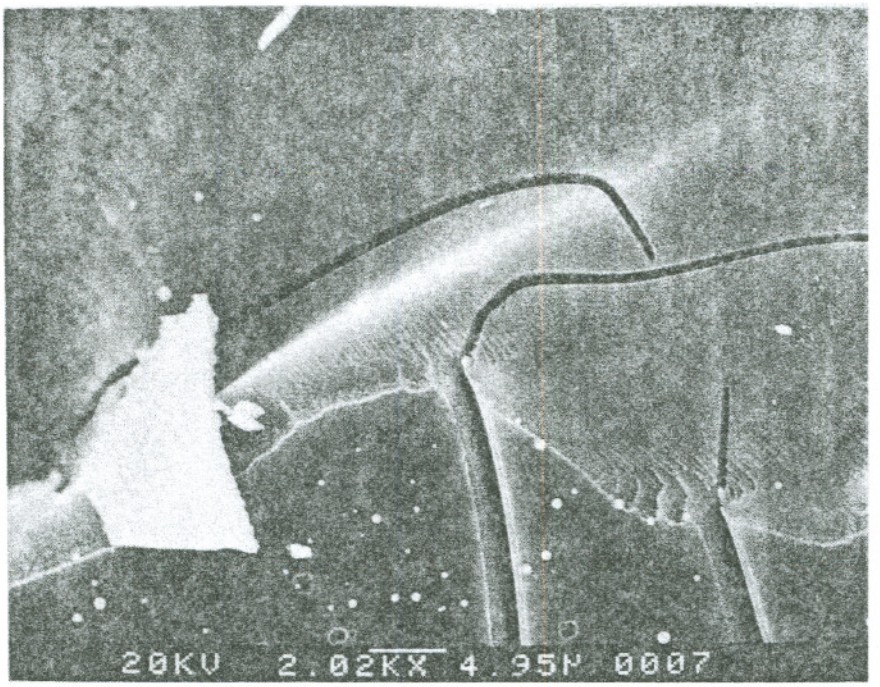

A

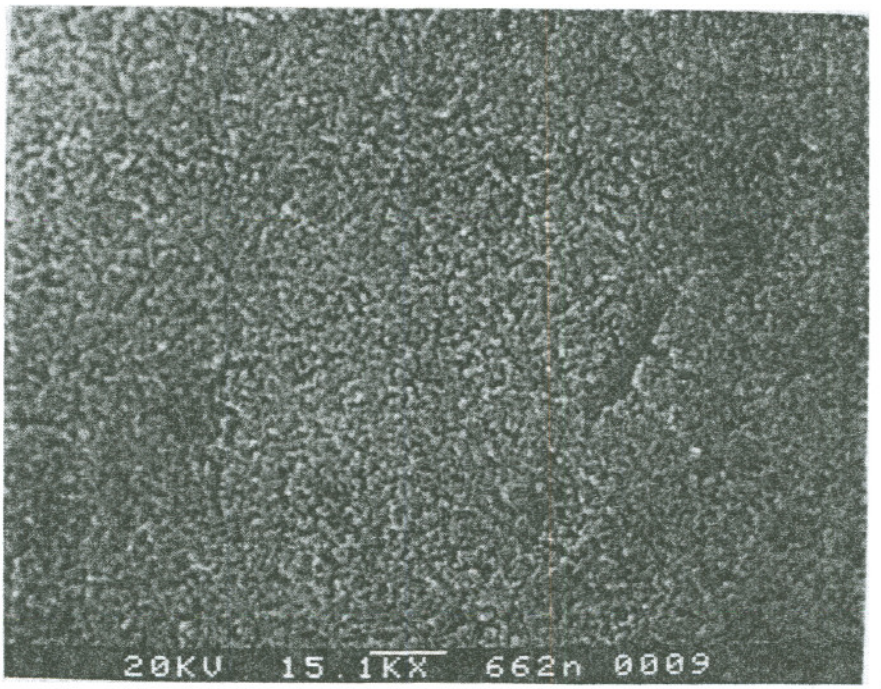

B

Figure 3.4 : Microstructure of pyrolyzed polysilazanes, 1400°C, N_2.

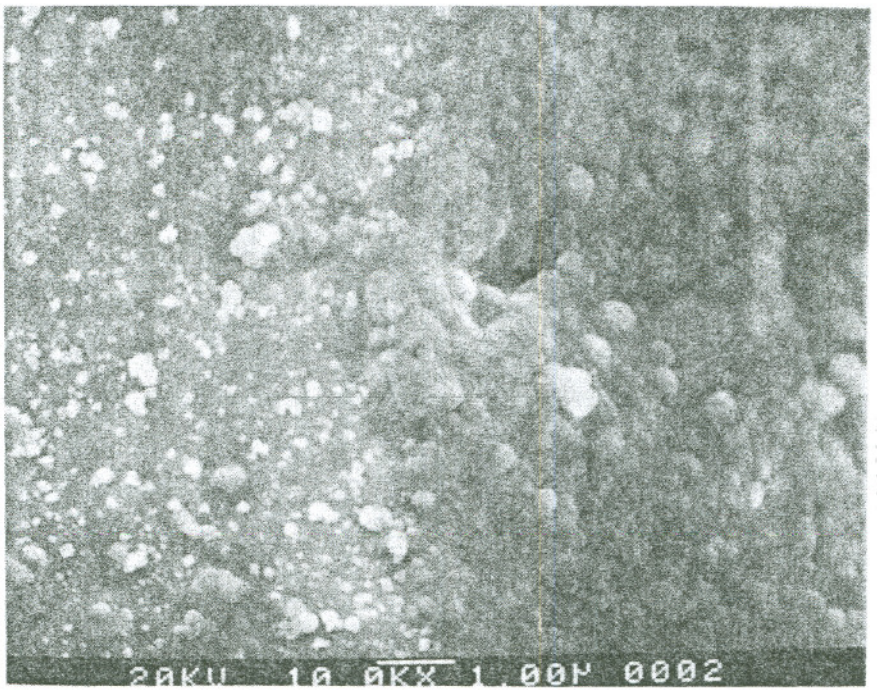

A

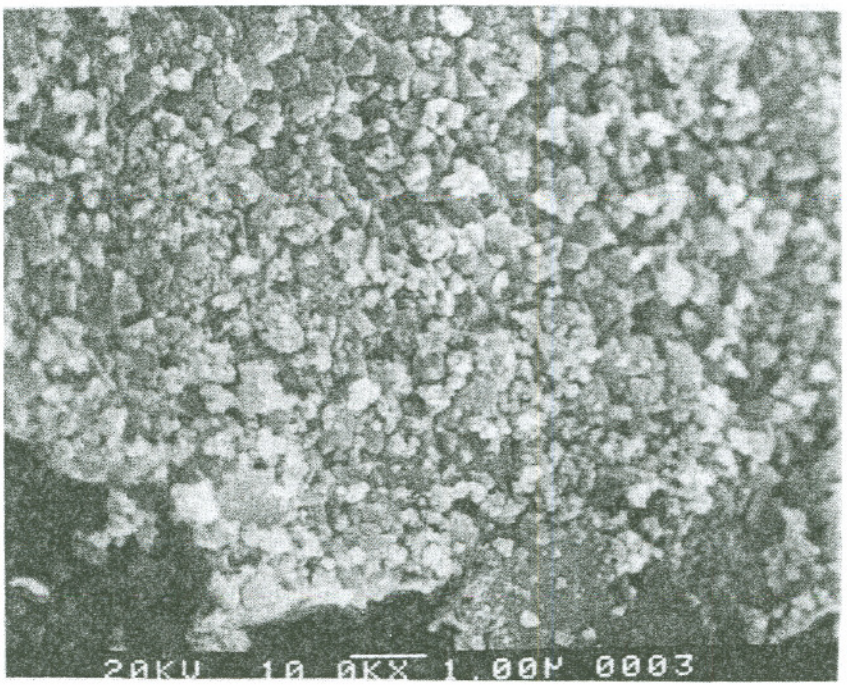

B

Figure 3.5 : Microstructure of pyrolyzed polysilazanes, 1600°C, N_2.

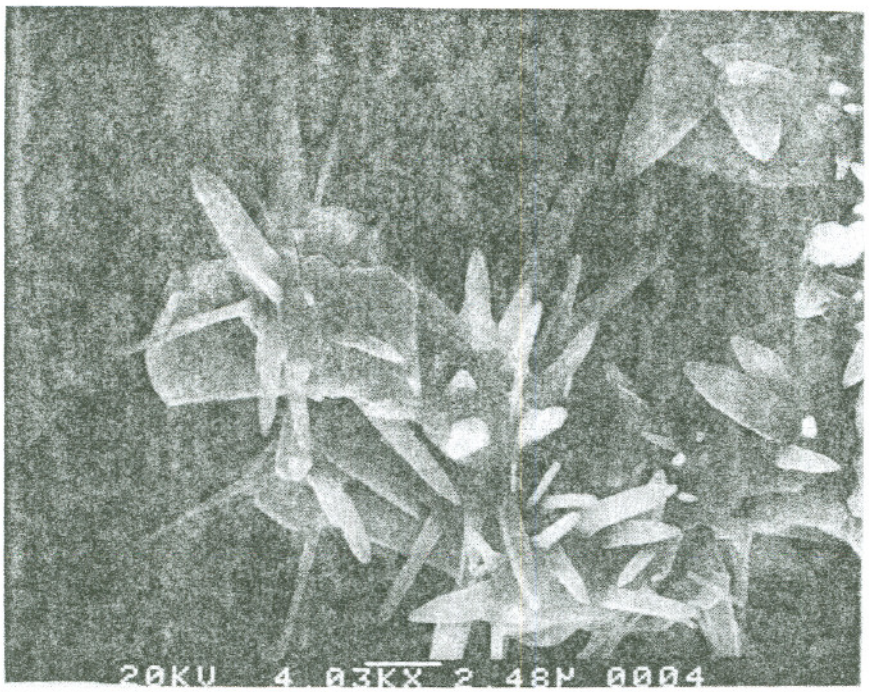

A

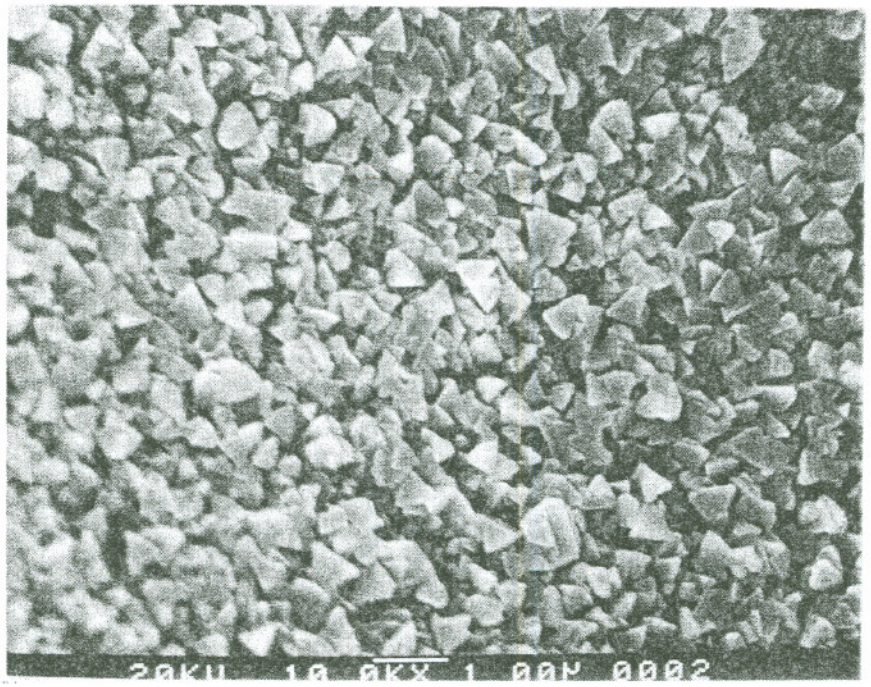

B

Figure 3.6 : Microstructure of pyrolyzed polysilazanes, 1700°C, N_2.

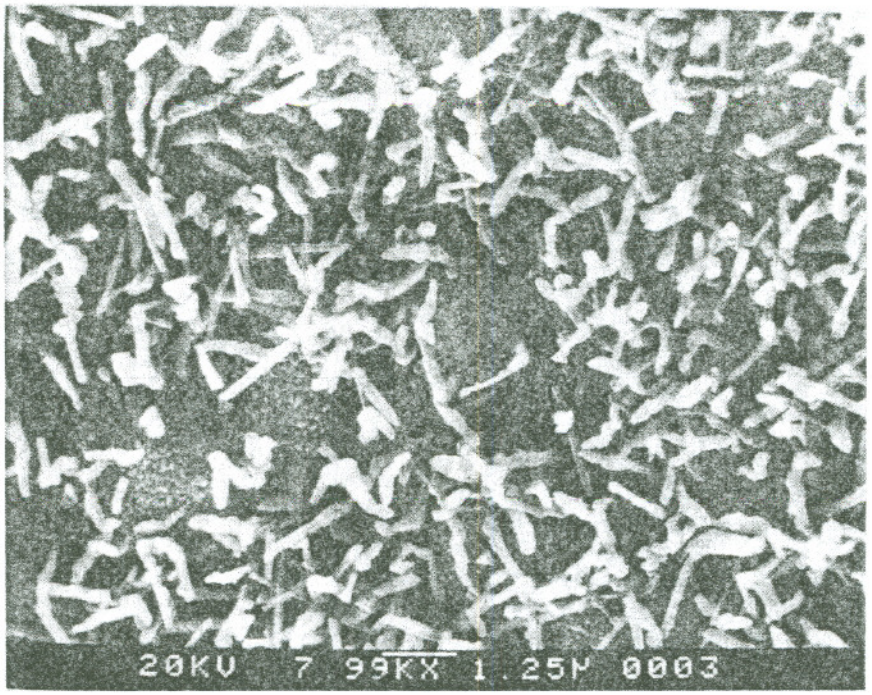

A

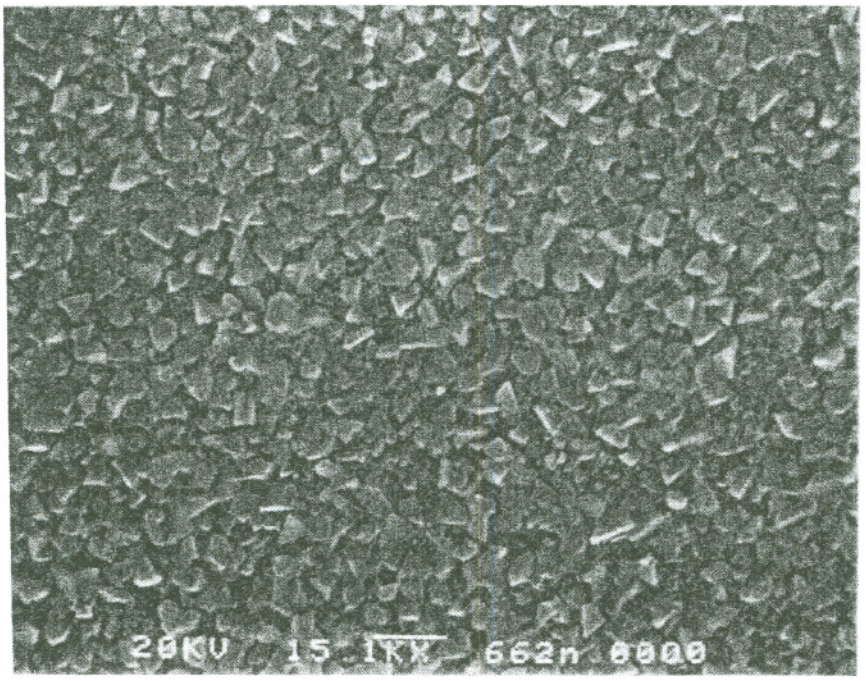

B

Figure 3.7 : Microstructure of pyrolyzed polysilazanes, 1400°C, vacuum.

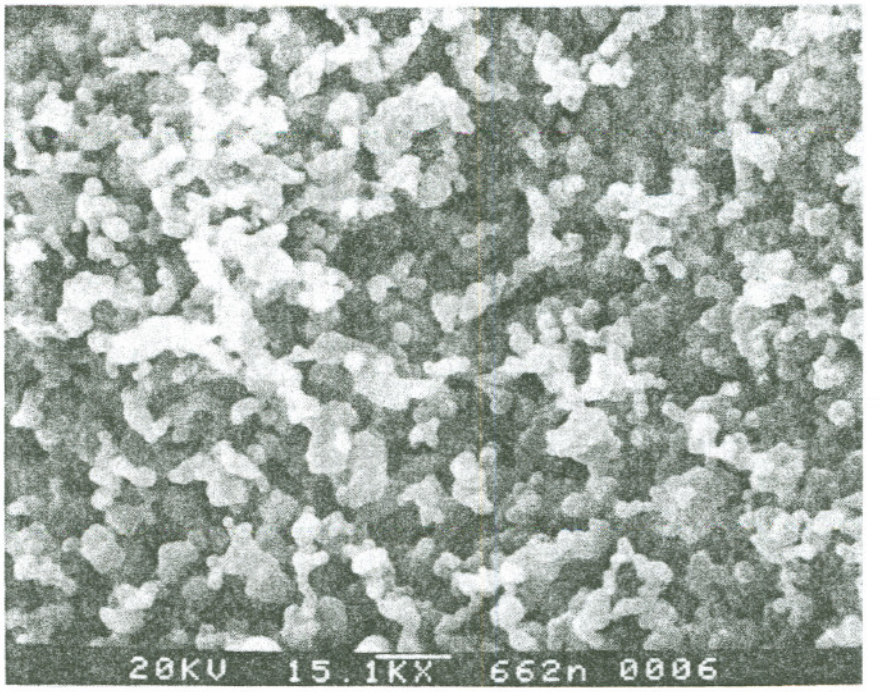

A

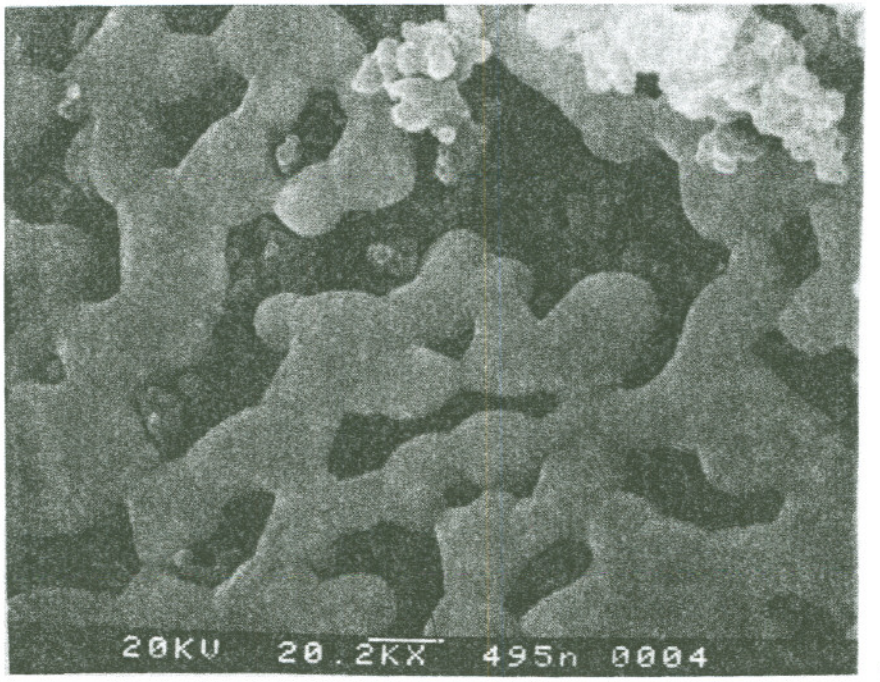

B

Figure 3.8 : Microstructure of pyrolyzed polysilazanes, 1500°C, vacuum.

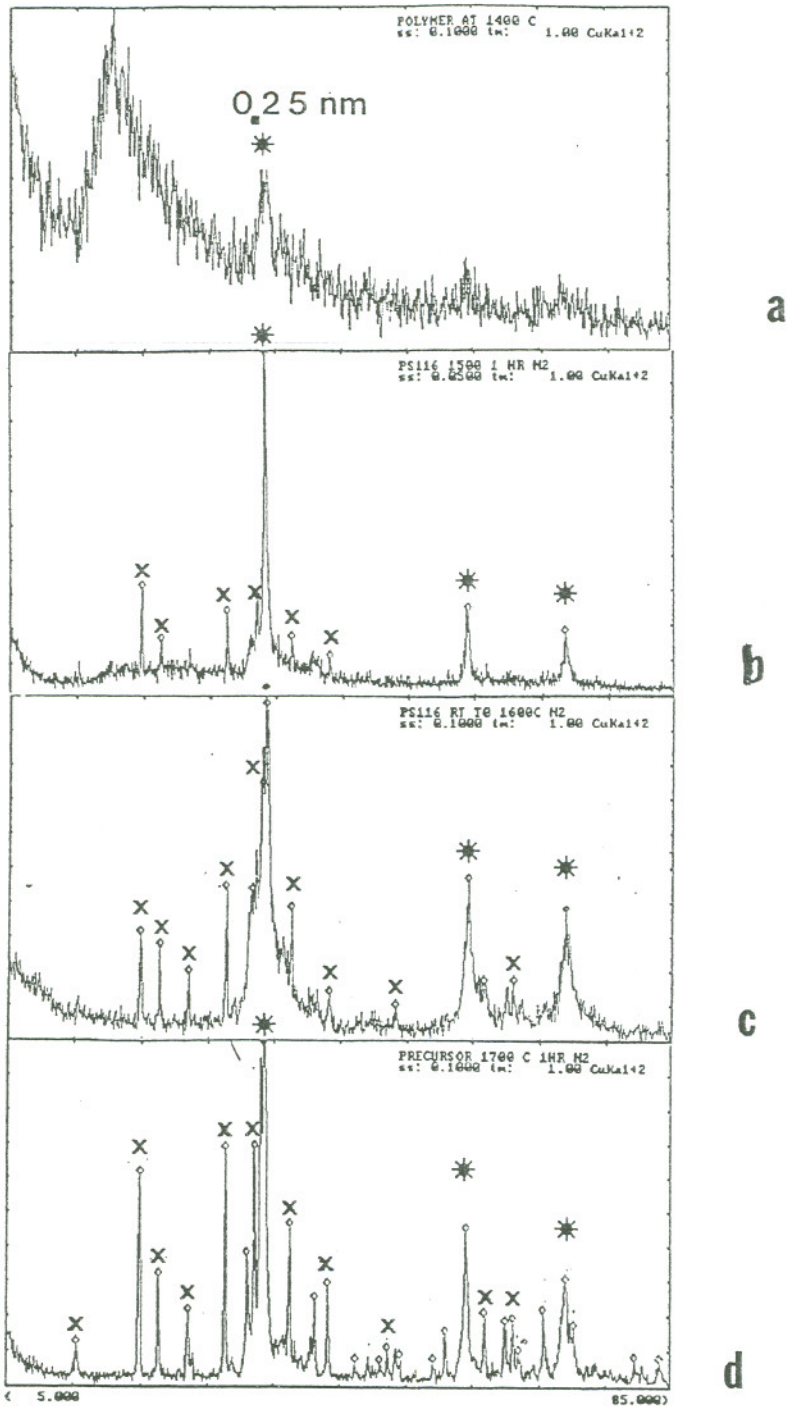

Figure 3.9 : X-ray diffraction spectra of pyrolyzed polysilazanes (N_2)
a: 1400°C, b: 1500°C, c: 1600°C, d: 1700°C.

✳ β-SiC
× α-Si_3N_4

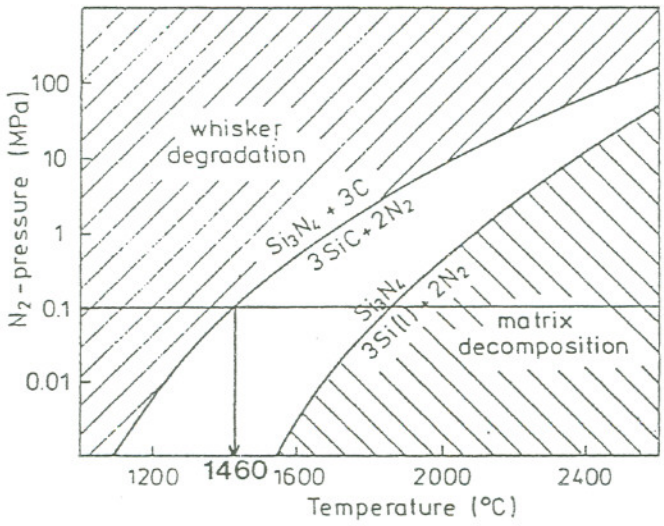

Figure 3.10 : Thermal stability diagram of SiC and Si_3N_4 in N_2.

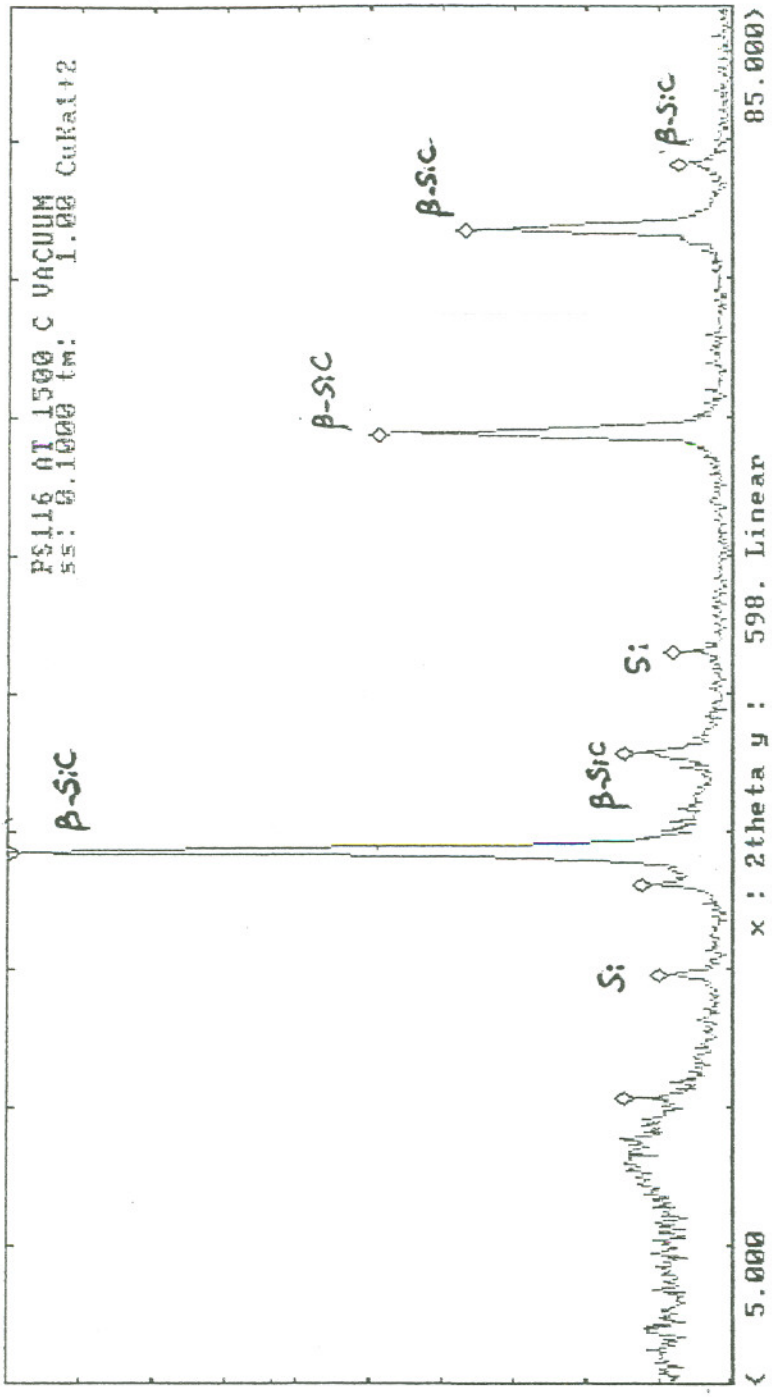

Figure 3.11 : X-ray diffraction spectrum of polysilazanes pyrolyzed at 1500°C in vacuum.

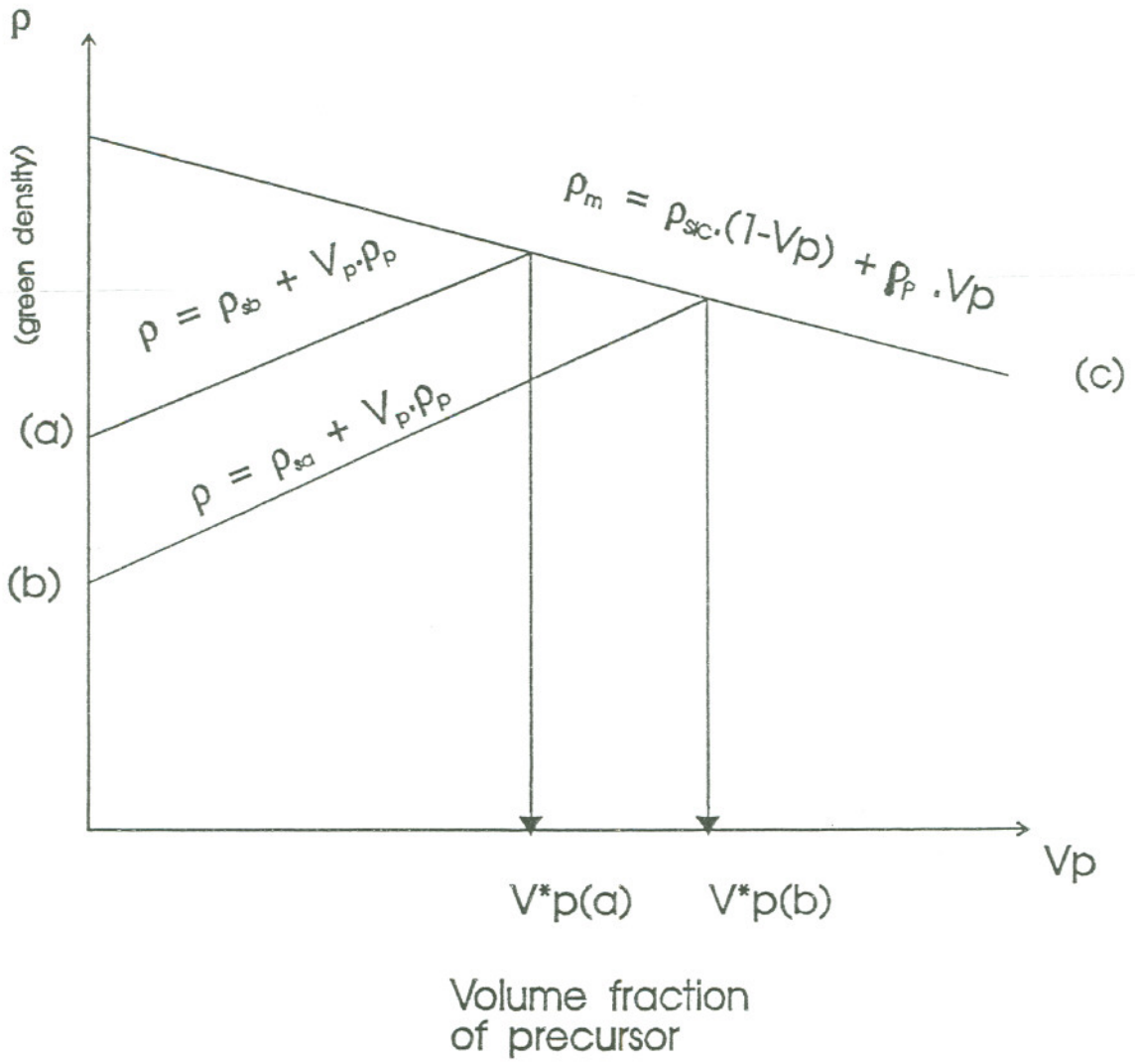

Figure 4.1 : Selection rule for initial precursor content.

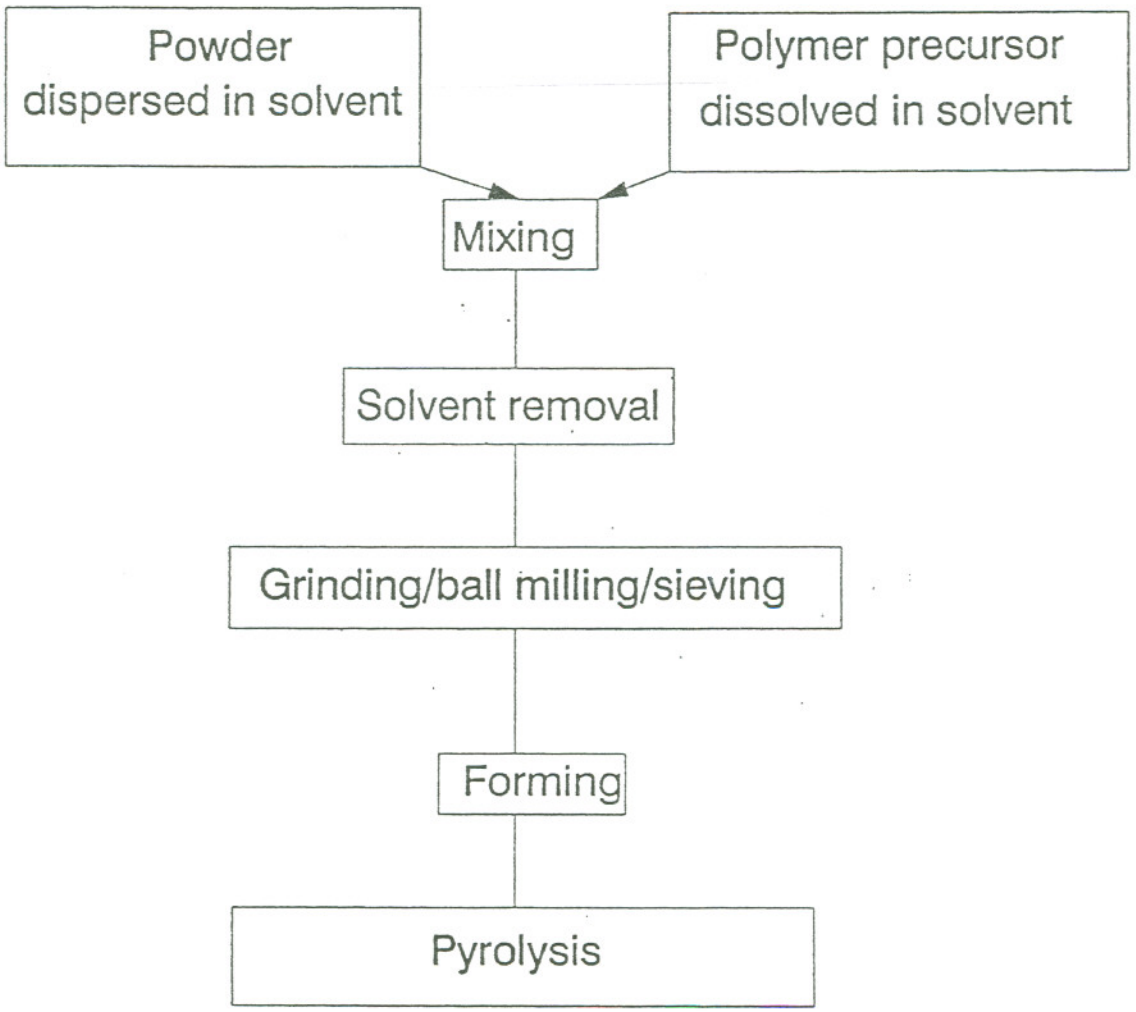

Figure 4.2 : Flow chart for conventional processing

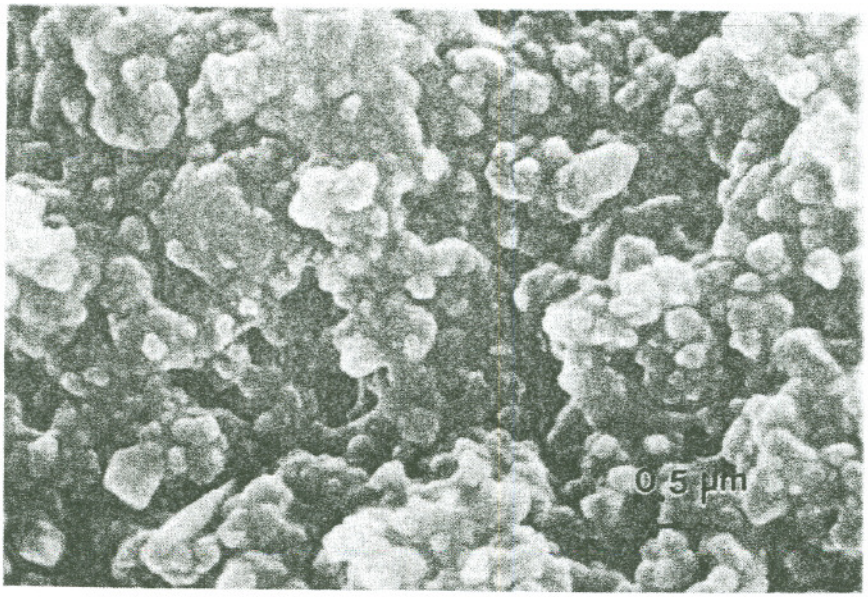

Figure 4.3 : Powder/ polysilazane mixture (conventional processing)

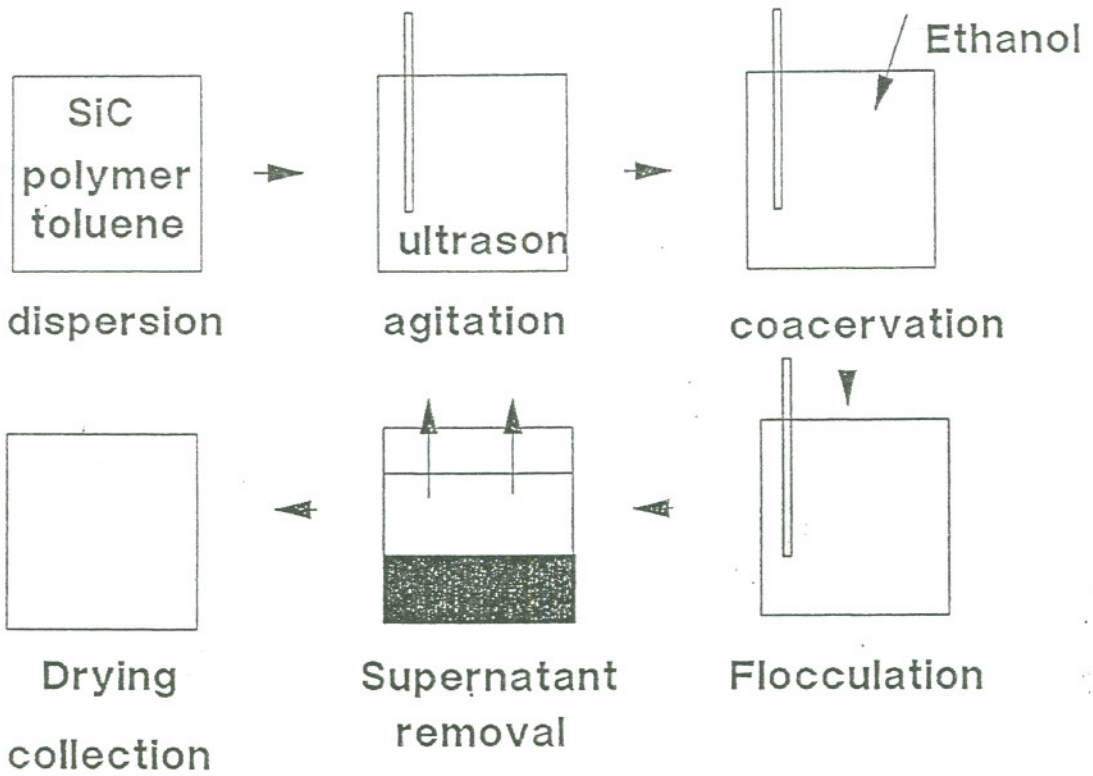

Figure 4.4 : Micro-encapsulation flow chart.

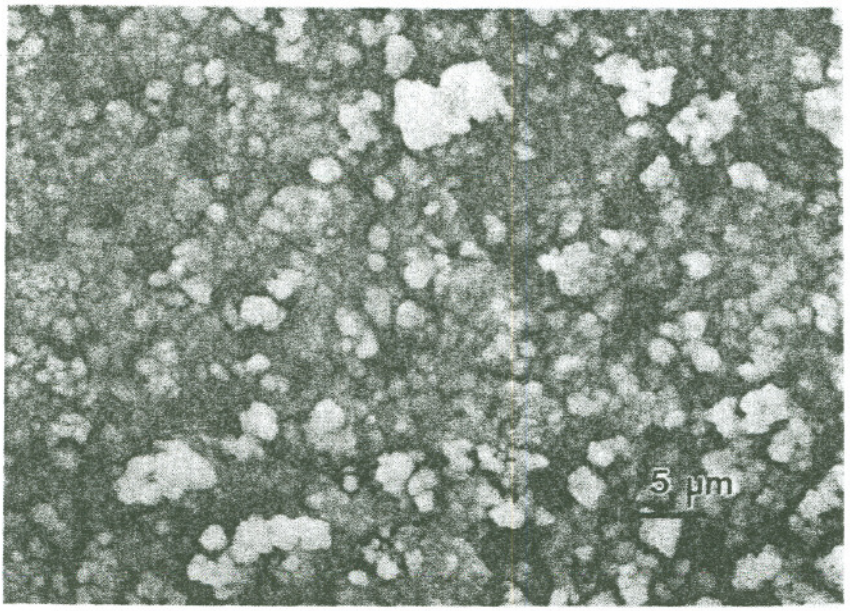

Figure 4.5 : Micro-encapsulated SiC powder

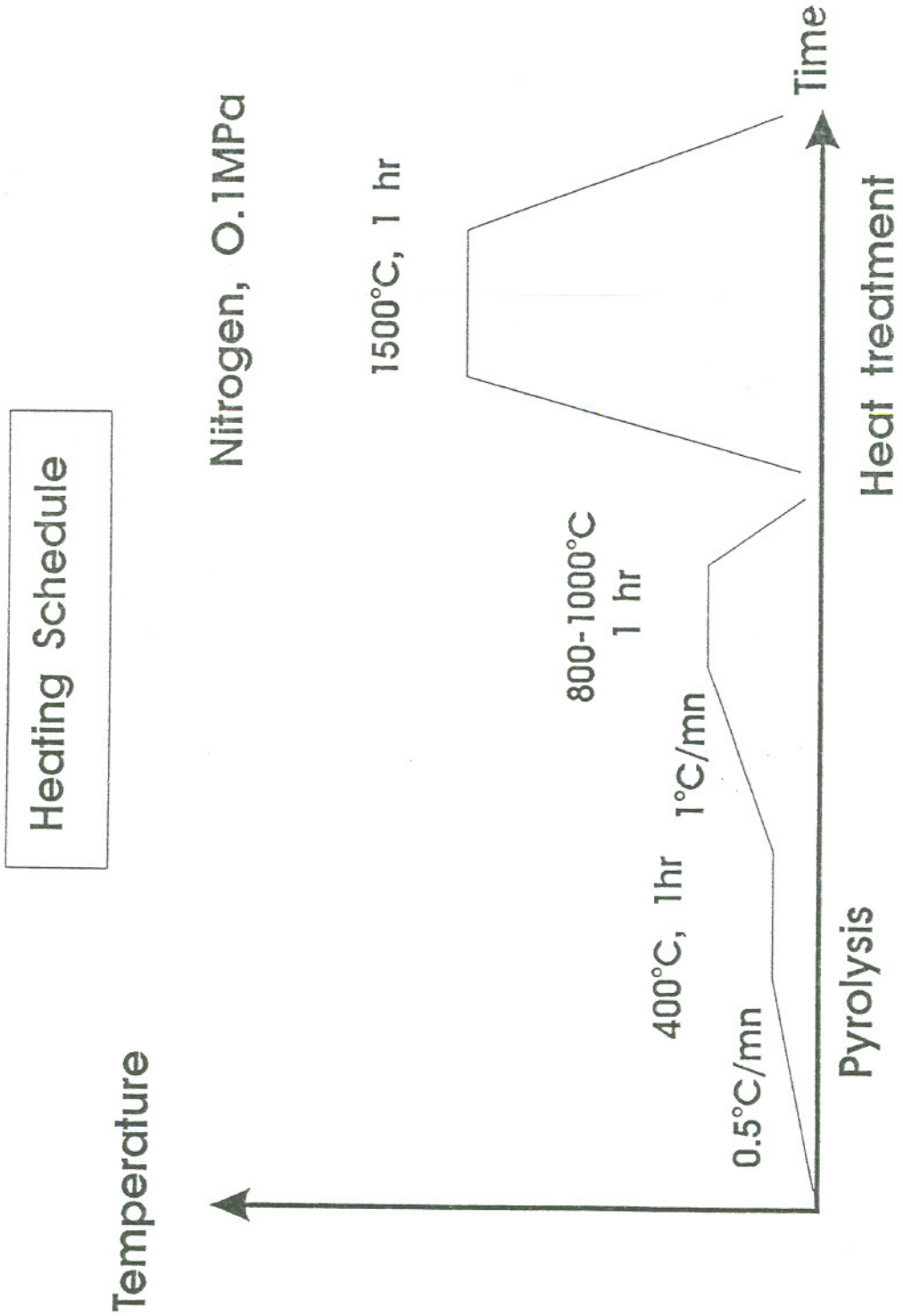

Figure 4.6 : Heating schedule for 20 wt% PS 116 / SiC samples.

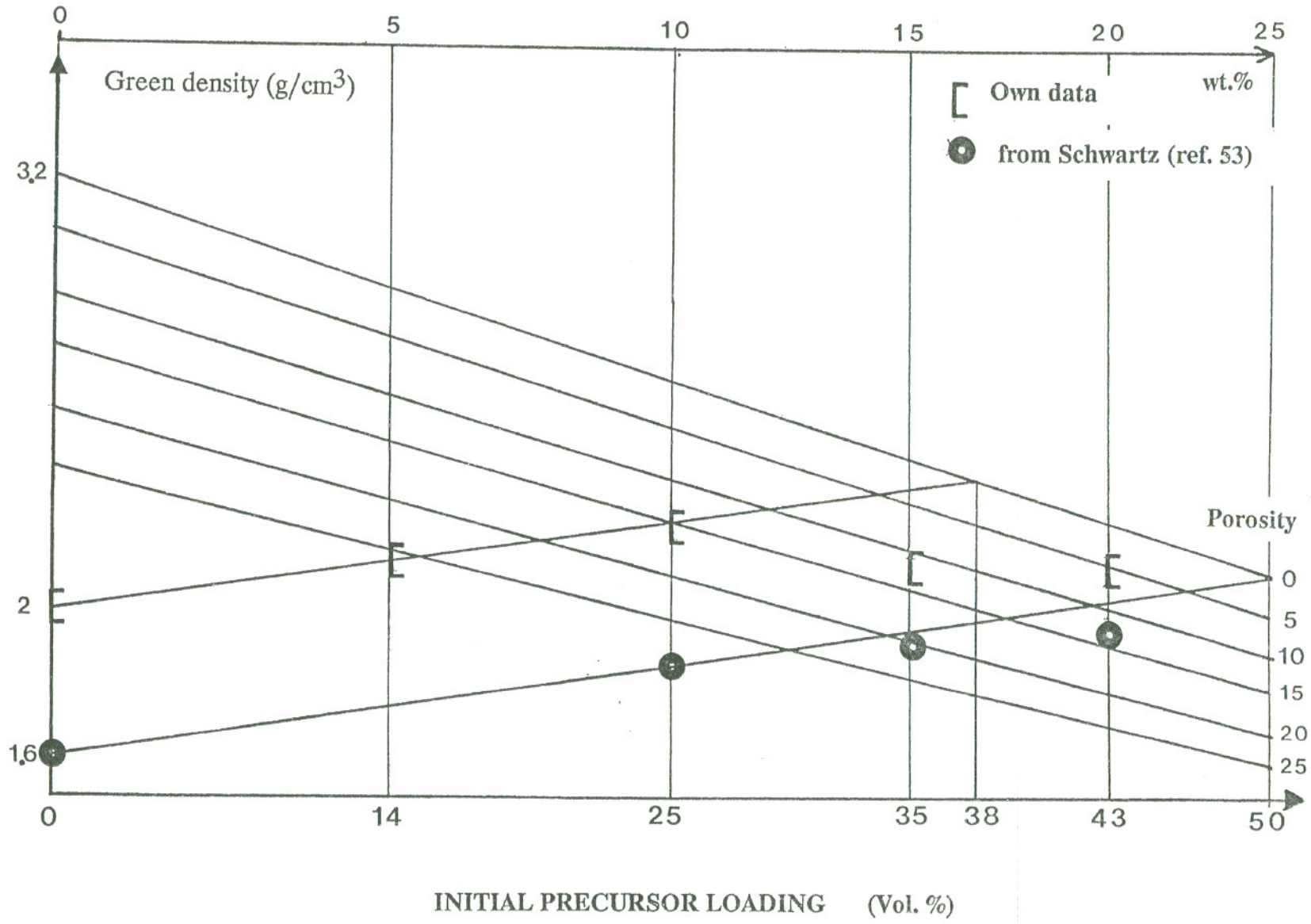

Figure 4.7 : Measured green densities vs. precursor content.

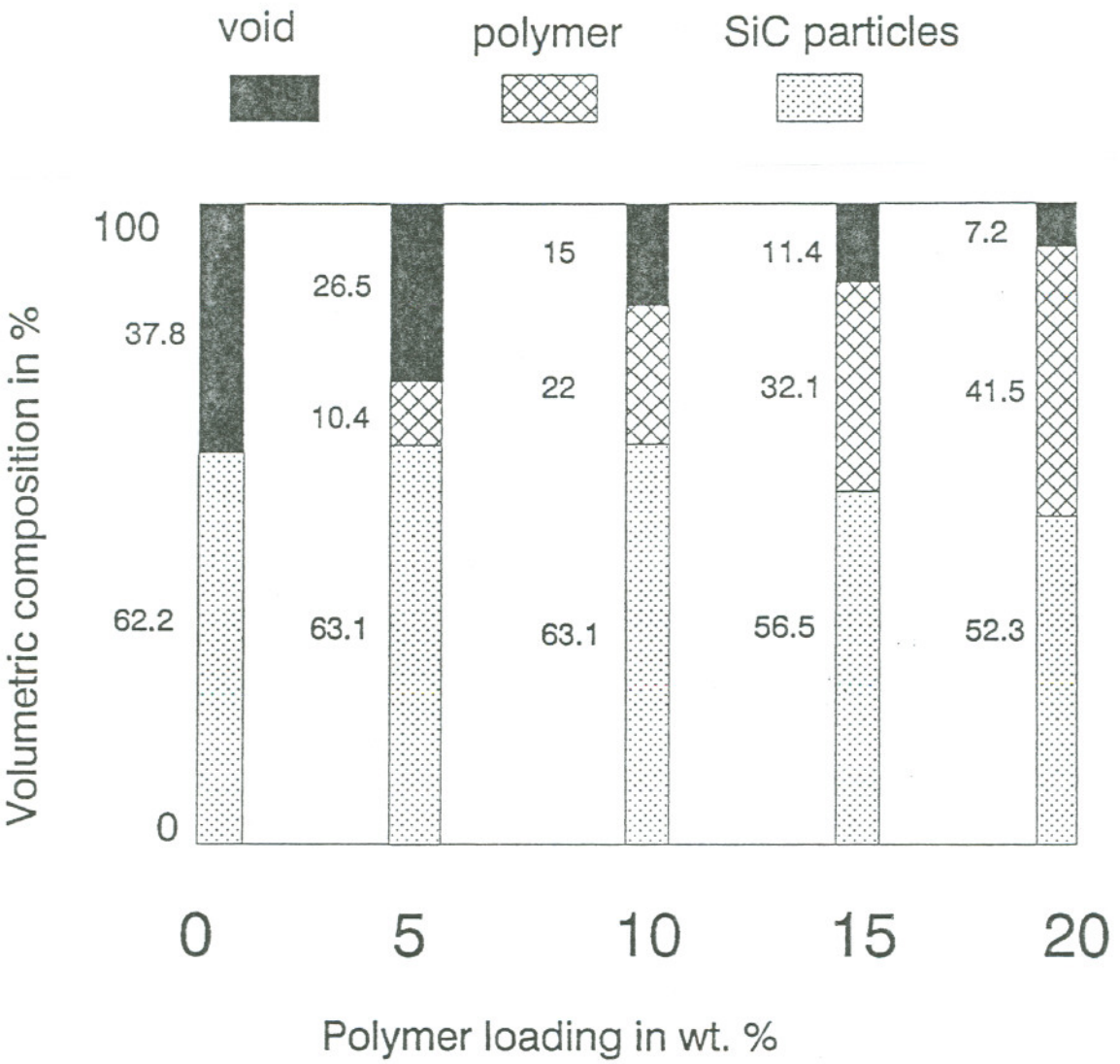

Figure 4.8 : Volumetric composition as a function of initial precursor content.

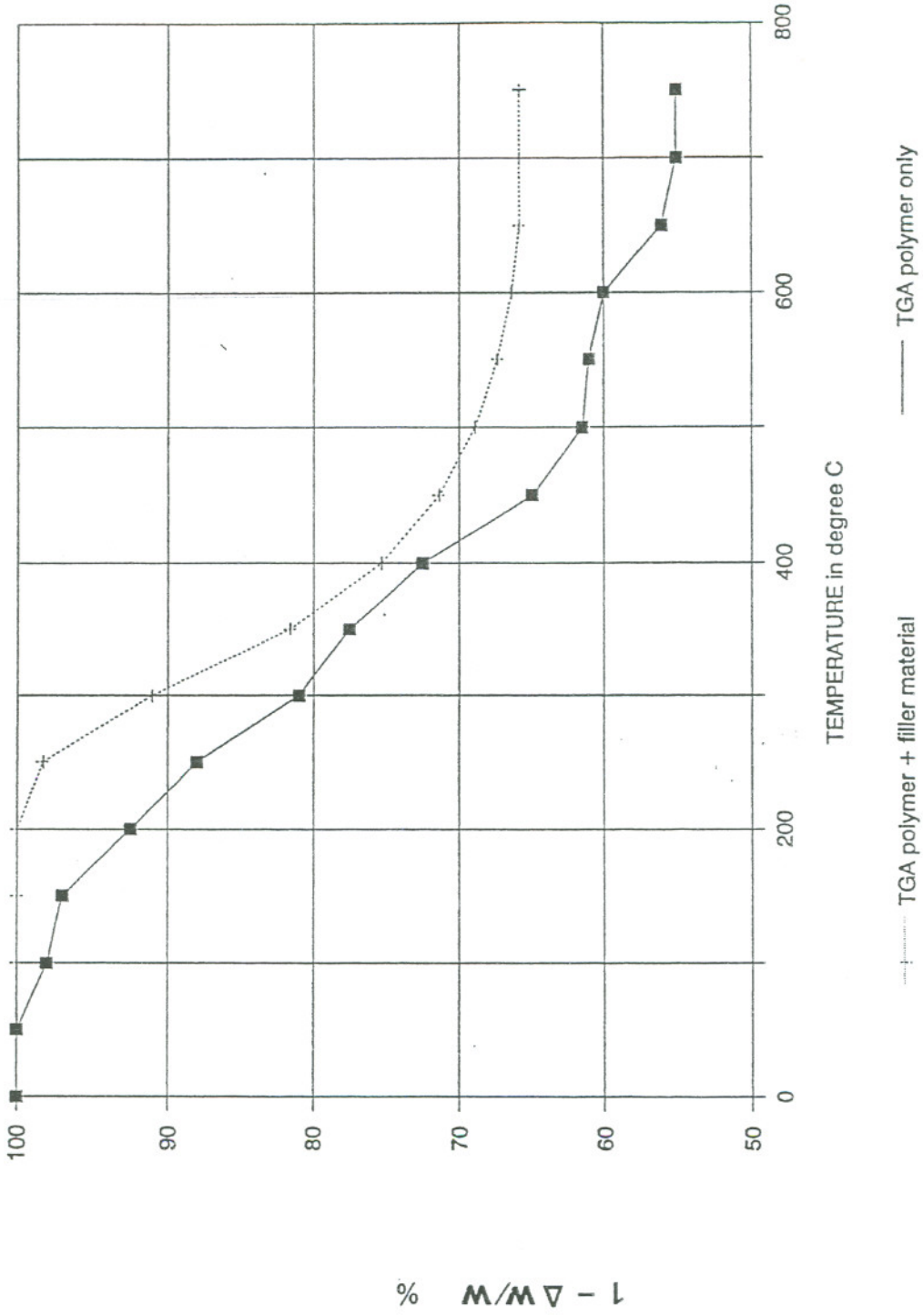

Figure 4.9 : Comparison of pyrolysis behaviors : Precursor vs. Precursor + SiC.

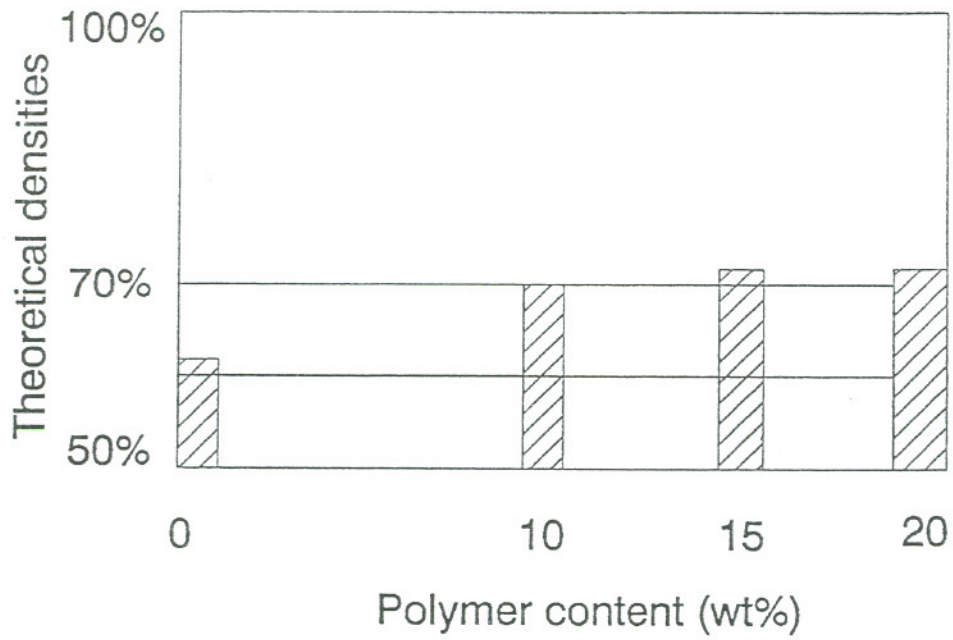

Figure 4.10 : Densities (relative to ρ_{SiC}) of pyrolyzed samples.

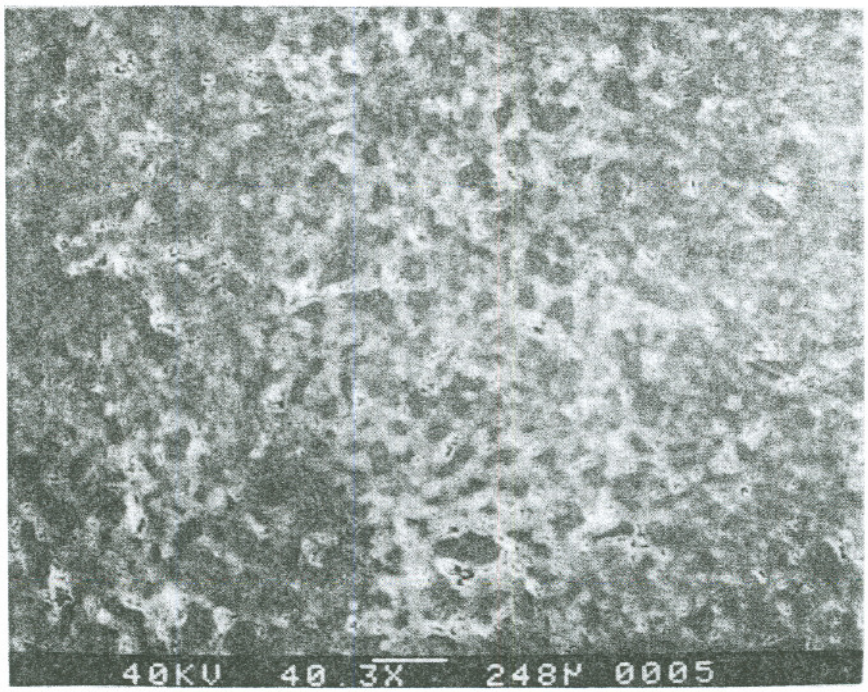

Figure 5.1 : Polished surface of sample pyrolyzed at 800°C.

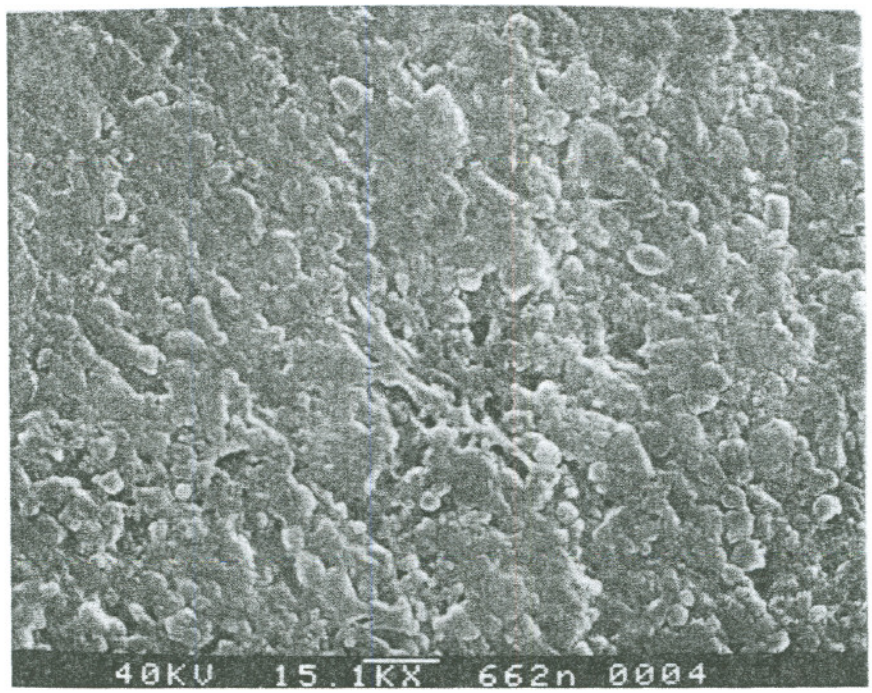

Figure 5.2 : High magnification of sample pyrolyzed at 800°C, showing dense area.

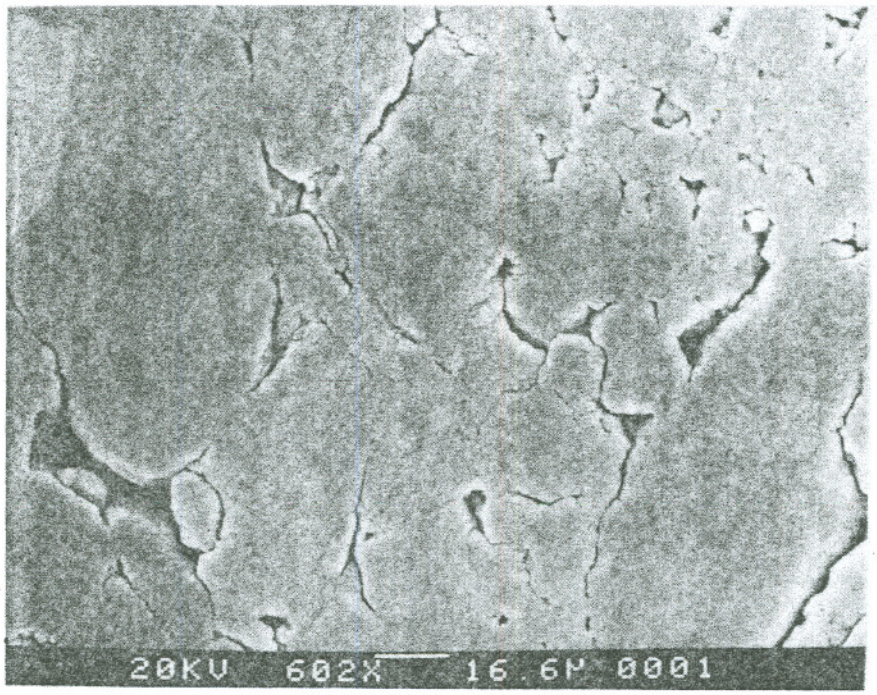

A

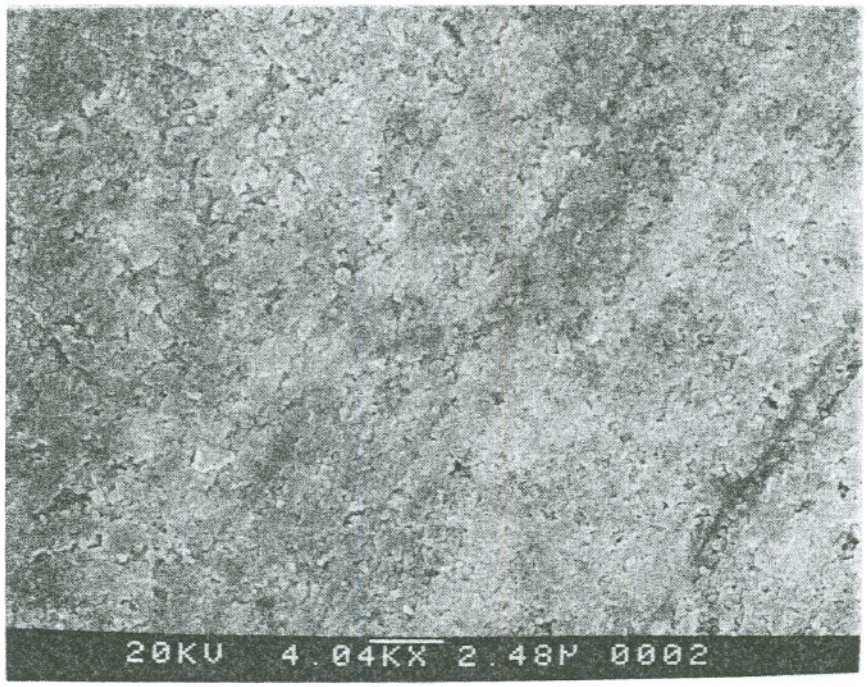

B

Figure 5.3 : Polished surface of sample pyrolyzed at 1000°C.

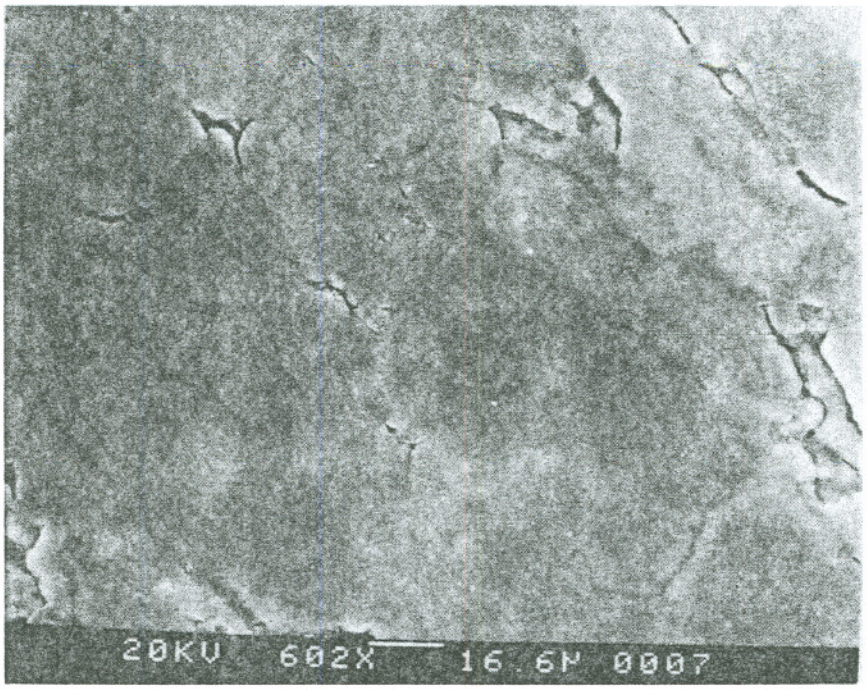

A

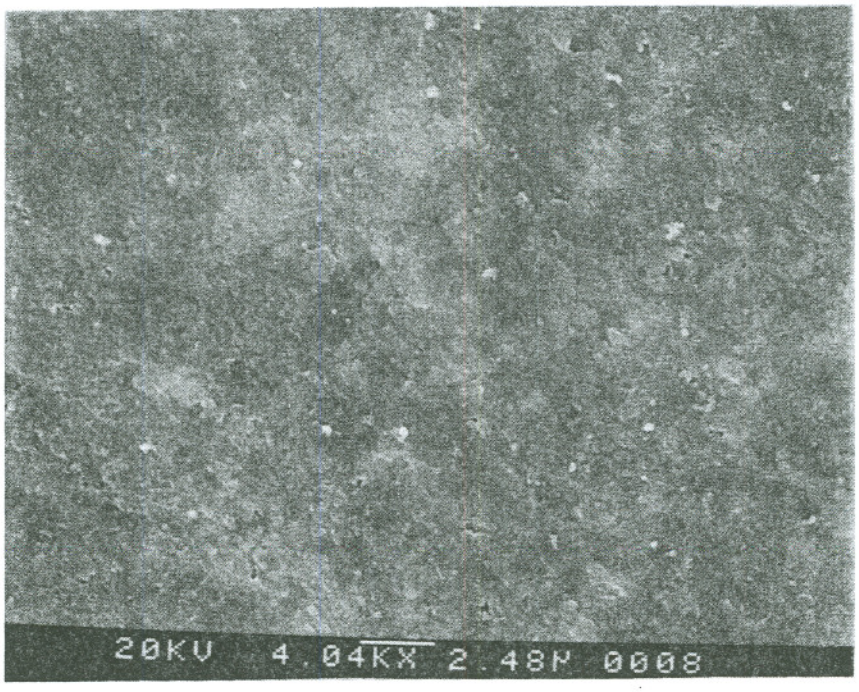

B

Figure 5.4 : Polished surface of sample pyrolyzed at 1200°C.

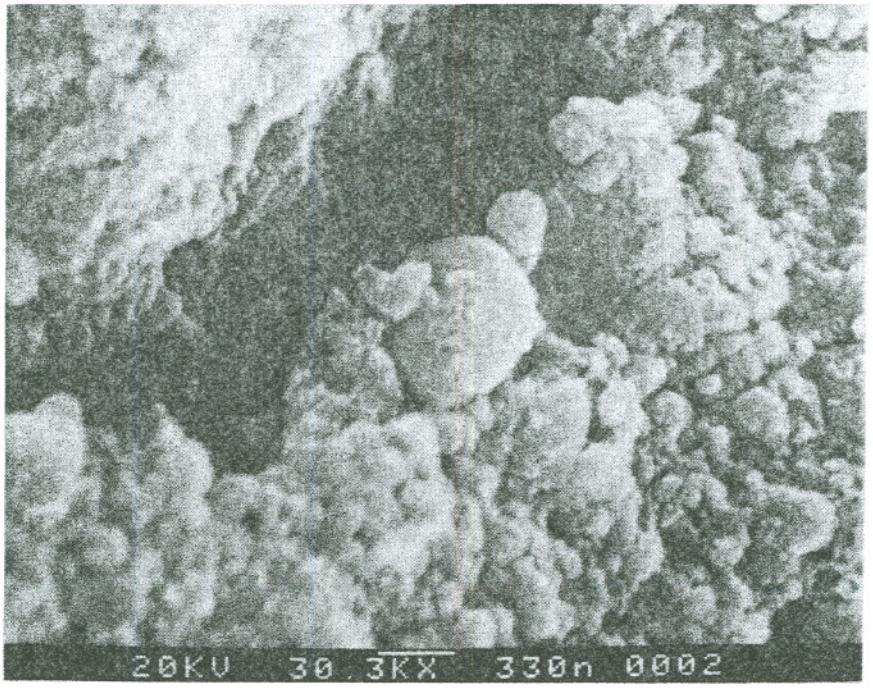

Figure 5.5 : Evidence of precursor derived phase (1000°C, N_2)

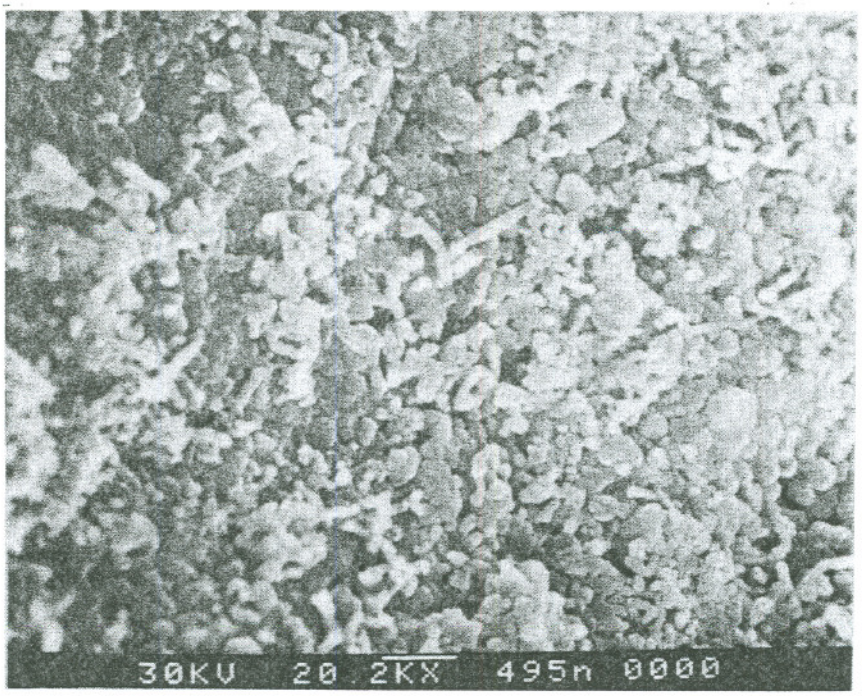

Figure 5.6 : Fracture surface of pyrolyzed sample (1500°C, N_2)

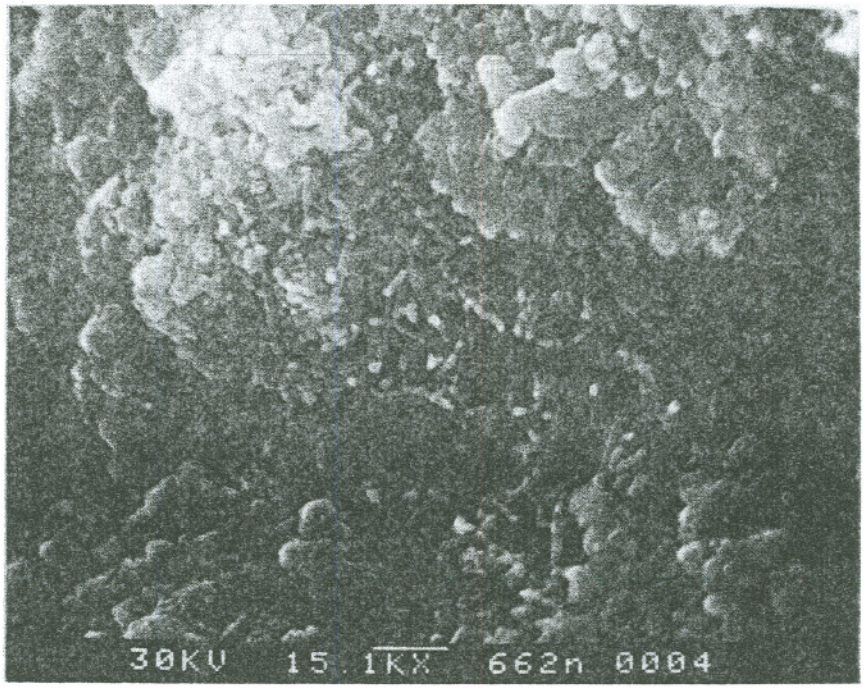

Figure 5.7 : Presence of whiskers in less dense regions.

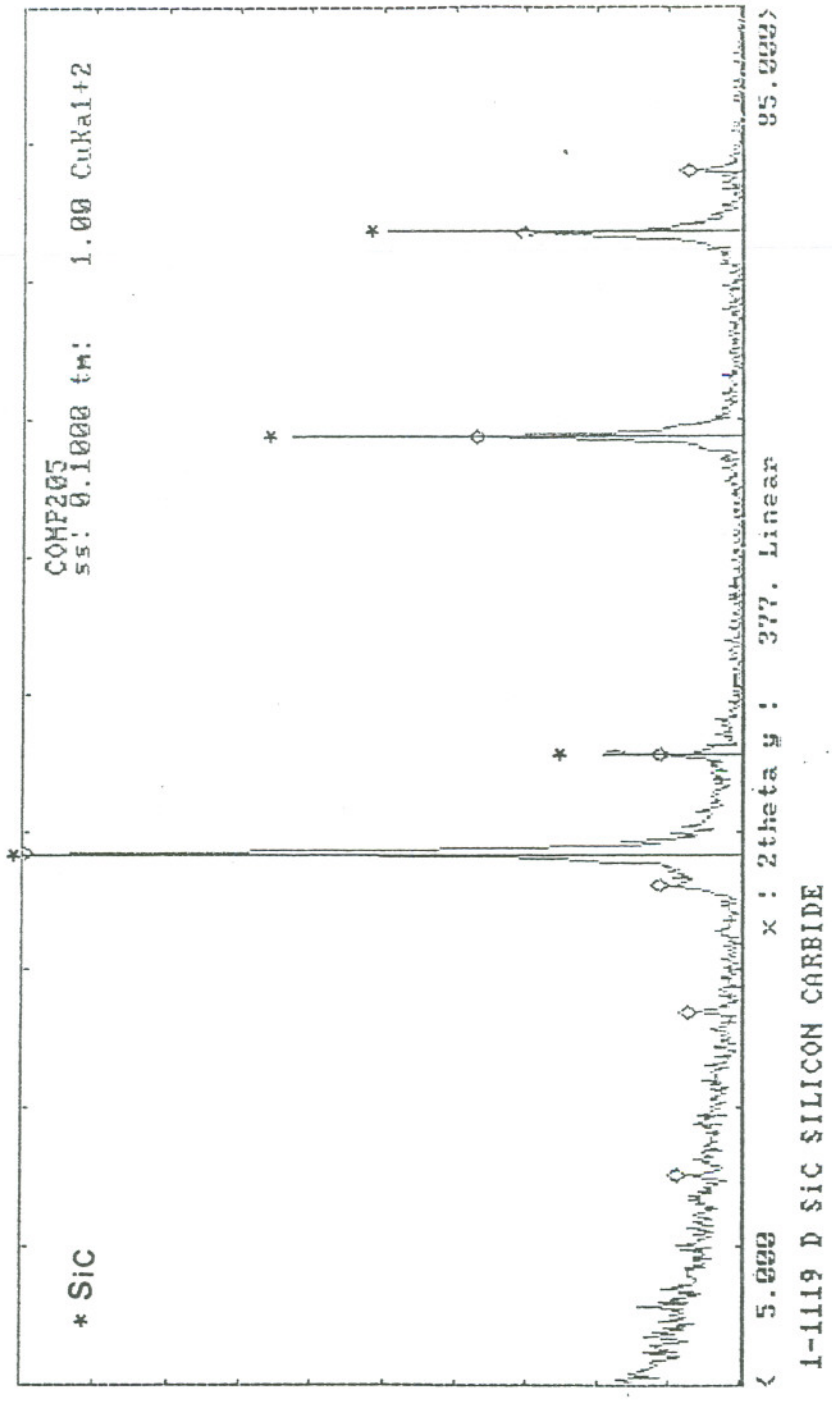

Figure 5.8 : X-ray diffraction of pyrolyzed sample (1500°C, N_2).

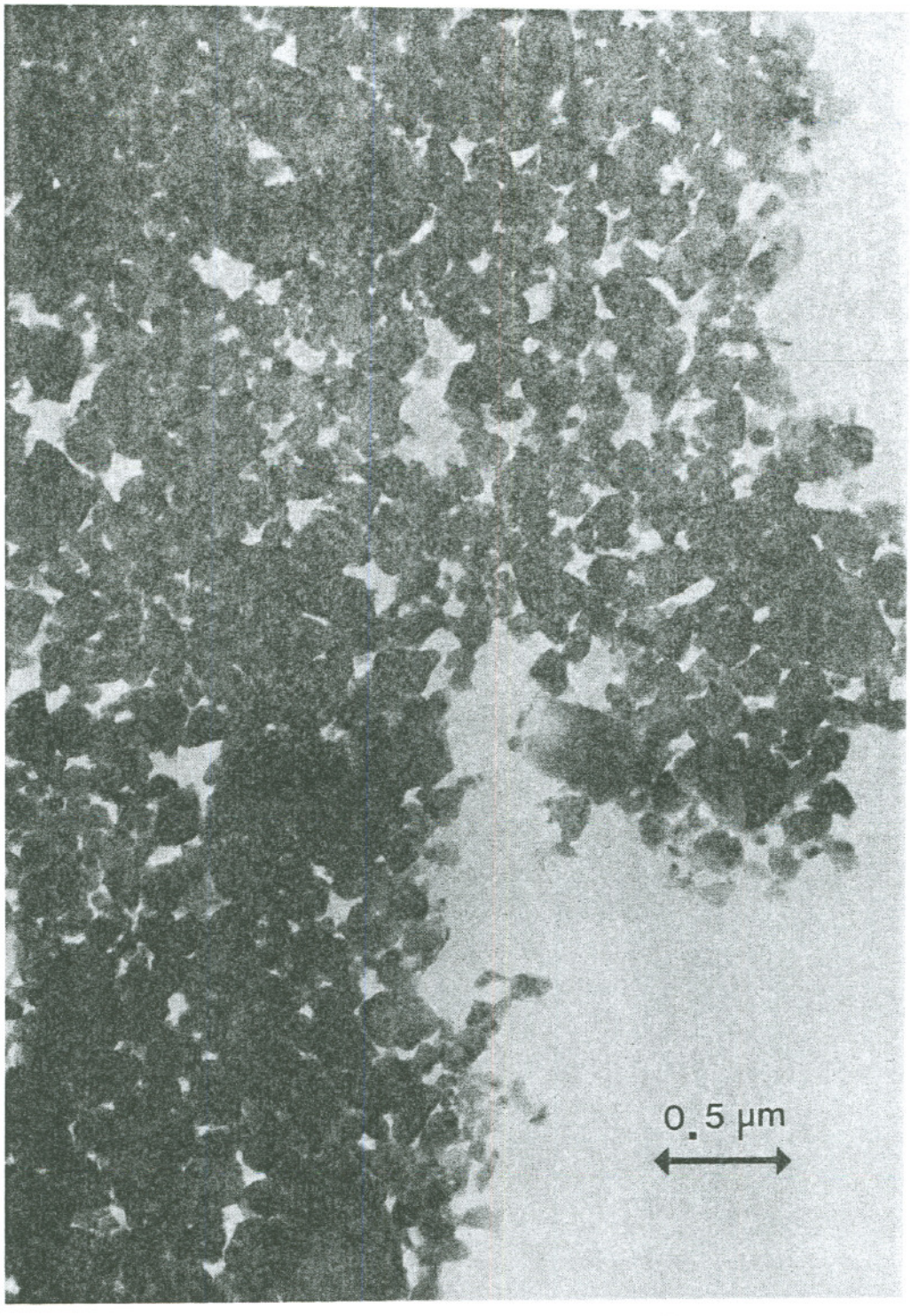

Figure 5.9 : TEM of pyrolyzed sample.

Figure 5.10 : Electron diffraction ring pattern : microcrystalline SiC.

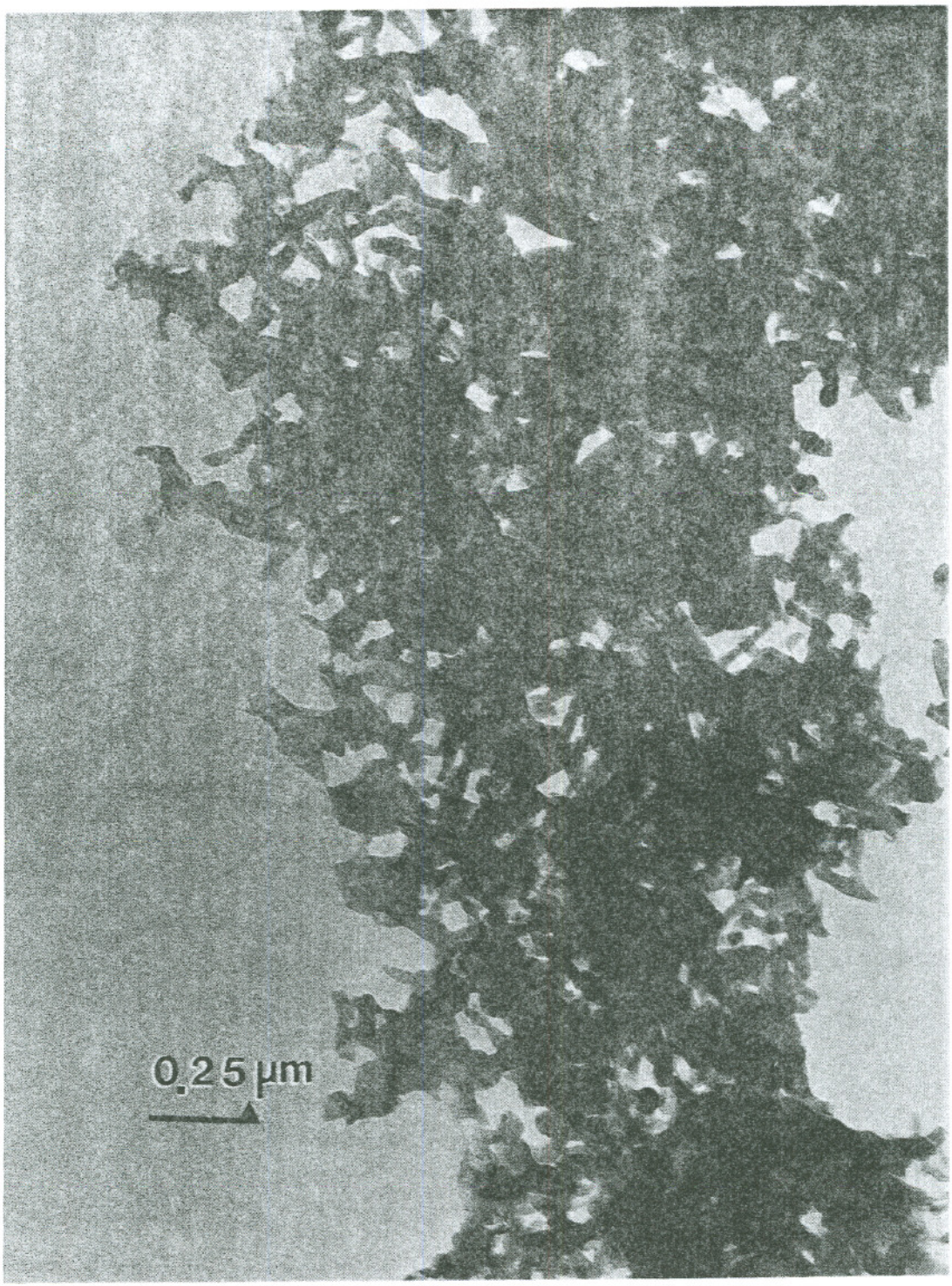

Figure 5.11 : TEM of elongated features (polymer derived phase).

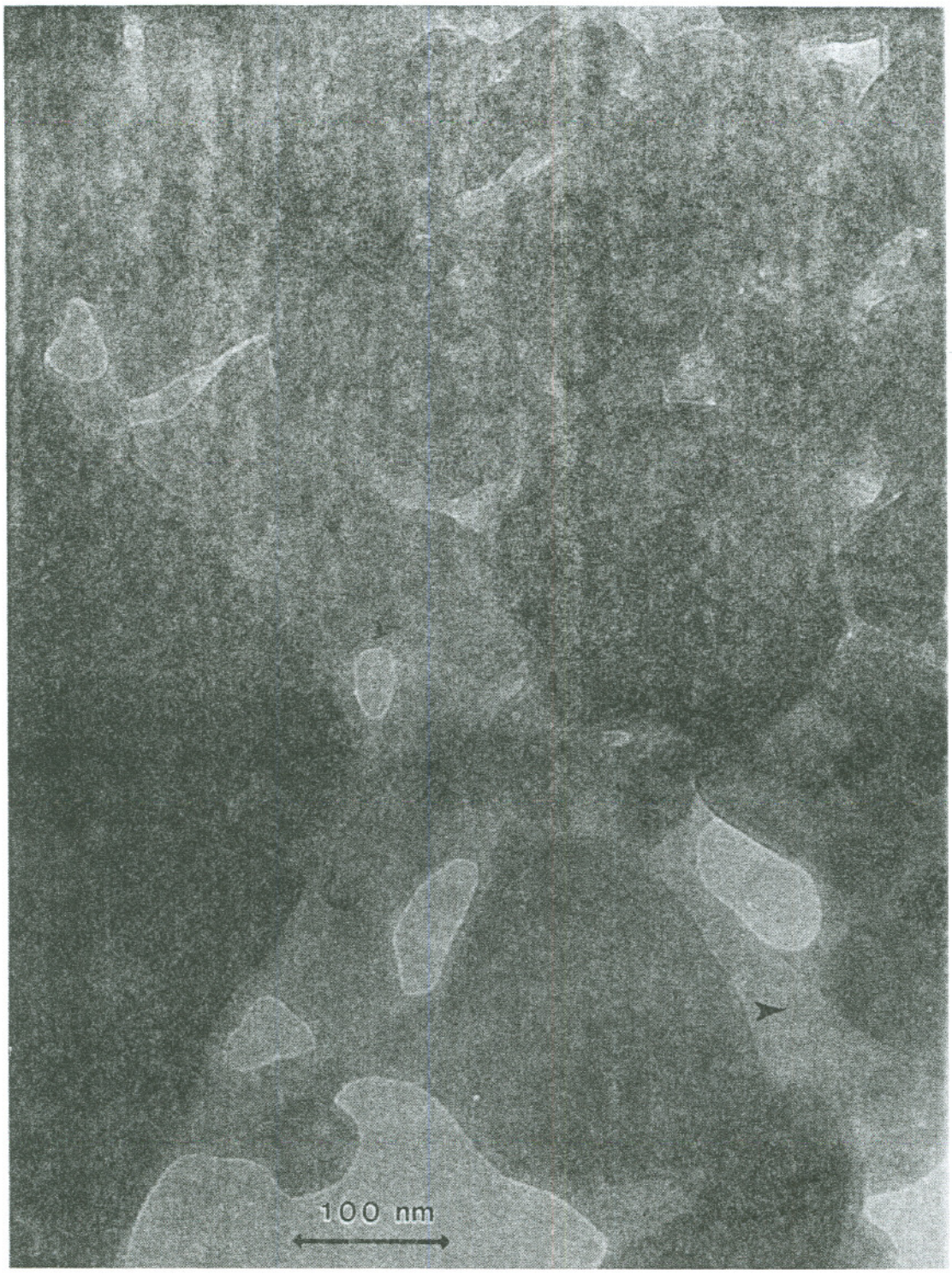

Figure 5.12 : TEM of amorphous phase (pdp) binding SiC particles.

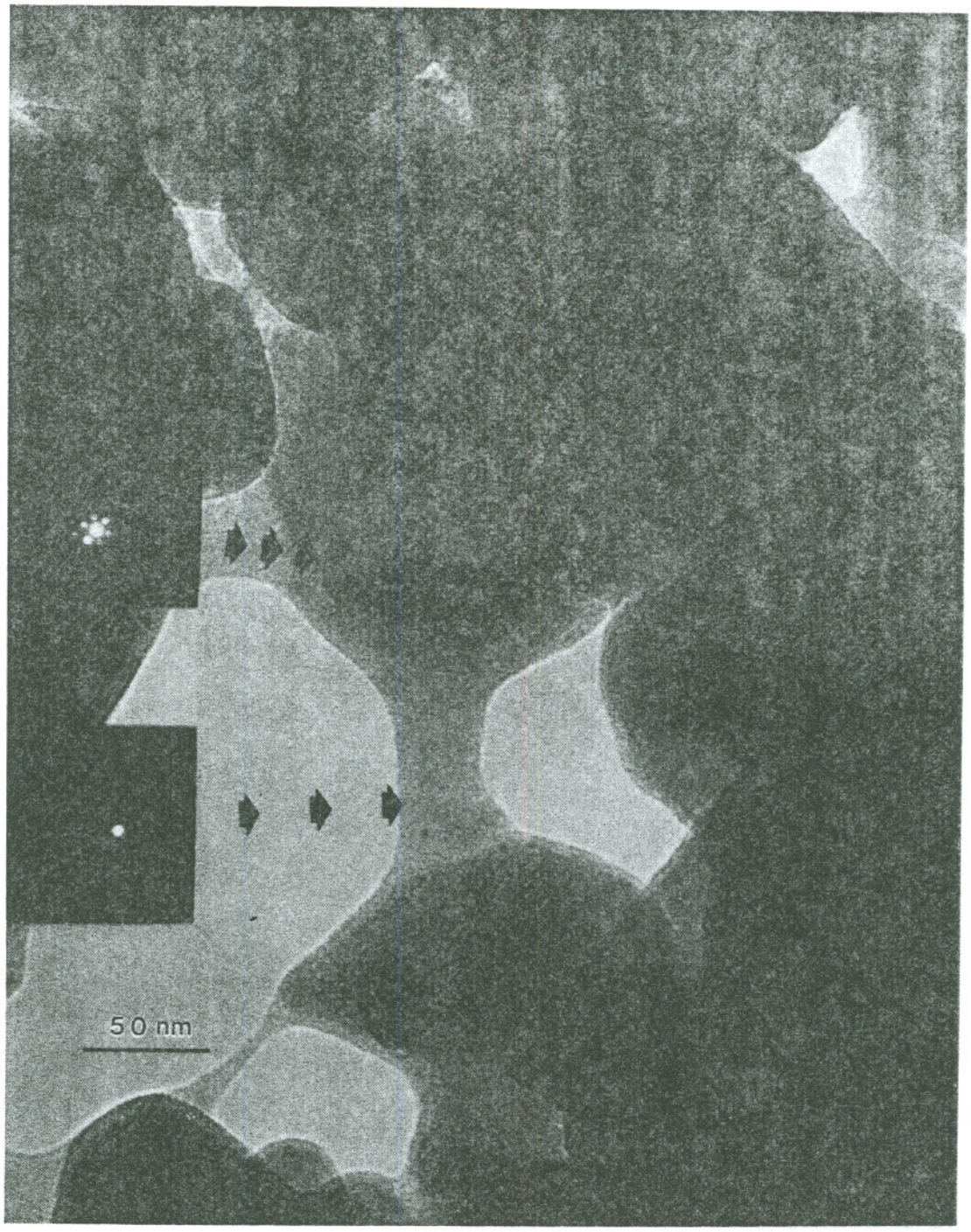

Figure 5.13 : TEM and microdiffraction of amorphous bridge.

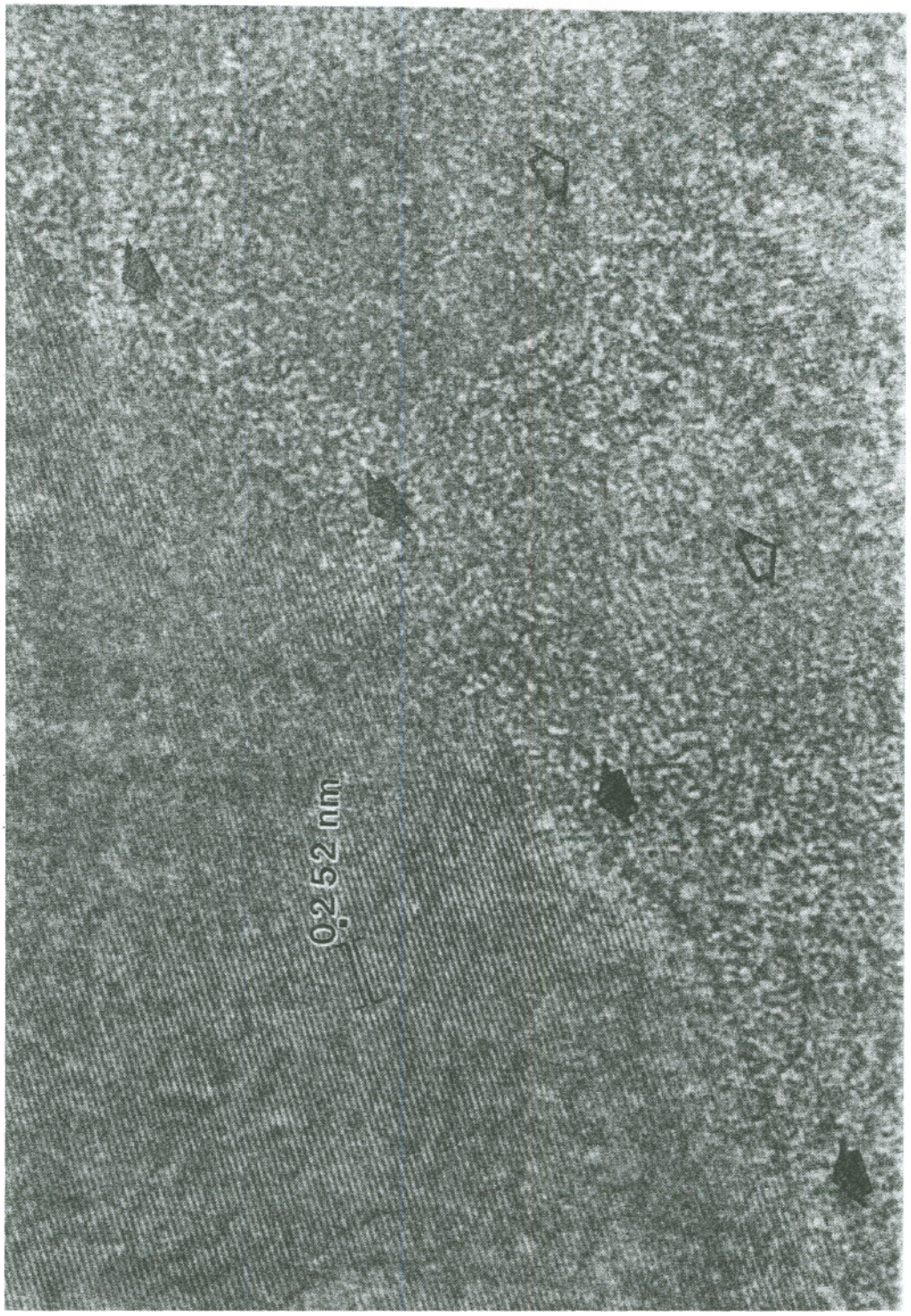

Figure 5.14 : High resolution micrograph of neck region between two SiC particles.

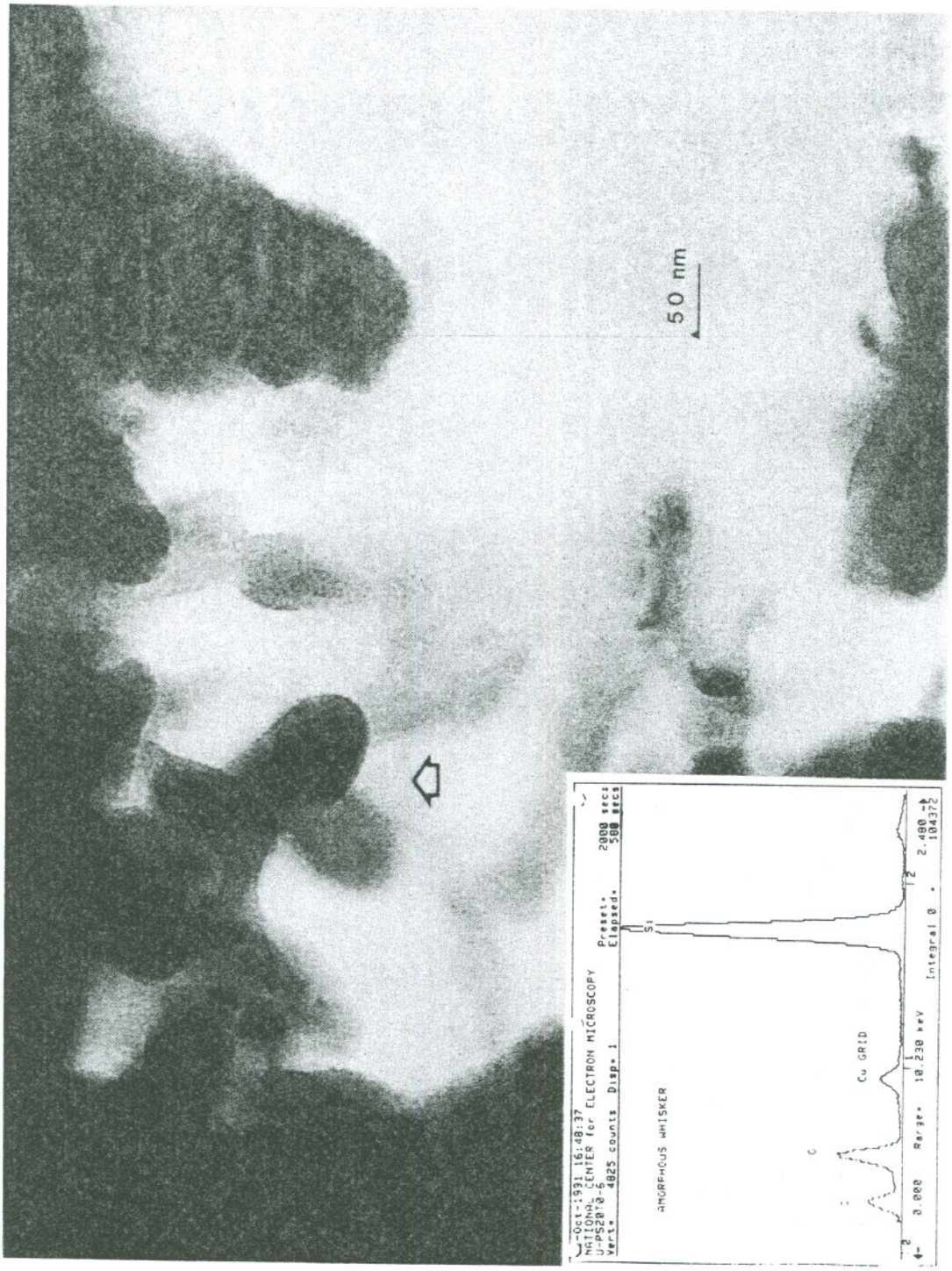

Figure 5.15 : Energy dispersive spectroscopy of amorphous region ($SiC_{2.7}O_{1.1}N_{0.1}$).

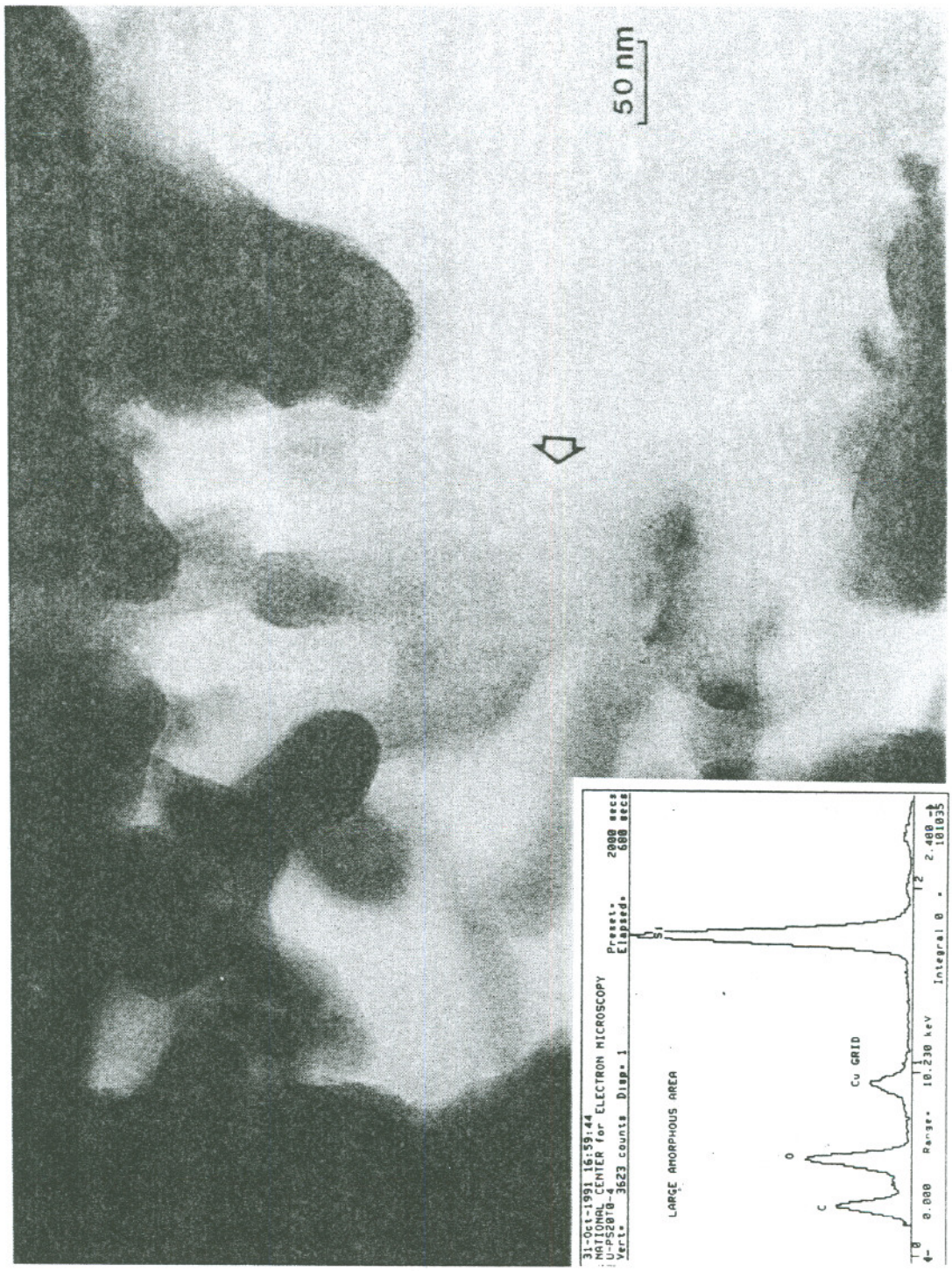

Figure 5.16 : Energy dispersive spectroscopy of amorphous region (see arrow) $SiC_{1.1}O_{0.6}$.

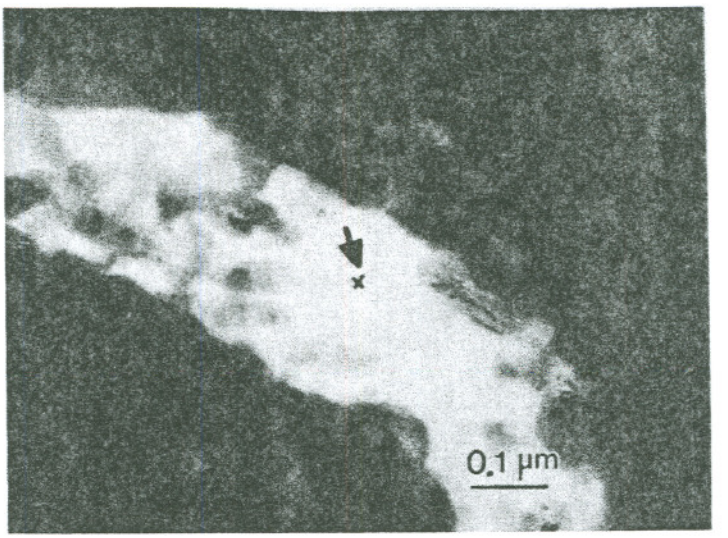

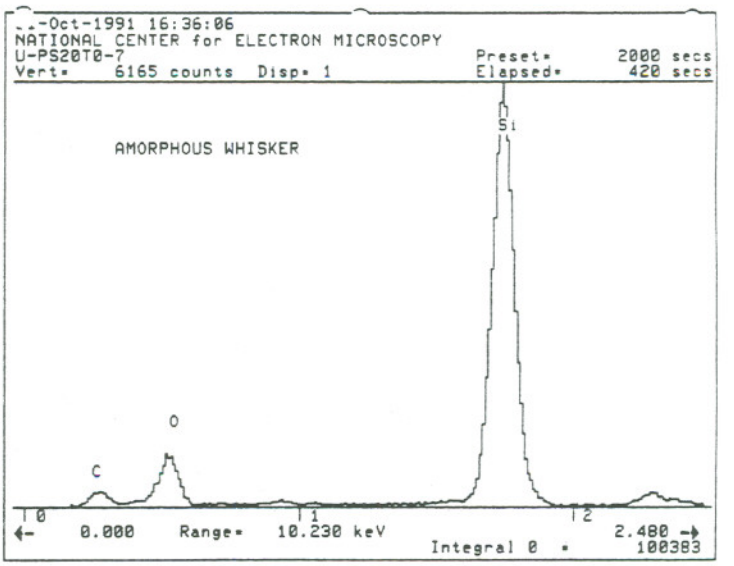

Figure 5.17 : Energy dispersive spectroscopy of amorphous whisker in crack-like opening. ($SiC_{0.3}O_{0.25}$).

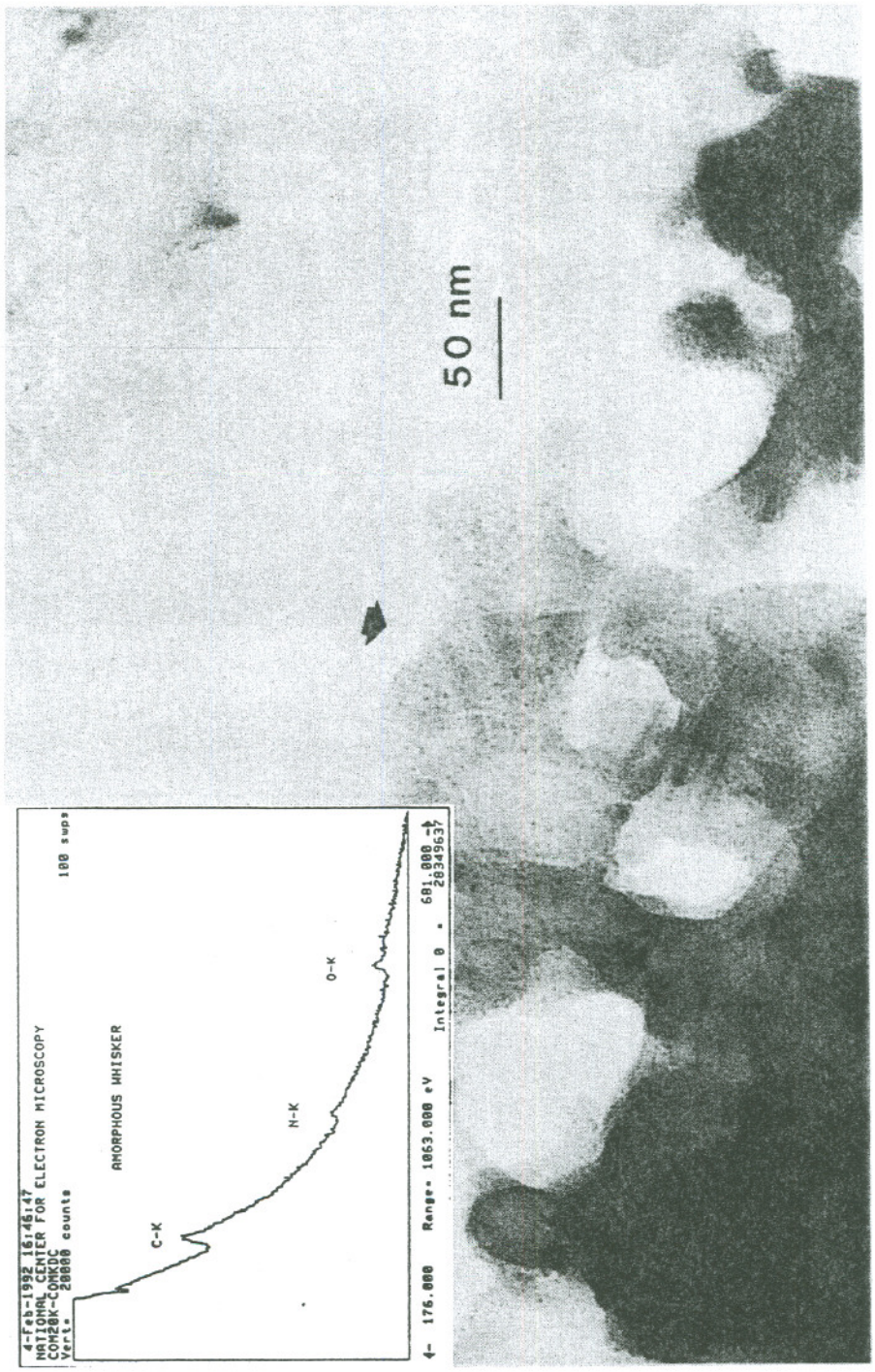

Figure 5.18 : Energy loss spectroscopy of precursor derived phase: N content less than 5 at.%.

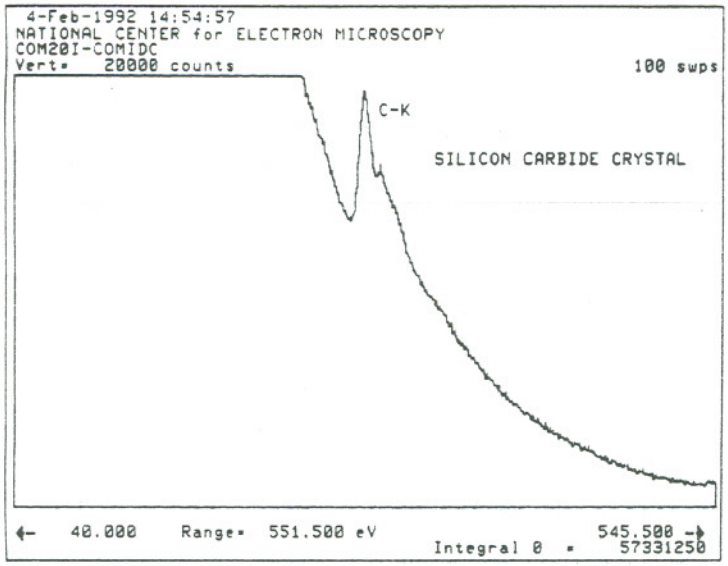

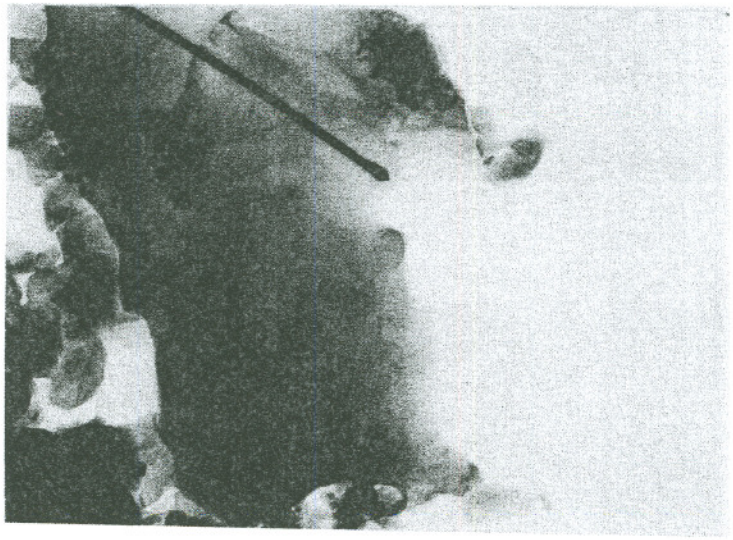

Figure 5.19 : Energy loss spectrum of SiC (reference).

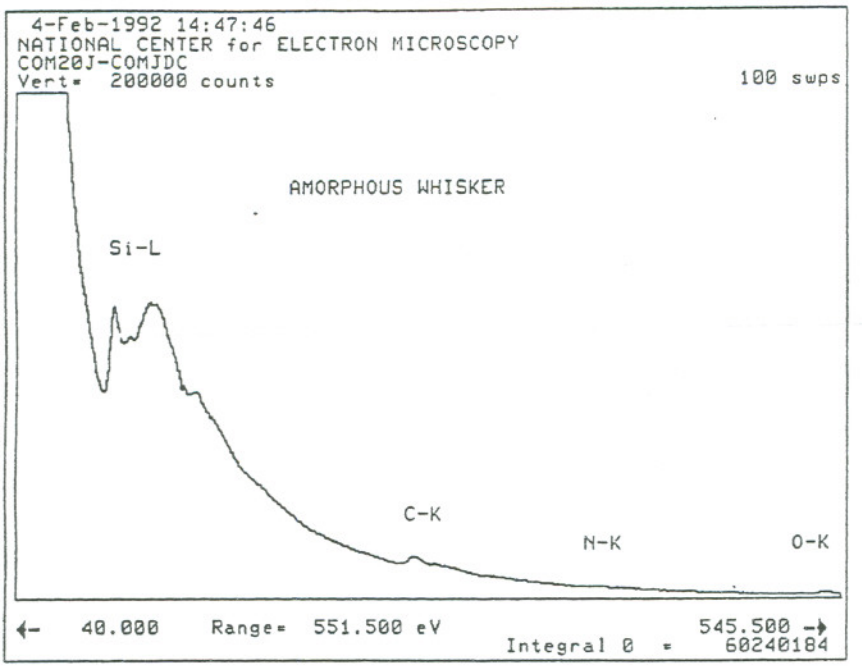

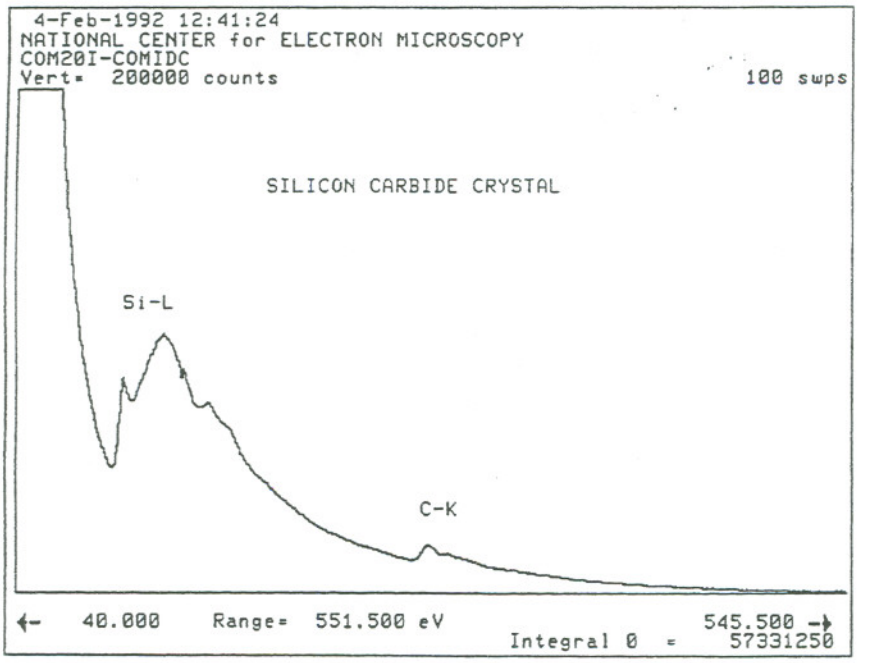

Figure 5.20 : Comparison between Si-L near edge structures in β-SiC and in precursor derived phase.

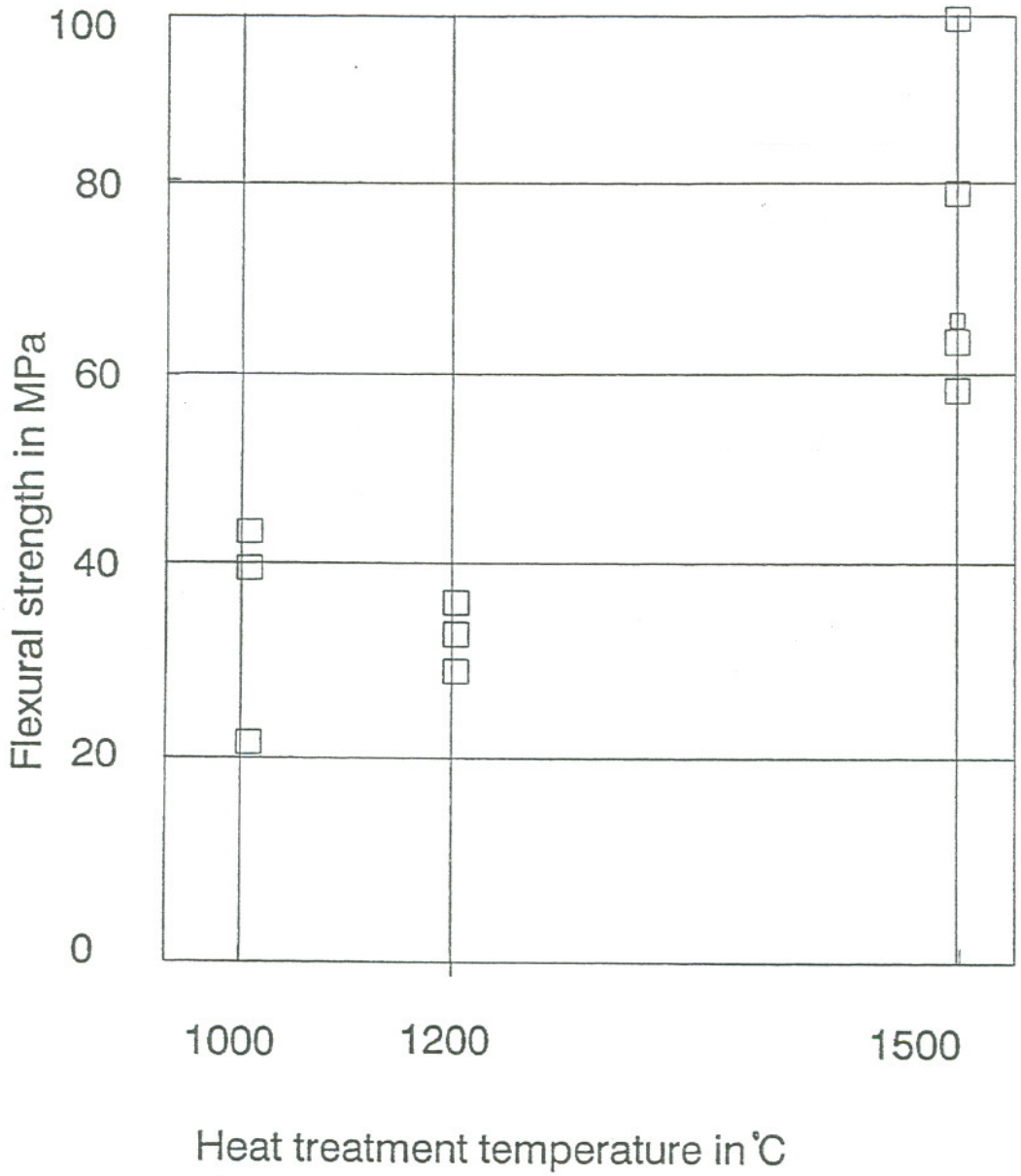

Figure 6.1 : Flexural strength as a function of heat treatment temperature.

Figure 6.2: Possible source of flaws: agglomerates formed during processing.

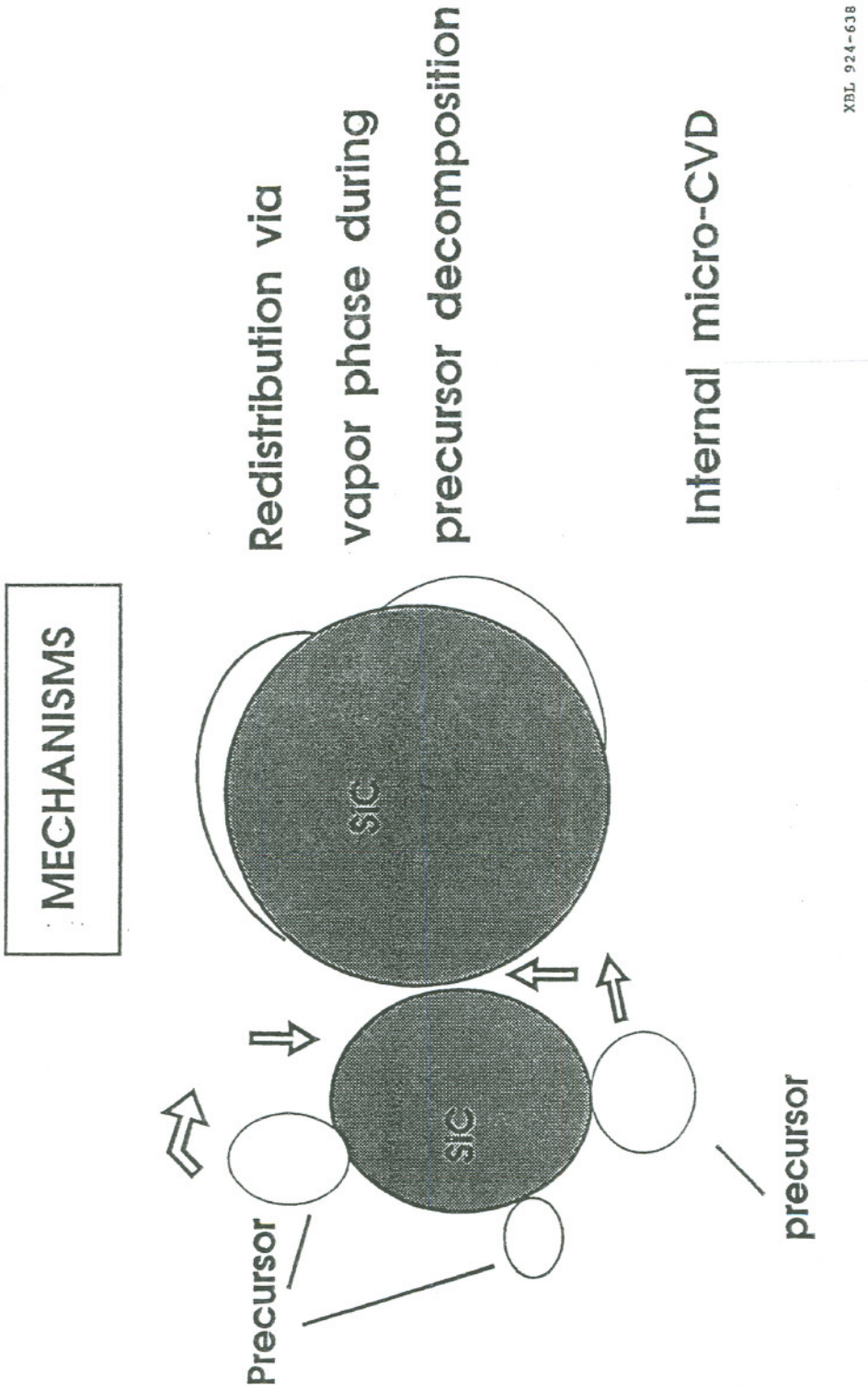

Figure 6.3 : Consolidation mechanism: redistribution of precursor via vapor phase transport during pyrolysis.

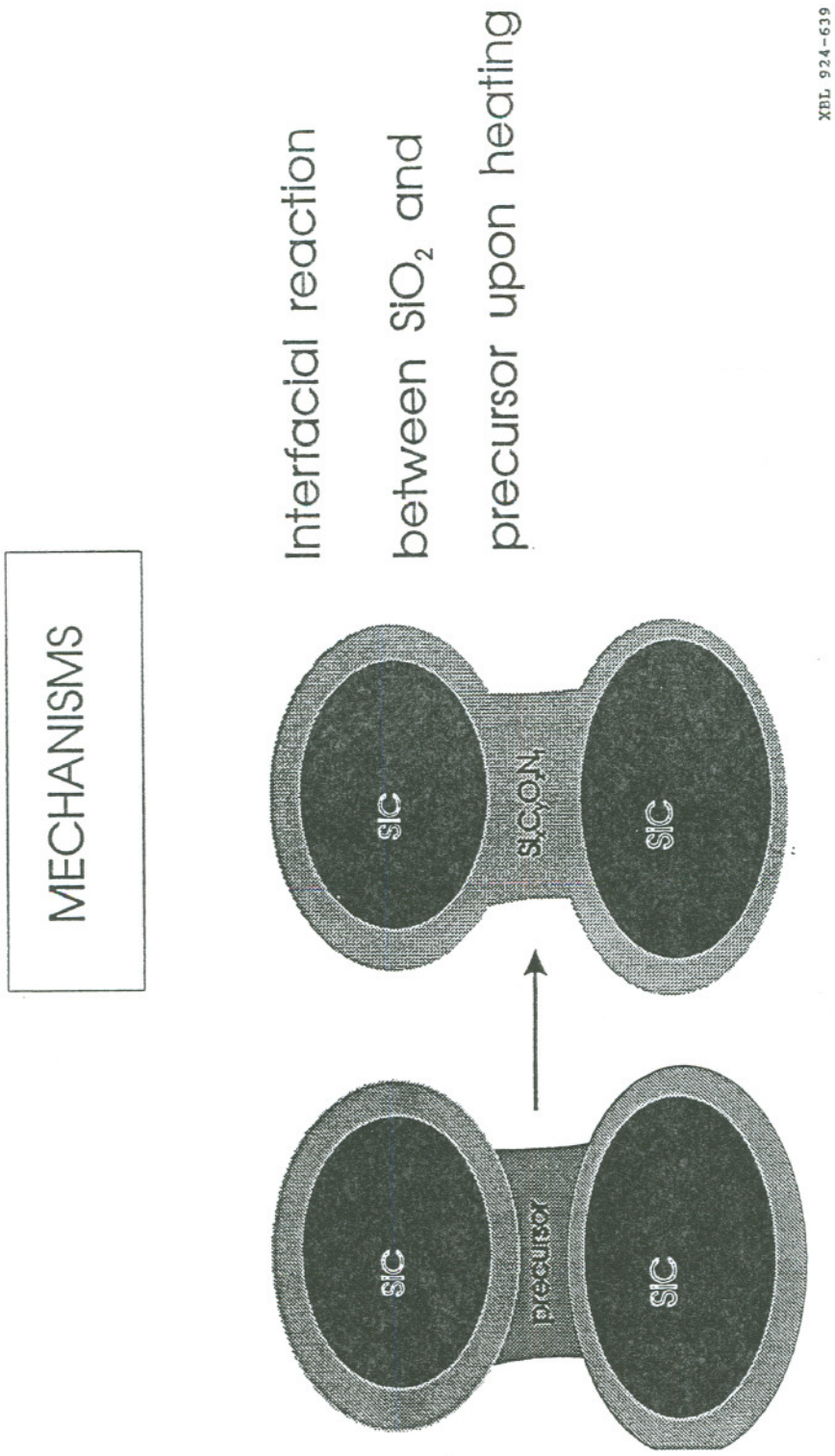

Figure 6.4 : Consolidation mechanism: interfacial reaction involving silica-rich surface layer and polymer derived phase.

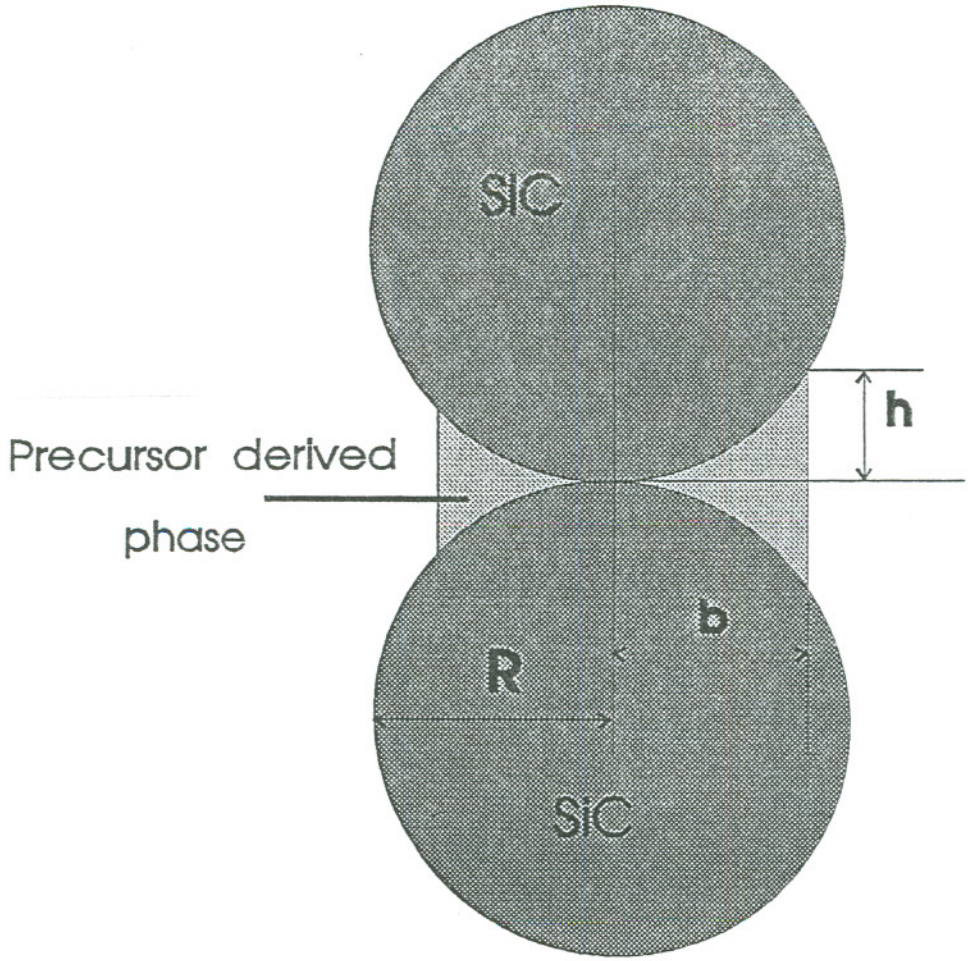

Figure 6.5 : Geometry of reinforced particle contact area.